



Lawrence Berkeley Laboratory

UNIVERSITY OF CALIFORNIA

RECEIVED
LAWRENCE
BERKELEY LABORATORY

APPLIED SCIENCE
DIVISION

SEP 16 1986

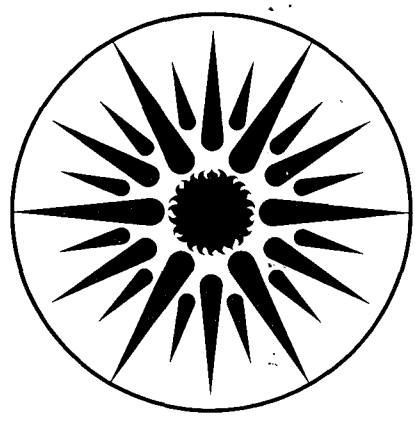
LIBRARY AND
DOCUMENTS SECTION

TECHNOLOGY BASE RESEARCH PROJECT FOR
ELECTROCHEMICAL ENERGY STORAGE
Annual Report for 1985

July 1986

TWO-WEEK LOAN COPY

*This is a Library Circulating Copy
which may be borrowed for two weeks.*



**APPLIED SCIENCE
DIVISION**

LBL-21342
e.2

DISCLAIMER

This document was prepared as an account of work sponsored by the United States Government. While this document is believed to contain correct information, neither the United States Government nor any agency thereof, nor the Regents of the University of California, nor any of their employees, makes any warranty, express or implied, or assumes any legal responsibility for the accuracy, completeness, or usefulness of any information, apparatus, product, or process disclosed, or represents that its use would not infringe privately owned rights. Reference herein to any specific commercial product, process, or service by its trade name, trademark, manufacturer, or otherwise, does not necessarily constitute or imply its endorsement, recommendation, or favoring by the United States Government or any agency thereof, or the Regents of the University of California. The views and opinions of authors expressed herein do not necessarily state or reflect those of the United States Government or any agency thereof or the Regents of the University of California.

LBL-21342

**ANNUAL REPORT
FOR 1985
TECHNOLOGY BASE RESEARCH PROJECT FOR
ELECTROCHEMICAL ENERGY STORAGE**

**Applied Science Division
Lawrence Berkeley Laboratory
University of California
Berkeley, California 94720**

Edited by Kim Kinoshita, Technical Manager

July 1986

This work was supported by the Assistant Secretary for Conservation and Renewable Energy, Office of Energy Storage and Distribution of the U.S. Department of Energy, under Contract No. DE-ACO3-76SF00098.

Table of Contents

EXECUTIVE SUMMARY	v
I. INTRODUCTION	1
II. EXPLORATORY RESEARCH	2
A. AMBIENT-TEMPERATURE LITHIUM CELLS	2
1. Inorganic Ambient-Temperature Rechargeable Lithium Battery	2
B. ALTERNATIVE SODIUM/SULFUR CELL DESIGNS	3
1. Sulfur-Chloraluminat Cathodes for Intermediate- Temperature Cells	3
2. The Hollow-Fiber Sodium/Sulfur Cell	3
C. THERMALLY REGENERATIVE SYSTEM	4
1. Materials for the Sodium Heat Engine	4
III. APPLIED SCIENCE RESEARCH	6
A. ALKALINE CELLS	6
1. Zinc Electrode Studies	6
2. A Semiconductor Electrochemistry Approach to the Study of Oxide Films on Nickel and Zinc	8
3. Spectroscopic Studies of Zincate Solutions	8
4. Battery Membrane Separators	10
5. Hybrid Separators for Alkaline Zinc Cells	11
6. Stable Ionic Polymers for Electrochemical Applications	12
B. ZINC/HALOGEN CELLS	12
1. Surface Morphology of Metals in Electrodeposition	13
2. Dendritic Zinc Deposition in Flow Batteries	14
3. Zinc Electrode Morphology in Acid Electrolytes	15
4. Transport in Aqueous Battery Systems	16

C. MOLTEN-SALT CELLS	16
1. Molten-Electrolyte Cell Research	16
2. Investigation of the FeS ₂ Electrode Capacity Decline In High-Temperature Cells	19
D. IMPROVED COMPONENTS FOR ALKALI/SULFUR CELLS	20
1. Electrochemical Properties of Solid Electrolytes	20
2. Improved β "-Alumina Oxide Electrolyte Through Transformation Toughening	21
3. Principles of Superionic Conduction	23
4. Glass Electrolytes and Advanced Cell Concepts	24
5. Electrical Conduction and Corrosion Processes in Fast-Ion Conducting Glasses	25
6. Glass Electrolytes For Lithium/Sulfur Cells	26
7. New Battery Materials	27
8. Transport Properties of Sodium-Polysulfide Melts	28
9. Experimental and Modeling Studies of the Sodium/Sulfur Cell	29
E. CORROSION PROCESSES IN HIGH-TEMPERATURE, HIGH-SULFUR-ACTIVITY MOLTEN SALTS	29
1. Polysulfide Containment Materials	29
2. Corrosion-Resistant Coatings for High-Temperature High-Sulfur-Activity Applications	32
3. Microcrystalline (Amorphous) Metal/Alloy Coatings Resistant to Molten Sulfur/Polysulfide	34
F. COMPONENTS FOR AMBIENT-TEMPERATURE NONAQUEOUS CELLS	35
1. Surface Layers on Battery Materials	35
2. Spectroscopic Studies of the Passive Film on Alkali and Alkaline Earth Metals in Nonaqueous Solvents	36
3. Polymeric Electrolytes for Ambient-Temperature Lithium Batteries	37

4. Metal Couples in Nonaqueous Electrolytes	38
G. CROSS-CUTTING RESEARCH	39
1. Analysis and Simulation of Electrochemical Systems	39
2. Ambient-Temperature Alkaline Sulfur-Polysulfide Electrodes	40
3. Electrode Kinetics and Electrocatalysis	41
4. Engineering Analysis of Gas Evolution	42
IV. AIR SYSTEMS RESEARCH	44
A. METAL/AIR CELL RESEARCH	44
1. Corrosion of Non-Metallic Electrode Materials	44
2. Electrocatalysts for Oxygen Electrodes	45
3. Research and Development of Bifunctional Oxygen Electrode	47
4. Electrical and Electrochemical Behavior of Particulate Electrodes	48
5. Zinc/Air Battery Systems	49
B. ALUMINUM/AIR BATTERY R&D	49
1. Aluminum/Air Power Cell Research and Development	49
C. FUEL CELL RESEARCH	56
1. Fuel Cells for Vehicles	56
2. Advanced Chemistry and Materials for Fuel Cells	59
3. Oxygen Reduction on Platinum in Fuel Cell Electrolytes	60
4. Investigation of Alloy Catalysts and Redox Catalysts for Phosphoric Acid Fuel Cells	61
5. A New Membrane-Catalyst Combination for Solid-Polymer-Electrolyte Systems	62
6. The Effects of Heat Treatment and Microstructure on Electrocatalyst Performance	63

EXECUTIVE SUMMARY

The U.S. Department of Energy's Office of Energy Storage and Distribution provides continuing support for an Energy Storage Program, which includes R&D on advanced electrochemical energy storage and conversion systems. A major goal of this program is to develop electrochemical power sources suitable for application in electric vehicles and/or electric load-leveling devices. The program centers on advanced secondary batteries and fuel cells that offer the potential for high performance and low life-cycle costs, both of which are necessary to permit significant penetration into commercial markets.

The DOE Electrochemical Energy Storage Program is divided into two projects: the Exploratory Technology Development and Testing (ETD) Project and the Technology Base Research (TBR) Project. ETD Project management responsibility has been assigned to Sandia National Laboratory (SNL), and the Lawrence Berkeley Laboratory* (LBL) is responsible for management of the TBR Project. The ETD and TBR Projects include an integrated matrix of research and development efforts designed to advance progress on several candidate electrochemical systems. The role of the TBR Project is to perform supporting research for the advanced battery systems under development by the ETD Project, and to evaluate new systems with potentially superior performance, durability and/or cost characteristics. The specific goal of the TBR Project is to identify the most promising electrochemical technologies and transfer them to industry and/or the ETD Project for further development and scale-up. This report summarizes the research, financial and management activities relevant to the TBR Project in CY 1985. This is a continuing project, and reports for prior years have been published, and they are listed at the end of the Executive Summary.

General problem areas addressed by the project include identification of new electrochemical couples for advanced batteries, determination of technical feasibility of the new couples, improvements in battery components and materials, establishment of engineering principles applicable to electrochemical energy storage and conversion, and the development of air-system (fuel cell, metal/air) technology for transportation applications. Major emphasis is given to applied research which will lead to superior performance and lower life-cycle costs.

* Participants in the TBR Project include the following LBL scientists: E. Cairns, K. Kinoshita and F. McLarnon of the Applied Science Division; and L. DeJonghe, J. Evans, R. Muller, J. Newman, P. Ross and C. Tobias of the Materials and Molecular Research Division.

The TBR Project is divided into three major project elements: Exploratory Research, Applied Science Research, and Air Systems Research. Highlights of each project element are summarized according to the appropriate battery system or electrochemical research area.

EXPLORATORY RESEARCH

The objectives of this project element are to identify, evaluate and initiate development of new electrochemical couples with the potential to meet or exceed advanced battery and electrochemical performance goals. Research projects were conducted on ambient-temperature Li cells, novel Na/S systems, and a thermally-regenerative system.

Ambient-Temperature Lithium Cells have the potential for high specific energy and specific power, but they typically exhibit short lifetimes when tested under deep-discharge regimens. An inorganic-electrolyte system, which offers improved Li electrode rechargeability and the capability to withstand limited overcharge, is under investigation.

- Duracell, Inc. has observed that prototype cells (2/3A size with wound electrode design) of the Li/LiAlCl₄-SO₂/C system showed a gradual loss of capacity of about 1% per cycle on continuous cycling; cell capacity decreased to 50% after about 40 cycles on deep discharge to 2.0 V. However, cells discharged to 25 or 50% depth-of-discharge have demonstrated over 200 cycles without showing degradation.

Alternative Sodium/Sulfur Cell Designs, which represent significant departures from the Na/ β'' -Al₂O₃/S configuration under development in the ETD Project, were investigated during 1985. In the first design, an intermediate-temperature (180-250 °C) molten-salt mixture substitutes for the high-temperature (300-350 °C) sulfur-polysulfide melt typically used in the positive-electrode compartment, and in the second design a glass electrolyte is used instead of the β'' -Al₂O₃ ceramic electrolyte. Each of these design variations could lead to a Na/S battery lower in cost than the present configuration.

- Experiments at the University of Tennessee on Na/ β'' -Al₂O₃/SCl₃⁺ in AlCl₃-NaCl cells indicate that the factor limiting the specific energy of this cell is the utilization of the active material. A better cell design is needed to optimize the utilization of active materials for long cycle life.

- Dow Chemical Company has observed that the sulfur-corrosion resistance of a promising glass formulation is strongly dependent on the preparative procedure; the glass prepared at 1200 °C, after thorough mixing of the components, has a corrosion resistance that is two times greater than that of the glass obtained at 1000 °C after less mixing.

Thermally-Regenerative Systems convert heat directly into electricity, and their conversion efficiencies are therefore Carnot-cycle limited. The system under investigation uses Na-ion-conducting β'' -Al₂O₃ to separate two Na reservoirs which are at different temperatures.

- Experiments are underway at Ford Motor Company to improve the performance and endurance of electrodes for their thermally regenerative electrochemical system (sodium heat engine). The studies indicate that sputtered TiN electrodes appear to have the potential for long life at temperatures of 800 to 900 °C.

APPLIED SCIENCE RESEARCH

The objectives of this project element are to provide and establish scientific and engineering principles applicable to batteries and electrochemical systems; and to identify, characterize and improve materials and components for use in batteries and electrochemical systems. Projects in this element provide research that supports a wide range of battery systems -- alkaline, metal/air, flow, solid-electrolyte, molten-salt, and non-aqueous. Other research efforts are directed at improving the understanding of electrochemical engineering principles, minimizing corrosion of battery components, analyzing the surfaces of electrodes, and electrocatalysis.

Alkaline Cells often use Zn as the negative electrode, and it is this electrode that typically limits the lifetime of these cells. Efforts are underway to identify cell components that will improve the cycle-life performance of the Zn electrode.

- Evaluations at LBL indicate that the addition of 25 wt% Ca(OH)₂ to the Zn electrode can significantly slow the rate of Zn redistribution. Post-test analyses show that an insoluble Ca-Zn compound forms and is uniformly distributed over the face of the electrode.

- SRI International has examined the photo-effect of passive Zn electrodes. The experiments show that these electrodes are n-type semiconductors, and impedance measurements indicate a higher resistance of the passive film in a fluoride-containing alkaline solution (which has been shown to extend the lifetime of the Zn electrode) compared to that in solution without fluoride ions.
- Raman spectroscopy studies of solutions having a wide range of Zn^{2+} and OH^- concentrations by Argonne National Laboratory (ANL) indicate only one dominant Zn^{2+} complex is present in aqueous Zn^{2+}/KOH solutions. The evidence suggests that Zn^{2+} -hydroxyl complexes, $Zn(OH)_x^{2-x}$, as opposed to ZnO^{2-} , are present in the alkaline solution.
- Sandia National Laboratory (SNL) is exploring synthesis techniques to prepare sulfonated polyphenylene membranes that are stable in alkaline ferro/ferricyanide electrolytes. A material with a high ion-exchange capacity (>30 meq/g) was obtained by sulfonation with fuming sulfuric acid.
- A number of membranes (polyvinyl alcohol cross-linked with crown ether) have been fabricated by Brigham Young University. They exhibit conductivities that approached the target of 0.01 mho/cm, but the transference number for hydroxide ions in the membranes was only 0.71.
- Hybrid separators developed by Pinnacle Research Institute (PRI) appear to possess excellent selectivity to zincate ions, and their hydroxide-ion and water transport properties are not altered by the presence of ion-exchange groups.

Zinc/Halogen Cells use flowing electrolytes to promote the transport of Zn ions across the cell and to remove halogen as the cell is charged. The cell performance is limited by the tendency of the electrodeposited Zn to assume unwanted shapes, and efforts are aimed at understanding the complex phenomena that control the Zn electrode morphology.

- A traveling-stage videomicroscope was used by LBL to investigate the morphology of Zn electrodeposited from a flowing acidic electrolyte. The growth of large protrusions and the development of well-defined ridges are evident during electrodeposition.
- Illinois Institute of Technology (IIT) has observed that the growth rate of protrusions on a rotating cylinder electrode in 1 M $ZnCl_2$ (+3 M KCl) increases with the

rotation rate to the power of approximately 0.6. Higher zinc halide concentrations and higher current densities also cause an increase in the growth rate of the protrusions.

- Brookhaven National Laboratory (BNL) has found that the presence of foreign metals (Bi, Pb, Cd) on the surface of Zn single crystals inhibited layer growth and promoted growth via a nucleation process during Zn deposition. Copper, on the other hand, did not inhibit layer growth and the kinetics of Zn deposition were accelerated.
- Lawrence Livermore National Laboratory (LLNL) has completed isopiestic measurements of the $\text{ZnCl}_2\text{-H}_2\text{O}$ system over the concentration range 4.6749 to 13.143 mol/kg. These data will be used to calculate activity coefficients.

Molten-Salt Cells based on Li alloy negative electrodes and metal disulfide positive electrodes can exhibit very high performance, ease of manufacture, and freeze-thaw capability. Two organizations are pursuing techniques to stabilize the performance of FeS_2 electrodes in these cells.

- ANL has found that the upper-plateau Li-Al/ FeS_2 cell with LiCl-LiBr-KBr electrolyte at 397 °C showed an utilization capacity (at 50 mA/cm²) of about 89% of theoretical through more than 300 cycles and 4000-h operation. Based on this performance, a 250-Ah monopolar cell is expected to achieve 175 Wh/kg at a 4-h rate and 200 W/kg at 80% depth-of-discharge.
- Gould, Inc. has observed that identical Li-alloy/ FeS_2 cells containing LiCl-LiF-LiI electrolyte, which were cycled at 350 and 450 °C, lost upper-plateau capacity at the rate of 0.15 and 0.23% per cycle, respectively. These findings are preliminary, but the two cells have accumulated 150 cycles over 4000 h and 64 cycles over 1700 h, respectively.

Improved Components for Alkali/Sulfur Cells, such as superior alternatives to the $\beta''\text{-Al}_2\text{O}_3$ ceramic electrolyte and high-temperature sulfur-polysulfide electrode used in Na/S cells and stable Li-ion conductors for Li/S cells, are under investigation.

- A novel, low-temperature secondary cell has been developed at LBL which contains a liquid Na negative, $\beta''\text{-Al}_2\text{O}_3$ electrolyte, and a new positive electrode. The cell

operates at 120 to 150 °C, and it can withstand freeze-thaw cycles without harm. Laboratory cells have been tested and show a specific energy of 80 Wh/kg.

- Rockwell International, Inc. is exploring fabrication techniques to reduce the large scatter in the strength of ZrO₂-toughened β"-Al₂O₃. The experiments indicate that a colloidal method, using a nonaqueous solution, helps to disperse the starting powder and allow classification of the powder to achieve the optimum particle size distribution for fabrication of the solid electrolyte.
- Rietveld analysis of the phase transformation and structure at 320 °C of NASICON (Na_{1+x}Zr₂Si_xP_{3-x}O₁₂) solid solutions has been completed by the Massachusetts Institute of Technology (MIT). The results show no evidence for an order-disorder transformation in the Na distribution. It is hoped that improved understanding of the NASICON structure will lead to similar materials that exhibit comparable Na-ion conductivity and ease of fabrication, yet are stable to liquid Na at elevated temperatures.
- ANL has completed evaluation of 24 soda-rich glasses in the soda-alumina-zirconia-silica system, and selected a glass with the composition (mol%) of 42 Na₂O, 8 Al₂O₃, 5 ZrO₂ and 45 SiO₂ for further testing in Na/S cells. This glass has an ionic conductivity of 7.1 x 10⁻³ ohm⁻¹cm⁻¹ at 300 °C, and its chemical stability in the cell environment is comparable to that of Dow glass and β"-Al₂O₃.
- MIT has observed that Ca-containing borate glasses remain highly conductive, in sharp contrast to the known depressing effect of Ca additions on alkali-ion transport in alkali-silicate glasses. This finding has technological importance since CaO additions are believed to improve the durability of glasses in contact with Li metal or its alloys.
- LBL has developed a lithium-chloroborate glass which is capable of supporting pseudo-steady-state current densities up to 15 mA/cm² for 15 to 20 h in a Li/S cell, but this glass lacks the necessary stability to withstand charge-discharge cycling.
- Stanford University is exploring the use of Li₂S-SiS₂ glasses as solid electrolytes. These materials have ionic conductivities comparable to those of the best known inorganic solid electrolytes. Preliminary evaluations (thermodynamic calculations and electrochemical measurements) of several ternary phases, Li-Si-S, Li-O-S and Si-O-S, have been completed.

- The method of restricted diffusion was used by LBL to determine differential diffusion coefficients of Na ions in sodium polysulfide melts. The experimental data can be correlated by the expression

$$D = 0.153 \exp(-5.89 \times 10^3/T) \exp(5.30x_e) \text{ cm}^2/\text{s}.$$

- Experimental measurements on the static-corrosion and dynamic-polarization behavior of materials in sulfur-polysulfide melts were completed by LBL, and the results were published in LBL reports (LBL-19518, LBL-20248, LBL-20249), and presented at the 1985 Fall Meeting of the Electrochemical Society in Las Vegas, NV.

Corrosion Processes in High-Temperature, High-Sulfur Activity Molten Salts are under investigation, and the aim is to develop low-cost container and current-collector materials for use in alkali/sulfur and other molten-salt cells.

- Measurements at ANL indicate that an alloy with an approximate composition of Al-10 Mg plus 15 vol% SiC would fulfill most of the requirements for a container material for Na/S cells. This alloy would be lightweight, relatively inexpensive, and corrosion-resistant to polysulfides and sulfur.
- The factors influencing the adherence of Mo coatings (CVD deposition) on low-carbon steels were delineated in experiments at IIT. A temperature of 900 to 950 °C, system pressure of 2.5 to 3.0 kPa, and a slight excess of H₂ provided the optimum conditions.
- A 40- μm thick Cr layer was successfully electrodeposited by ANL on Type 304 stainless steel from a molten-salt electrolyte containing 58 mol% LiCl-42 mol% KCl eutectic plus CrCl₂. Analysis indicates the Cr layer shows strong adherence to the stainless steel.

Components for Ambient-Temperature Nonaqueous Cells, particularly metal/electrolyte combinations that improve the rechargeability of these cells, are under investigation.

- Measurements at LBL show that Li₃N layers formed by reaction of Li with gaseous nitrogen are microporous. These layers were shown by impedance spectroscopy to be insufficiently protective in nonaqueous solution for use in rechargeable Li electrodes.

- Case Western Reserve University (CWRU) has completed assembly of the ultrahigh vacuum apparatus for investigations of alkali and alkaline-earth metals on metal substrates. Preliminary experiments indicate that clean alkali-metal films, free of carbon contaminants, can be produced in the apparatus.
- The University of Pennsylvania has found that PbBr_2 , in addition to MgCl_2 , form complexes with poly(ethylene oxide) (PEO). The lead halide-PEO complexes are the first polymeric electrolytes with divalent cations that have been reported. This work suggests that many salts of divalent cations and monovalent anions may form conductive complexes with PEO and related polymers.
- LBL is exploring the electroreduction of Mg from $\text{Mg}(\text{BF}_4)_2$ in propylene carbonate. This study shows that the presence of a few parts per million of moisture in the electrolyte prevents the formation of detectable amounts of Mg.

Cross-Cutting Research is carried out to address fundamental problems in electrocatalysis and current density distribution, solutions of which will lead to improved electrode structures and performance in batteries and fuel cells.

- Mathematical models were developed at LBL to identify the physical phenomena that govern the performance of electrochemical systems. Models were developed that (i) simulate the behavior of Li-alloy/ FeS_2 cells employing LiCl-KCl electrolyte, (ii) calculate the frequency response of a rotating-disk electrode, and (iii) calculate the concentration, potential, and current distribution in a thin-gap channel flow cell.
- The kinetic parameters for the aqueous sulfide-polysulfide redox couple, which is used as the counter electrode in several photoelectrochemical cells and has been proposed for use in redox cells, were measured by LBL. Exchange current densities of the order 1 mA/cm^2 were found, which are significantly higher than those reported previously.
- Electrochemical experiments at LBL indicate that repeated formation/reduction of a monolayer of oxide on Au did not change the structure of the surface; this is in direct contrast to the results obtained with Pt.
- Modeling studies by LBL on gas evolution at smooth electrodes indicate that the current density near the bubble/electrode interface is enhanced, which results from the local depression of the supersaturation potential in this region. This

enhancement effect diminishes with increasingly sluggish kinetics, and it is seen to disappear completely in the limit of Tafel polarization.

AIR SYSTEMS RESEARCH

The objectives of this project element are to identify, characterize and improve materials for air electrodes; and to identify, evaluate and initiate development of metal/air battery systems and fuel-cell technology for transportation applications.

Metal/Air Cell Research projects address bifunctional air electrodes, which are needed for electrically rechargeable metal/air (Zn/air, Fe/air) cells; and novel alkaline Zn electrode structures, which could be used in either electrically recharged or mechanically recharged cell configurations.

- Recent experiments at LBL on the graphitization of carbon blacks indicate that there is a new family of graphitic material having particularly attractive BET-area/ I_2 -adsorption ratios, and which appear to be nearly an order of magnitude better in corrosion resistance than acetylene black.
- Analytical measurements by CWRU indicate that heat treatment of organic macrocycles supported on carbon results in the decomposition of the macrocycle, but the pyrrole nitrogen is retained. This nitrogen provides binding sites for adsorbed transition metals, such as Co and Fe, with the catalytic activity due mostly to the metal in an atomic state of dispersion.
- Energy Research Corporation (ERC) has found a perovskite of the composition $La_{0.5}Sr_{0.5}CoO_3$ that can be operated as a bifunctional air electrode for 800 cycles at 10 mA/cm² (charge) and 20 mA/cm² (discharge). Its polarization characteristics are comparable to those of Westinghouse's technology.
- An investigation has been completed at LBL on the effect of potential fluctuations on the morphology of Zn electrodeposited on fluidized-bed and particulate Zn electrodes in alkaline electrolytes. In most cases the fluctuations have a marked effect on both macrostructure and microstructure. Investigations to date indicate that a fluidized-bed electrode might be most suitable for charging a Zn/air cell (depositing Zn) but that a moving-bed electrode would be more suitable for discharge.

- PRI was awarded a contract from a RFP on metal/air battery R&D issued by LBL during 1985. PRI will investigate methods to improve the performance of particulate Zn electrodes for Zn/air cells.

Aluminum/Air Battery R&D, managed by LLNL, is directed at improving cell components and solving system integration problems, including the following: (i) air cathode development, (ii) hydrargillite crystallization and separation, (iii) integrated experiments involving a coupled cell/crystallizer, (iv) cell design, and (v) development of improved Al anodes. Major achievements of the program include:

- Experiments were performed at LLNL in which a single cell was run for over 5 h at 70 °C with 99.999% pure Al anode. The presence of stannate ions in solution, which is present to reduce Al corrosion, was found to deposit as Sn on cell components (cell hardware and pump valves). This observation suggests that additives other than stannate ions are required to suppress corrosion.
- Experiments at Eltech Systems Inc., Electromedia, Inc., and CWRU have identified Norit (Ultracarbon) containing 5 to 10% CoTMPP as a promising air cathode material that exhibit long life (over 3000 simulated-drive cycles*). The performance of these air electrodes in KOH electrolyte is approximately 240 mV higher (at 600 mA/cm²) than the corresponding performance in NaOH electrolyte.
- Alcan International Ltd. has developed a proprietary Al anode which has anodic polarization characteristics similar to that of RX-808 (Reynolds alloy) and corrosion behavior approaching a target of 10 mA/cm² equivalent corrosion rate. Its polarization is not appreciably changed by operation at 80 °C or the use of KOH electrolyte, but the corrosion rate is somewhat increased under these conditions.
- Eltech has developed a new cell design, EL-2, to overcome many of the problems identified with the M-4 design. An improved modular cathode, better gasket sealing, and a better anode current-collection design were achieved.
- LLNL is exploring alternative methods to hydrocyclones for separation of hydrargillite. Theoretical calculations and preliminary measurements indicate that lamella settlers offer an attractive alternative to hydrocyclones.

* Not true vehicle driving cycles, but represents cycles for comparative test of electrode cycle life.

Fuel Cell Research, managed by Los Alamos National Laboratory (LANL), includes research in several areas of electrochemistry, theoretical studies, fuel-cell testing, fuel processing, and membrane characterization. Major achievements of the fuel-cell program include:

- LANL demonstrated that the Pt catalyst loading in proton-exchange membrane fuel cells can be dramatically reduced by pretreating commercial Prototech electrodes with solubilized Nafion. Their performance was comparable to that of conventional electrodes, despite a Pt loading that is an order of magnitude lower.
- LANL has concluded from studies using isotopic-labeled O_2 that CH_3OH reforming on ZnO-CuO catalysts does not follow the cracking-shift route; instead methanol adds to an oxide vacancy, and in that position, reacts with lattice oxygen atoms to generate CO_2 .
- Theoretical studies at LANL have been extended to Pt_3 molecules. These studies indicate that the three atoms are located at the corners of an equilateral triangle with an internuclear separation of 2.69 Å.
- Testing of a 20-kW fuel-cell system, which was delivered by ERC, was completed at LANL. The transient characteristics of the fuel processor were quantified. A time constant of about 15 s was recorded for a change in reformat temperature in response to a step change in the burner temperature.
- BNL is investigating the electrochemistry and characterization of metal-organic macrocycles. None of the 20 synthesized tetrasulfonated metal phthalocyanines (M-TsPc) exhibited interaction with C_1 compounds, which indicates that they are not active for compounds with C-H bonds.
- International Fuel Cells, Inc. (United Technologies Corporation) has concluded from thermogravimetric analysis and Mossbauer spectroscopy that the central FeN_4 group remained intact after heat-treatment of Fe-TMPP supported on carbon at $950^\circ C$. This material was more active for O_2 reduction in H_3PO_4 than the Co analog.
- Hamilton Standard-Electrochemical concluded from their study on solid-polymer-electrolyte fuel cells that (i) the development of a low-cost, ion-exchange membrane that exhibits similar performance to Nafion for over 1000-h operation is feasible, and

(ii) material costs for both the anode and cathode can be reduced by 50% while maintaining similar performance to a fuel cell containing noble-metal loadings of 4 mg/cm².

- The University of Virginia observed that an alloy of 25 at% Cr-75 at% Pt produced activity for O₂ reduction in H₃PO₄ that was comparable to that of Pt. However, the performance of the alloy never exceeded that of Pt, contrary to the results obtained with dispersed alloy catalysts, which indicated higher activity after Cr addition to Pt.
- Oxygen reduction measurements in K₂CO₃ and KOH have been completed by LBL. The kinetic currents at 0.9 V (versus RHE) are 2 to 2.5 times higher in K₂CO₃ than in KOH at the same concentration. However, lower O₂ solubilities in carbonate electrolytes may lead to higher mass-transfer overpotentials in a fuel cell.

PLANNED ACTIVITIES IN 1986

New research projects planned include:

1. An RFP will be issued for research on novel concepts for rechargeable lithium cells.
2. Applied research on the characterization of components for secondary batteries.

MANAGEMENT ACTIVITIES

During 1985, LBL managed 30 subcontracts and conducted a vigorous research program in Electrochemical Energy Storage. LBL staff members attended project review meetings, made site visits to subcontractors, and participated in technical management of various TBR projects. LBL staff members also participated in the following reviews, meetings, and workshops:

- Sixth Meeting of the DOE Advanced Fuel Cell Working Group, LBL, Berkeley, CA, January 9-11, 1985.
- DOE/SNL/LBL/EPRI Lead Center Coordination Meeting, Washington, DC, January 22, 1985.

- Electrochemical Energy Storage Program Lead Center Review, Washington, DC, January 23, 1985.
- Review of Ceramatec's Programs on Beta"-Alumina and Related Technologies, Salt Lake City, UT, January 24-25, 1985.
- EPRI Na/S Battery Research Program, EPRI, Palo Alto, CA, February 5, 1985.
- Golden Gate Metals and Welding Conference, San Francisco, CA, February 12, 1985.
- Sodium Heat Engine Review, ANL, Argonne, IL, February 12-13, 1985.
- Annual Meeting of the AIME, New York, NY, February 24-28, 1985.
- Frontiers of Experimental and Theoretical Electrochemistry Workshop, LANL, Los Alamos, NM, February 25-26, 1985.
- Electric Vehicle Battery Review Meeting, Washington, DC, April 23, 1985.
- Spring Meeting of the Electrochemical Society, Toronto, Ontario, Canada, May 12-17, 1985.
- NRC Committee Meeting on Electrochemical Aspects of Energy Conservation and Production, Toronto, Ontario, Canada, May 16, 1985.
- Aluminum/Air Battery Review Meeting, Toronto, Ontario, Canada, May 17, 1985
- National Fuel Cell Seminar, Tucson, AZ, May 19-22, 1985.
- Beta Battery Workshop VI, Snowbird, UT, May 19-23, 1985.
- Electrochemical Energy Storage Program Lead Center Meeting, Washington, DC, July 10-11, 1985.
- Sixth Read Conference on Electrodeposition, University Park, PA, July 22-26, 1985.
- NRC Committee Meeting on Chemical Engineering Frontiers, Panel on Energy and Natural Resources Processing, Itasca, IL, July 31-August 1, 1985.
- NRC Committee Meeting on Energy Conservation and Production, Washington, DC, August 15-16, 1985.
- 20th Intersociety Energy Conversion Engineering Conference, Miami Beach, FL, August 18-23, 1985.
- 36th Meeting of the International Society of Electrochemistry, Salamanca, Spain, September 22-27, 1985.
- Fall Meeting of the Electrochemical Society, Las Vegas, NV, October 13-18, 1985.
- Aluminum/Air Battery Review Meeting, Las Vegas, NV, October 18, 1985.
- Seventh Battery and Electrochemical Contractors' Conference, Crystal City, VA, November 18-21, 1985.

MILESTONES FOR THE TECHNOLOGY BASE RESEARCH PROJECT

Milestones accomplished in Fiscal Year 1985 by the TBR Project include:

- LLNL initiated testing of an Al/air cell (M-4) that is coupled to a crystallizer. This test showed that the crystallizer design was adequate to obtain separation of crystal from the electrolyte flow stream. The major finding from this test is that the stannate ions (inhibitor to reduce Al corrosion) present in solution are reduced and precipitate as metallic Sn on various components in the system.
- Testing of the M-5 cell design (500 cm²) was completed by Eltech Systems Corp. This Al/air cell contained an anode of 99.98% Al and a cathode of CoTMPP. The cell operated at 1.21 V (200 mA/cm²) at the start of testing in 4 N NaOH at 55 °C. The initial test demonstrated that the results with small cells (2.5-cm x 2.5-cm electrodes) can be correlated with data from larger cells (500 cm²).
- Eltech Systems Corp. completed a new design (EL-2) for an Al/air cell that provided major improvements over the old design (M-5). Cell EL-2 demonstrated improvements in the sealing mechanism for the air cathodes, reliability of components, and ease of assembly of multi-cell stacks.
- A glass electrolyte with the composition (in mol%) 42 Na₂O, 8 Al₂O₃, 5 ZrO₂, and 45 SiO₂ has been selected by ANL for testing in Na/S cells. The chemical stability of this glass in Na/S cell environment is comparable to that of β"-Al₂O₃ and Dow glass.
- A research program at International Fuel Cells, Inc. seeks to reduce the cost of electrocatalysts for air electrodes in phosphoric acid fuel cells. Various organic macrocyclics were evaluated as possible alternatives to Pt for O₂-reduction electrocatalysis. FeTMPP showed stable performance in half-cell tests, but its performance decayed badly in fuel-cell tests. Based on these results a decision was made not to pursue endurance testing of FeTMPP in fuel cells. Instead, it was decided to continue with studies to determine the cause of performance decay and to proceed with tests on the variations in electrode fabrication that are needed to improve the performance of electrodes containing organic macrocyclics.
- Hamilton Standard-Electrochemical has tested solid-polymer-electrolyte fuel cells with an active area of 0.05 ft². This cell size is adequate for laboratory tests, but is not a suitable size for cell stacks for use in a vehicle propulsion system where the active electrode area should be at least 1 ft². Despite the encouraging results obtained in this program, the progress to date did not warrant a scale-up of the cell from 0.05 to 1 ft².

ANNUAL REPORTS

1. "Technology Base Research Project for Electrochemical Energy Storage - Annual Report for 1984," LBL-19545 (May 1985).
2. "Annual Report for 1983 - Technology Base Research Project for Electrochemical Energy Storage," LBL-17742 (May 1984).
3. "Technology Base Research Project for Electrochemical Energy Storage, - Report for 1982" LBL-15992 (May 1983).
4. "Technology Base Research Project for Electrochemical Energy Storage - Report for 1981," LBL-14305 (June 1982).
5. "Applied Battery and Electrochemical Research Program Report for 1981," LBL-14304 (June 1982).
6. "Applied Battery and Electrochemical Research Program Report for Fiscal Year 1980," LBL-12514 (April 1981).

ACKNOWLEDGEMENT

This work was supported by the Assistant Secretary for Conservation and Renewable Energy, Office of Energy Storage and Distribution of the U.S. Department of Energy under Contract No. DE-AC03-76SF00098. The fuel cell effort at LANL was partially supported by the U.S. Department of Energy, Office of Vehicle and Engine Research and Development. The support from the Department of Energy and the contributions to this project by the participants in the Technology Base Research Project are gratefully acknowledged.

SUBCONTRACTOR FINANCIAL DATA - CY 1985

Subcontractor	Principal Investigator	Project	Contract Value (K\$)	Duration (months)	Expiration Date	Status in FY 1986
EXPLORATORY RESEARCH						
Ambient Temperature Lithium Cells						
Duracell International, Inc.	A. Dey	Li/SO ₂	1500	48	12-85	R
Alternative Sodium/Sulfur Cell Designs						
University of Tennessee	G. Mamantov	Na/SCl ₄ (NaCl-AlCl ₃)	19	12	3-85	T
Dow Chemical Company	P. Pierini	Sodium/Sulfur	290	12	8-85	T
Thermally-Regenerative System						
Ford Motor Company	T.K. Hunt	Sodium Heat Engine	253	16	5-85	T
APPLIED SCIENCE RESEARCH						
Lawrence Berkeley Laboratory	E. Cairns, L. DeJonghe J. Evans, R. Muller, J. Newman, P. Ross, and C. Tobias	Electrochem. Energy Storage	1500	12	9-85	C
Alkaline Cells						
SRI International	M. Madou	Semiconductor Electrode	71	12	3-85	T
Argonne National Laboratory	J. Battles	Spectroscopic Studies	25	12	9-85	T
Brigham Young Univ.	D. Bennion	Zn/NiOOH Separators	77	12	7-85	T
Pinnacle Research	R. Yeo	Zn/NiOOH Separators	100	13	7-85	T
Zinc/Halogen Cells						
Illinois Institute of Technology	J.R. Selman	Zn Deposition	71	12	8-86	C
Brookhaven National Laboratory	J. McBreen	Zn Morphology	100	12	9-85	C
Lawrence Livermore Nat'l Laboratory	D. Miller	Transport Properties	65	12	9-85	C
Molten-Salt Cells						
Argonne National Laboratory	J. Battles	Molten-Salt Cells	330	12	9-85	C
Gould, Incorporated	H.F. Gibbard	Li/FeS ₂	200	20	4-86	R
Stanford University	R. Huggins	New Battery Materials	300	12	11-85	C

SUBCONTRACTOR FINANCIAL DATA - CY 1985

Subcontractor	Principal Investigator	Project	Contract Value (K\$)	Duration (months)	Expiration Date	Status in FY 1986
Improved Components for Alkali/Sulfur Cells						
Rockwell International, Inc.	F. Lange	Improved $\beta''\text{Al}_2\text{O}_3$	145	12	4-86	T
Massachusetts Institute of Technology	B. Wuensch	Superionic Conductors	83	12	7-85	C
Massachusetts Institute of Technology	H. Tuller	Li Conducting Glasses	99	12	5-86	C
Argonne National Laboratory	J. Battles	Glass Electrolytes	300	12	9-85	C
Corrosion Processes in High Temperature, High-Sulfur Activity Molten Salt						
Argonne National Laboratory	J. Battles	Polysulfide Containment	200	12	9-85	C
Illinois Institute of Technology	R. Selman	Corrosion Resistant Coatings	163	12	9-85	C
Argonne National Laboratory	J. Battles	Amorphous Coatings	50	6	3-86	T
Components for Ambient-Temperature Lithium Cells						
Case Western Reserve University	D. Scherson	Spectroscopic Studies	58	12	11-85	C
University of Pennsylvania	G. Farrington	Polymeric Electrolytes	82	12	2-86	C
AIR SYSTEMS RESEARCH						
Metal/Air Cell Research						
Case Western Reserve University	E. Yeager	Air Electrodes	213	12	3-86	C
Energy Research Corporation	M. Klein	Bifunctional O_2 Electrode	195	12	9-85	T
Pinnacle Research Institute	L. Morris	Zn/Air Battery	225	12	11-86	C
Aluminum/Air Battery R&D						
Lawrence Livermore Nat'l Laboratory	A. Maimoni	Al/Air Battery R&D	450	12	9-85	C
Eltech Systems Corporation	L. Gestaut	Al/Air Battery	600	24	1-86	C
Fuel Cell R&D						
Los Alamos National Laboratory	J. Huff	Fuel Cell R&D	784	12	9-85	C
Brookhaven National Laboratory	J. McBreen	Fuel Cell Research	290	12	9-85	C
United Technologies Corporation	J.A. Bett	Alloy Catalysts	627	24	4-85	T
Hamilton Standard (formerly G.E.)	J.F. McElroy	Solid Polymer Electrolyte	997	35	12-85	T
University of Virginia	G. Stoner	Alloy Electrocatalyst	82	28	1-86	T

* C = continuing, T = terminating, R = subject included in a request for proposals (RFP) issued by LBL in FY 1986.

I. INTRODUCTION

This report summarizes the progress made by the Technology Base Research (TBR) Project for Electrochemical Energy Storage during calendar year 1985. The primary objective of the TBR Project, which is sponsored by the Department of Energy (DOE) and managed by Lawrence Berkeley Laboratory (LBL), is to identify electrochemical technologies that can satisfy stringent performance and economic requirements for electric vehicles and stationary energy storage applications. The ultimate goal is to transfer the most promising electrochemical technologies to the private sector or to another DOE project (e.g., Sandia National Laboratories' Exploratory Technology Development and Testing Project) for further development and scale-up.

Besides LBL, which has overall responsibility for the TBR Project, technical management of several projects is shared with Lawrence Livermore National Laboratory (LLNL) and Los Alamos National Laboratory

(LANL). Brookhaven National Laboratory (BNL) and Argonne National Laboratory (ANL) participate in the TBR Project by providing key research support in several of the project elements.

The TBR Project consists of three major project elements:

- Exploratory Research
- Applied Science Research
- Air Systems Research

The objectives and the specific battery and electrochemical systems addressed by each project element are discussed in the following sections, which also include technical summaries that relate to the individual projects. Financial information that relates to the various projects and a description of the management activities for the TBR Project are described in the Executive Summary.

II. EXPLORATORY RESEARCH

The major thrust of this project element is to evaluate promising electrochemical couples for advanced batteries for electric vehicles. The advanced battery systems that were investigated are ambient-temperature rechargeable Li cells, new Na/S cell designs, and a thermally regenerative electrochemical system using Na.

A. AMBIENT-TEMPERATURE LITHIUM CELLS

These cells have the potential for high specific energy and specific power, but they typically exhibit short lifetimes when tested under deep discharge regimens. An inorganic-electrolyte system, which offers improved Li-electrode rechargeability and the capacity to withstand limited overcharge, is under investigation.

Inorganic Ambient-Temperature Rechargeable Lithium Battery

(A. Dey, Duracell, Inc.)

The objectives of this program is to develop an ambient-temperature rechargeable Li battery which can deliver 500 to 800 cycles at 80% depth of discharge (DOD), with a specific energy of about 150 Wh/kg. Continued efforts at Duracell on the development of rechargeable Li batteries with an inorganic SO₂ electrolyte has led to the discovery of a new electrochemical system. The new system consists of a Li negative electrode, a carbon positive electrode, and a low-cost LiAlCl₄/SO₂ electrolyte.

The system has an open-circuit voltage (OCV) of 3.24 V and discharges with a rather flat voltage similar to prior Li/SO₂ cells with Li₂B₁₀Cl₁₀/SO₂ or LiGaCl₄/SO₂ electrolyte.

However, the discharge reaction does not produce lithium dithionite by reducing of liquid SO₂, as commonly observed in other types of Li/SO₂ cells. No dithionite can be directly identified from the discharge of the positive electrode. In cells with excess electrolyte, the capacity is limited by the amount of carbon, and the capacity depends strongly on the type of carbon material. Experimental cells have been cycled at 1-3 mA/cm² discharge rates to a 2.6 V cut-off and a 1 mA/cm² charge rate; and several hundred cycles have been obtained without showing capacity loss.

The chemistry of the system allows the cell to withstand limited overcharge. On overcharge, Cl₂ and AlCl₃ are generated. Both reaction products are highly soluble in electrolyte and are able to diffuse through the separator and react with the excess Li deposited during overcharge to regenerate the electrolyte salt, LiAlCl₄.

Prototype 2/3A-size cells with wound electrode design were evaluated. The wound cell delivers about 0.4 Ah at C/4 rate, and it has a specific energy of about 90 to 100 Wh/kg. Since the 2/3A-size cell has very poor packaging efficiency, it is believed that the specific energy can be further improved to reach a goal of 150 Wh/kg, when the system is scaled up to larger-size cells. The system also has good shelf life; small wound cells stored for 9 months at ambient temperature did not show any loss of capacity.

The wound cells showed a gradual loss of capacity of about 1% per cycle on continuous cycling; cell capacity decreases to 50% after about 40 cycles on deep discharge to 2.0 V. However, cells discharged to 50% or 25% depth have demonstrated over 200 cycles without showing degradation. Cells on

shallow-discharge cycling usually failed due to development of internal shorts, probably caused by degradation of the separator.

B. ALTERNATIVE SODIUM/SULFUR CELL DESIGNS

Two cell designs that represent significant departures from the Na/ β'' -Al₂O₃/S configuration under development in the ETD Project were investigated. In the first design an intermediate-temperature (180-250 °C) molten-salt mixture substitutes for the high-temperature (300-350 °C) sulfur-polysulfide melt typically used in the positive-electrode compartment, and in the second design a glass electrolyte is used instead of the β'' -Al₂O₃ ceramic electrolyte.

Sulfur-Chloraluminate Cathodes for Intermediate-Temperature Cells

(G. Mamantov, University of Tennessee)

The objective of this program was to investigate the electrochemical and chemical processes taking place in the Na/ β'' -Al₂O₃/S/Cl₃⁺ in AlCl₃-NaCl cell, which operates at 180 to 250 °C. More than 40 cells were tested during this contract. With few exceptions, the cells have all been constructed of Pyrex glass, and either tungsten or Reticulated Vitreous Carbon (RVC) have been used as current collectors for the positive electrodes.

Factors that affect the performance of these cells (i.e., specific energy, specific power, energy efficiency, cycle life) were investigated. For the best-performing cells, the cell resistances were as low as 12 ohm-cm² at 200 °C and 20 mA/cm². At high discharge rates, cell resistances have been as low as 6 ohm-cm² at 150 to 300 mA/cm² and ~250 °C; this effect may be caused by an increase in temperature due to resistive heating. Electrochemical

measurements indicate that most of the polarization occurred at the β'' -Al₂O₃/molten salt interface, and it was dependent on the initial melt composition.

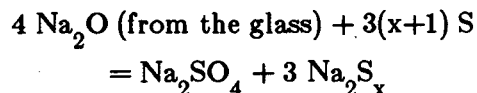
Another factor limiting the specific energy of the cell is the utilization of the active material. The incomplete utilization observed on discharge at high current densities may be due to non-equilibrium conditions within the cell. It is clear that a better cell design is needed to optimize the utilization of active materials for long cycle life.

The Hollow Fiber Sodium/Sulfur Cell

(P. Pierini, Dow Chemical Company)

The objective of this project is to improve the lifetime and reliability of hollow-fiber electrolytes for Na/S cells. By use of very sensitive techniques involving anion chromatography, a method was developed that can determine S attack (via Reaction I) on Na-ion conducting glass that results in corrosion depths of as little as 100Å.

Reaction I:



Reaction rates and kinetics of S attack on 17 different glasses in the ternary system Na₂O-B₂O₃-SiO₂ were determined at 300 and 400 °C. The goal of this work was twofold: first, to test the hypothesis that S reactivity of an improved Na-resistant glass (T806) was responsible for the early failure of cells using T806 glass as the electrolyte, and second, to identify glasses more resistant to S for potential use in Na/S cells.

Although Dow's standard glass (D406) is one of the least-reactive glasses at 300 °C, it is the most reactive at 400 °C. It was hoped that there would be large breaks in S reactivity at some threshold level of Na₂O content for the

range of compositions examined. However, this was not observed. As a result, the studies were focused more critically on S corrosion of the D406 and T806 glasses. The total corrosion was measured at 325, 350 and 400 °C at time intervals of 14 and 30 days. Excellent fits for D406 glass at all temperatures and times were obtained, which can be described by the equation

$$Q = 2fC_o \left[D_o t / \pi \right]^{1/2} \exp(-E_a / 2RT)$$

where Q is the Na₂O consumed per unit area of glass surface in mg/cm², C_o is the concentration of Na₂O, f is the fraction of Na₂O that actually participates in the reaction, and E_a is the activation energy (obtained from Arrhenius plots of ln Q versus 1/T). Excellent straight-line fits of Q versus t^{1/2} were obtained with D406 glass at the three temperatures, and at 400 °C with T806 glass. The observed t^{1/2} dependence of Q is very suggestive of a reaction mechanism limited by solid-state diffusion.

Additional observations of the glass-S corrosion (Reaction I) are:

- Reactivity of powdered T806 glass decreases twofold when the glass is prepared at 1200 °C with thorough mixing, in contrast to glass prepared at 1000 °C with only two to three stirrings.
- Reactivity of both T806 and D406 in the form of powders is significantly reduced by the addition of 0.5 wt% organic to the S.
- Reactivity (400 °C) for a fixed mass of glass powder increases by 40% when the mass of S is decreased from 200 to 10 mg.
- Reactivity of 80-μm glass rods is significantly below that measured for glass powders.

C. THERMALLY REGENERATIVE SYSTEM

Thermally regenerative systems convert heat directly into electricity, and their conversion efficiencies are therefore Carnot-cycle limited. The system under investigation uses Na-ion conducting β"-Al₂O₃ to separate two Na reservoirs which are at different temperatures.

Materials for the Sodium Heat Engine (T. Hunt, Ford Motor Company)

The Sodium Heat Engine (SHE) is a direct thermal-to-electrical-energy conversion device that uses sodium beta"-alumina solid electrolyte (BASE) as a Na-conducting membrane. SHE cells have demonstrated output power densities as high as 1.1 W/cm² of electrode area, and they should be capable of high efficiency even in units of relatively small total output power.

The Mo electrodes obtained by sputtering or CVD exhibit the best initial performance, yielding power densities that are extremely close to the theoretical limit. Their maximum output power at operating temperatures of 800 to 900 °C typically degrades with time to values approximately one-third of those observed initially. The objectives of this research are to achieve an understanding of (i) the problem of electrode stability, and (ii) the detailed manner in which this high-power system functions. These investigations show that the superior initial performance of Mo electrodes is due to the presence of sodium molybdate, which forms at the interface between the electrode and electrolyte and within the electrode, when O₂ is present in the Na-Mo system. Sodium molybdate melts at ~680 °C, and provides a molten salt to assist in charge transfer at the interface and Na transport to and through the electrode. The loss of output

power is now understood as being due to the evaporation or decomposition of sodium molybdate.

Previous studies of the stability of β'' - Al_2O_3 were extended to include investigations of the surfaces of the ceramic material in contact with both the Na negative electrode and the positive permeable electrode materials at high temperature. Beta''-alumina samples were heated in Na at temperatures up to 1000 °C, and the surfaces were examined for indications of decomposition products. No evidence of β'' - Al_2O_3 decomposition or degradation was found which would suggest durability of this material in SHE applications.

A variety of electrode materials was tested for performance and durability on a time scale of hundreds of hours. Sputtered TiN electrodes appear to have the potential for long life at temperatures of 800 to 900 °C at power levels approaching 0.5 W/cm². Liquid Sn and Sn-Zr alloy electrodes were tested at several temperatures, and they show excellent performance as well as endurance which appears to be limited only by loss of electrode material due to evaporation. In certain cir-

cumstances where SHE operation at temperatures in the 650 to 700 °C range may be desirable, these liquid metal electrodes may provide important options.

During these studies it was discovered that β'' - Al_2O_3 powder can be flame-sprayed as a porous layer onto the surface of conventionally formed BASE tubes, while retaining the proper BASE crystal structure. Additional experiments demonstrated the feasibility of impregnating the porous, flame-sprayed layers with Mo metal deposited from solution to produce a mixed-conductor electrode material. This material can provide both electronic conduction and a distributed, ionically conducting surface layer. It has also been shown that co-deposition of BASE and Mo metal powders obtained by flame-spraying can provide a mixed conductor coating in a single step. The performance and endurance of such flame-sprayed electrodes appear to depend strongly on the details of their deposition but has not yet reached the levels established for BASE/Mo cermet electrodes produced by more conventional methods.

III. APPLIED SCIENCE RESEARCH

The objectives of this project element are to provide and establish scientific and engineering principles applicable to batteries and electrochemical systems; and to identify, characterize and improve materials and components for use in batteries and electrochemical systems. Projects in this element provide research that supports a wide range of battery systems -- alkaline, flow, molten salt, nonaqueous, and solid-electrolyte. Other projects are directed at research on improving the understanding of electrochemical engineering principles, corrosion of battery components, surface analysis of electrodes, and electrocatalysis.

A. ALKALINE CELLS

Zinc is often used as the negative electrode in alkaline cells, and it is this electrode that typically limits the lifetime of these cells. Efforts are underway to identify cell components that will improve the cycle-life performance of the Zn electrode.

Zinc Electrode Studies

(E. Cairns and F. McLarnon,
Lawrence Berkeley Laboratory)

The purpose of this research is to study the behavior of Zn electrodes used in secondary batteries and to investigate practical means for improving their performance and lifetime. The approach used in this investigation is to study life- and performance-limiting phenomena under realistic cell operating conditions. Systems of current interest include ambient-temperature rechargeable cells with Zn electrodes: Zn/air, Zn/NiOOH, Zn/AgO, Zn/Cl₂, Zn/Br₂, and Zn/Fe(CN)₆⁻³.

Experiments are underway to develop reference micro-electrodes as useful analytical tools, and use them to measure species concentration changes in secondary porous alkaline Zn electrodes. Cadmium, zinc and α -palladium reference micro-electrodes are currently being investigated. The use of Cd electrodes was discontinued due to poor stability. Stable and reproducible Zn electrode potentials were measured at various hydroxide and zincate concentrations; the results shown in Fig. 1 agree with and supplement the work of Dirkse (1) and Hampson, Herdman and Taylor (2).

The addition of Ca(OH)₂ to the Zn electrode was investigated as a practical means of reducing Zn species solubility in strong alkaline electrolytes. The Ca(OH)₂-free electrode showed significant Zn redistribution after 55 to 150 cycles (5-h charge rate, 2.5-h discharge rate). Many areas of the electrode were bare of Zn or showed very little material. The Ca(OH)₂-containing electrodes also showed considerable Zn redistribution, but there were no bare areas and there remained a uniform "background" amount of Zn material over the electrode. KEVEX X-ray analysis showed that this material was a Ca-Zn compound. The 25%-Ca(OH)₂ cells appeared to behave the best of the cells tested. Cells X-rayed at cycles 100 and 150 showed very few differences, implying that the background Zn material is fairly stable. The Zn-electrode overpotential in the 25%-Ca(OH)₂ cell was higher than that of the Ca(OH)₂-free cell, and the current density during charge had to be decreased by 25% for the cell to function properly.

Several pulse-charging modes were evaluated in which the frequency, peak current

density (pcd), and on-time/off-time ratios were varied. A cell pulse-charged at a pcd of 15.7 mA/cm², 30-ms on/90-ms off, retained over two-thirds of its Zn-covered area when cycling was stopped at cycle 125. Comparison of SEM photographs of the discharged Zn electrodes for cells charged with constant current showed the pulse-charged Zn electrode to have a more densely textured surface than the constant-current charged electrode. This effect may be attributed to the larger number of nucleation sites generated during pulse-charging.

A one-dimensional, time-dependent model is being developed to predict the cause and extent of Zn redistribution and passivation as the electrode is cycled. This model will take into account changes in current density, overpotential and species concentration. The equations for the model are complete, and the appropriate computer program is being written.

Transient potential and current step experiments have been carried out to determine exchange current densities for the Zn electrode in electrolytes of various KOH and zincate concentrations. The 99.999% pure Zn disc electrodes were fabricated from 1-mm diameter wires polished with successive abrasives to a final polish with 0.3 μm Al₂O₃. Zinc counter and reference electrodes were used, and the electrolyte solutions were deaerated. Preliminary results for experiments of 200-ms duration show exchange current densities in the 0.1 to 0.25 mA/cm² range.

References

1. T.P. Dirkse, *J. Electrochem. Soc.* **101**, 328 (1954).
2. N.A. Hampson, G.A. Herdman and R. Taylor, *J. Electroanal. Chem.* **25**, 9 (1970).

Publications

1. J.T. Nichols, F.R. McLarnon and E.J. Cairns, "Zinc Electrode Cycle-Life Performance in Alkaline Electrolytes Having Reduced Zinc Species Solubility," *Chem. Eng. Comm.* **97**, 355 (1985).
2. J.H. Flatt, F.R. McLarnon and E.J. Cairns, "Optical and Electrochemical Study of Model Zinc Electrode Pores in Alkaline Electrolyte," LBL-20025 (1985).
3. M.J. Isaacson, E.J. Cairns and F.R. McLarnon, "Activity Coefficients in Concentrated Potassium Hydroxide-Potassium Zincate Electrolytes," Extended Abstracts of the 36th Meeting of the International Society of Electrochemistry, Abstract No. 12080 (1985).
4. R. Jain, F.R. McLarnon and E.J. Cairns, "Evaluation of Calcium Hydroxide Additive in Secondary Zinc Electrodes," Extended Abstracts of the 168th Meeting of the Electrochemical Society (1985) p. 136.

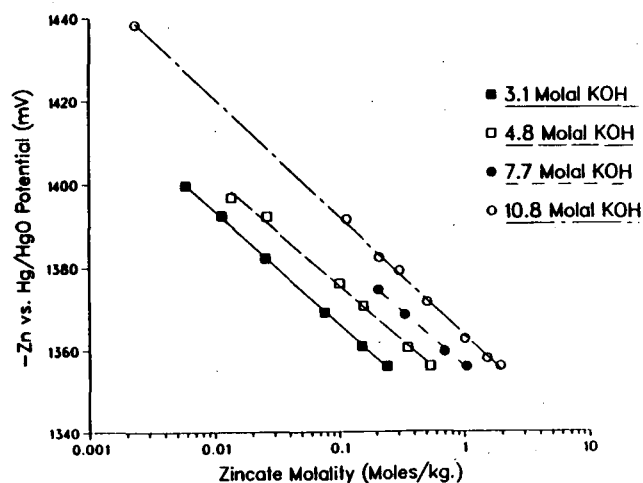


Fig. 1. Variation of Zn electrode rest potential with K₂Zn(OH) molality at constant hydroxyl-ion molality. Potentials are measured versus an Hg/HgO reference electrode in the same solution, and the temperature is 25 °C.

XBL 861-242

A Semiconductor Electrochemistry Approach to the Study of Oxide Films on Nickel and Zinc

(M. Madou, SRI International)

An investigation into the effects of additives to Ni and Zn battery electrodes was made to determine which solid-state properties contribute to the efficient operation of these electrodes.

Cobalt is more effective as an additive when it incorporates in the electrode from solution, rather than when it is added to the active material beforehand. The positive effect of zincate ions on Ni electrodes reported by some authors was not observed; an electrical effect is thus unlikely. An improvement in the structure, as reported by others, is still possible, but the reported capacity improvement could only be confirmed on unrealistically thin battery plates. Fluoride ions have a negative effect on Ni electrodes (i.e., greatly reduces oxygen overpotential), and it offsets the positive effect of Li ions. The positive effect of Co on Ni electrodes is very similar to that of Li. This study suggests that to achieve a beneficial effect, the ions should be (i) small (about 0.6 Å), (ii) preferably non-electroactive, (iii) able to act as acceptors in the NiO lattice, and (iv) they should poison the oxygen evolution reaction on Ni or at least not influence it. PbO appears to be a potentially beneficial additive for the Ni electrode as well; however, it is electroactive. Magnesium has a surface catalytic effect to decrease the oxygen overpotential, which reduces the charge capacity of the Ni electrode.

On Zn electrodes, Fe decreases the hydrogen overpotential, and therefore it should be avoided. Fluoride ions, which have been proposed as an additive to improve cycling of Zn electrodes, reduces the charge/discharge current peaks by over a factor of ten. Zincate ions, which will always be present when Zn is

used in an alkaline electrolyte, reduces the hydrogen overpotential at low concentrations and tends to increase it at high concentrations. Lead oxide has a beneficial effect on the Zn electrode as well and seems like a good additive for Zn/NiOOH cells.

The photocurrent experiments on passive Zn electrodes reveal the presence of an n-type semiconductor (possibly two separate phases). The impedance measurements indicate a higher resistance of the passive film on Zn in a fluoride-containing alkaline solution compared to that in an alkaline solution without the fluoride additive. More details of the impedance spectra of the passive Zn electrode have not yet been explained.

Spectroscopic Studies of Zincate Solutions

(V. Maroni, Argonne National Laboratory)

The purpose of this project was to investigate the coordination chemistry of Zn^{2+} ions in concentrated aqueous KOH. Laser Raman and ^{67}Zn nuclear magnetic resonance (NMR) spectroscopic techniques were used to study solutions having a wide range of Zn^{2+} and OH^- concentrations.

Raman spectra typifying the results obtained are shown in Fig. 2. The upper and lower curves in Figs. 2a and 2b show the effect of rotation of the plane of polarization for the exciting line. The polarized band at 465 cm^{-1} and the depolarized one at $\sim 415\text{ cm}^{-1}$ only appear in Zn^{2+} -containing solutions. The polarized band at $\sim 265\text{ cm}^{-1}$ is not due to the presence of Zn^{2+} since it appears in the spectrum of aqueous KOH, and its intensity relative to the 465 cm^{-1} band is most sensitive to the amount of OH^- in solution, not Zn^{2+} , as the insets in the upper right-hand corner of Figs. 2a and 2b show. Furthermore, the large

polarization of the 465 cm^{-1} band indicates that the Zn^{2+} species have a highly symmetrical structure. When these same experiments were conducted using D_2O instead of H_2O , the 465 cm^{-1} band shifted to a lower frequency by $\sim 13\text{ cm}^{-1}$. This is essentially the predicted shift for the totally symmetric stretching mode of a uniformly complexed $\text{Zn}(\text{OH})_x^{2-x}$ species when the OH^- ligands (group mass = 17 amu) are substituted by OD^- ligands (group mass = 18 amu); thus, the presence in solution of Zn^{2+} /hydroxyl complexes (as opposed to ZnO^{2-} ions) is established.

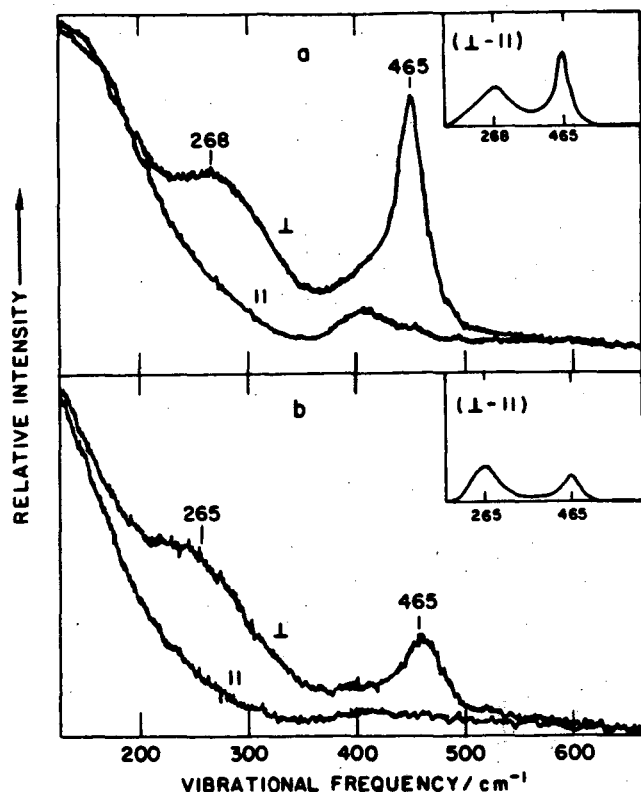


Fig. 2. Parallel (||) and perpendicular (⊥) polarized Raman spectra of ZnO solutions in aqueous KOH. Insets in the upper right-hand corner show the difference spectra (⊥ - ||). Set (a) is for 2.8 M ZnO in 18 M KOH; set (b) is for 0.8 M ZnO in 11 M KOH.

The ^{67}Zn NMR investigations were performed on zincate solutions of varying $\text{OH}^-/\text{Zn}^{2+}$ ratio and a solution of 1.5 M Zn^{2+} (90% enriched in ^{67}Zn) in 1 M HClO_4 as a reference. Typical results are shown in Fig. 3. The resonance for the octahedral $\text{Zn}(\text{H}_2\text{O})_6^{2+}$ complex in 1.5 M $\text{Zn}^{2+}/\text{HClO}_4$ was observed at the expected NMR frequency based on published results (1,2); its half-width was $\sim 30\text{ Hz}$, which is also consistent with prior work. In the 0.6 M $\text{Zn}^{2+}/\text{KOH}$ solution (90% enriched in ^{67}Zn), a shift in resonance signal of +221 ppm relative to 1.5 M $\text{Zn}^{2+}/\text{HClO}_4$ was observed, and the half-width of the resonance signal increased to $\sim 280\text{ Hz}$. The more concentrated Zn^{2+} solution in aqueous KOH ($\sim 20\%$ enriched in ^{67}Zn) showed an even broader resonance signal, but this signal narrowed and converged to the peak frequency in curve b of Fig. 3 as progressive dilutions were made (by addition of water). In previous studies (1,2) of tetrahedral $[\text{ZnX}_4]^{2+4q}$ complexes (where $\text{X} = \text{Cl}^-, \text{Br}^-, \text{CN}^-, \text{and } \text{NH}_3$, and $q =$ the charge on the ligand) in aqueous media, similar chemical shifts (150 to 300 ppm) relative to Zn^{2+} in HClO_4 were observed, and the conclusion was drawn that the chemical shift is due to a transformation from a coordination number of six (in HClO_4) to four (in $[\text{ZnX}_4]^{2+4q}$). The large increase in half-width, however, is unprecedented for 0.5 - 2.0 M Zn^{2+} in any coordination environment and suggests that the Zn^{2+} cations may have a short interaction distance, perhaps due to hydrolytic aggregation into $\text{Zn}(\text{OH})_4^{2-}$ units.

References

1. B.W. Epperlein, H. Kruger, O. Lutz, and A. Schwenk, *Z. Naturforsch.* **29A**, 1553 (1974).
2. G.E. Maciel, L. Simeral, and J.J.H. Ackerman, *J. Phys. Chem.* **81**, 263 (1977).

Publication

1. K.J. Cain, C.A. Melendres and V.A. Maroni, "Raman and ^{67}Zn NMR Studies of the Structure of Zn(II) Solutions in Concentrated Aqueous Potassium Hydroxide," Extended Abstracts of the 168th Meeting of the Electrochemical Society (1985) p. 126.

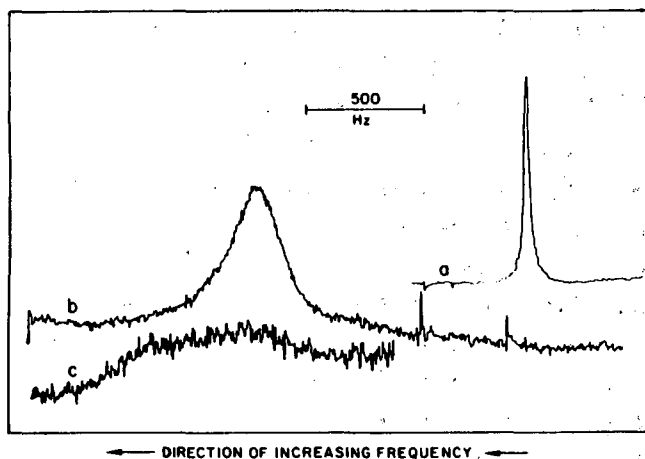


Fig. 3. ^{67}Zn NMR spectra of Zn^{2+} solutions. Curve a is for 1.5 M Zn^{2+} in ~ 1 M HClO_4 , curve b is for 0.6 M ZnO in 16 M KOH , and curve c is for 2.8 M ZnO in 18 M KOH .

Battery Membrane Separators

(D. Bennion, Brigham Young University)

The objective of this project is to develop anionic-exchange membranes which are stable in concentrated hydroxide solution. Anionic-exchange membranes which are made presently do not show long-term stability in caustic solution. It is hypothesized that the use of anionic-exchange membranes in secondary alkaline Zn cells will reduce dendrite formation and shape change at the Zn electrode, thus improving cycling behavior and cell life.

This study has focused on the fabrication and testing of membranes made by incorporating crown ethers or other macrocyclic compounds into a polymer structure. By locating a cation such as K^+ or Na^+ inside the cavity of the crown ether, fixed cationic sites can be created in the membrane. These fixed cationic sites will enhance anion transport (OH^-) and limit cation transport (K^+ , Na^+ or Zn^{2+}) through the membrane. Approximately twenty different macrocyclic compounds have been synthesized, and a number of these have been tested in a variety of polymer structures, such as polypropylene and vinyl chloride-vinylidene chloride.

During this year, work has centered on polyvinyl alcohol membranes. Sheibley and coworkers (1,2) have found that these membranes, normally unstable in aqueous solutions, can be stabilized by cross-linking with dialdehyde compounds. In this study membranes were prepared by adapting their techniques, using crown-ether compounds as the cross-linking agent. One of the chief advantages of this technique is that the crown ethers are chemically bonded to the polymer structure and are expected to be well distributed throughout the membrane. The crown ethers used were either dialdehyde or methylketone derivatives of dibenzo-18-crown-6. Membranes were prepared with 1 to 5% cross-linking.

These membranes were tested for their ionic conductivity, solution uptake, lifetime, and hydroxide transference number in 4.0 M KOH . Ionic conductivities ranged from 0.02 to $0.033 \text{ ohm}^{-1}\text{cm}^{-1}$, well within the range for battery application. The hydroxide transference number, measured in an electro dialysis experiment, was 0.69, essentially the same as in an aqueous solution without the membrane. The solution uptake (weight of solution absorbed/dry weight of the membrane) was two to six, two orders of magnitude greater than for a Nafion membrane. It was thought

that by increasing the macrocycle content that the swelling could be reduced. A membrane which contained 50 wt% of the dialdehyde crown ether showed a solution uptake of 1.02. However, the transference number of the hydroxide in this membrane was only 0.71. It is thought that by further reducing the swelling of the membrane the OH⁻ transference number can be improved. The membranes when soaked in strong caustic solution retained their integrity for periods of one to three months. Further improvements can probably be made in the lifetime by optimizing the amount of cross-linking in the membrane. These polyvinyl alcohol membranes demonstrate promise as anionic-exchange membranes.

Work also proceeded in developing two-dimensional computer codes modeling a Zn-NiOOH cell.

References

1. D.W. Sheibley, M.A. Manzo, and O.D. Gonzalez-Sanaori, *J. Electrochem. Soc.* **130**, 2255 (1983).
2. L.C. Hsu and D.W. Sheibley, *J. Electrochem. Soc.* **129**, 2251 (1982).

Hybrid Separators for Alkaline Zinc Cells (R. Yeo, Pinnacle Research Institute)

The objective of this project is to develop hybrid separators to improve the cycle life of alkaline Zn cells. The hybrid separators were synthesized and fabricated by Dr. J. Lee (RAI Research Corporation). The major emphasis this year has been to determine the transport properties of the hybrid separators.

The electrolyte uptake of the hybrid separators was found to be about 60 wt%.

The higher the percent graft of the separator, the higher the water uptake and the lower the KOH uptake that are observed. The high electrolyte uptake suggests that hybrid separators can provide low cell internal resistance and high cell capacity. In concentrated KOH solutions, t_{-} is 0.66 for microporous separators and 0.132 to 0.64 for cation-exchange separators, whereas t_w is 0.76 for microporous separators and ~1.2 for cation-exchange separators. The cation transport number increases with decreasing electrolyte concentration due to the Donnan exclusion effect. The water transport number increases with decreasing electrolyte concentration because of the greater degree of hydration of the cation.

The experimental results strongly suggest that the hybrid separators exhibit excellent selectivity against zincate ions, while the hydroxide ion and water transport through the hybrid separators are not altered by the presence of ion-exchange groups.

A mathematical model that is based on the separator transport properties has been successfully formulated to analyze the change of the electrolyte concentration and volume during cell cycling. The measured active-material distribution over the Zn electrode, fluid flow rates across the separator, and the electrolyte concentration change during cell cycling are in close agreement with predicted values. The predicted cycle lives based on various separator properties and cell operating conditions are in accord with experimental observations. The results of this modeling study could provide some direction for the future development of high-performance alkaline Zn cells. It has been clearly shown that cell separators play an important role in the cycle life of these cells.

Publications

1. R.S. Yeo and J. Lee, "Novel Hybrid Separators for Alkaline Zinc Batteries," in *Advances in Battery Materials and Processes*, J. McBreen, R.S. Yeo, D-T. Chin and A.C.C. Tseung, eds., The Electrochemical Society Inc., Pennington, NJ (1984) p. 206.
2. R.S. Yeo and D.D. Ellenberger, "Theoretical Analysis of Failure Mechanism of Zinc Electrode," Extended Abstracts of the 168th Meeting of the Electrochemical Society (1985) p. 138.

Stable Ionic Polymers for Electrochemical Applications

(C. Arnold and R. Assink,
Sandia National Laboratories)

The objective of this project is to develop an inexpensive, chemically stable membrane for the Zn/ferricyanide battery. The approaches taken are (i) to evaluate custom-made fluorocarbon-based grafted membranes, and (ii) to synthesize and evaluate sulfonated polysulfones.

Membranes made from aromatic polysulfones were found to be stable and efficient when evaluated in the Zn/ferricyanide battery, which utilizes a strong oxidizing electrolyte (alkaline ferricyanide). Even higher stabilities should be possible with other aromatic polymers. The above-mentioned sulfonated polysulfone was derived from Udel P-1700, a commercial polysulfone which contains both aliphatic and aromatic structures. The aliphatic portion of these polymers would be susceptible to oxidative attack under conditions more severe than those encountered in the Zn/ferricyanide battery. One of the objectives of this project was to synthesize aromatic ionomers which do not have aliphatic groups. Sulfonated polyphenylene is an example of such a polymer, and it should be an inexpensive

material since it can be synthesized in two steps from benzene and a sulfonating agent.

In the first attempt to prepare sulfonated polyphenylene, anhydrous FeCl_3 was used as the oxidative coupling agent and sulfuric acid was used as the sulfonating agent. The polyphenylene made using FeCl_3 as the coupling agent had a high organic chlorine content (~14%), indicating that chlorination as well as polymerization had occurred. Sulfonation of this product at 100 °C with H_2SO_4 gave a product that had an ion-exchange capacity of only 1.27 meq/dg; this means that only one in five phenylene units had been sulfonated. Better-quality polyphenylene was obtained when a mixture of AlCl_3 and CuCl_2 was used as the coupling agent. This polymer contained only 1% organic chlorine and was obtained in high yields (about 80%). Sulfonation with fuming H_2SO_4 gave a sulfonated polyphenylene with an ion-exchange capacity >3. Since sulfonated polyphenylenes are only partially soluble in common solvents, techniques are being developed to blend these materials into films of sulfonated polyphenylenes. It is anticipated that these blended polymers will have high conductivities.

During 1986 an NMR spectrometer will be used to characterize membrane performance and degradation, and a pulsed field-gradient unit and special probe will be employed to measure diffusion constants. Model compounds will be synthesized and used to elucidate the degradation mechanism in aqueous oxidizing media.

B. ZINC/HALOGEN CELLS

Flowing electrolytes are used in zinc/halogen cells to promote the transport of Zn ions across the cell and to remove halogen as the cell is charged. The cell performance is limited by the tendency of the electrodeposited

Zn to assume unwanted shapes, and efforts are aimed at understanding the complex phenomenon that control the Zn electrode morphology.

Surface Morphology of Metals in Electrodeposition

(C. Tobias, Lawrence Berkeley Laboratory)

The objective of this project is to gain understanding of the detailed processes and their interactions involved in the macrocrystallization of metals. Of particular interest is the influence of hydrodynamic flow on electrocrystallization, and the distribution of charge-transfer rates on advancing and receding metal profiles, as determined by the electric and concentration fields in the solution, and by the kinetics of the charge-transfer reaction.

To clarify the effect of simultaneous H_2 evolution on the morphology of Zn electrodeposited from a flowing [$1000 < Re < 4000$] chloride electrolyte with a supporting electrolyte of KCl, current efficiencies were measured by weight and by titration with EDTA. The results may be summarized as follows: (1) The current efficiency is very near 100% for current densities in the range of 25-140 mA/cm². (2) At low current densities the deposit dissolves (corrodes), while H_2 discharge occurs at high current densities. (3) The value at which the current efficiency declines increases with flow rate. (4) The current efficiency is affected by the nature of the substrate used. (5) The current efficiency increases with increasing pH in the range of $0.5 < pH < 5.0$; it also increases with increasing Zn concentration in the range of 65-195 g/l.

The developing morphology of Zn is investigated *in situ* using a traveling-stage videomicroscopy. The visual magnification ranges from 56x to 400x. Surfaces are examined after deposition by scanning electron

microscopy. Large nuclei line up parallel to the direction of flow; this orienting starts upstream and progresses downstream. The protrusions join by a mechanism that involves enhanced growth parallel to the direction of flow. After striations are fully formed, growth occurs over the entire electrode, resulting in well-defined ridges after long deposition times. Hydrogen-bubble evolution does not cause the development of striations.

To further study the coalescence and alignment of protrusions, a microprofiled electrode (MPE) was conceived and designed. The 5 x 10-mm Pt electrode is currently being manufactured in the UC Berkeley Microelectronics Laboratory, using advanced VSLI processing techniques. The MPE has periodically spaced hemispherical Pt surface features, with radii of approximately 2 μ m, on an otherwise optically smooth surface. After such an electrode is imbedded in an epoxy base and placed in a flow cell designed for the *in situ* optical observation and video recording described above, the effect of coalescence of protrusions and melding of striations on the deposition of Zn will be evaluated.

A model is developed for the calculation of advancing microprofiles during electrodeposition in the presence of certain leveling additives. The model is based on the diffusion-adsorption theory of leveling in which the higher rate of inhibitor transport to the protruding regions of a deposit produces a preferential inhibition at these points, which, in turn, causes an attenuation of microroughness.

Publications

1. J.O. Dukovic and C.W. Tobias, "A Model for Current Distribution with Passivating Kinetics," Extended Abstracts of the National Association of Corrosion Engineers, Corrosion Research Symposium, Boston, MA (1985) p. 69. LBL-18819.

2. J.L. Faltemier, T. Tsuda and C.W. Tobias, "Imprints of Hydrodynamic Flow in Zinc Deposited from Acid Electrolytes," Extended Abstracts of the 168th Meeting of the Electrochemical Society (1985) p. 113.
3. L. McVay, C.W. Tobias and R.H. Muller, "Continuous Optical Observation of Developing Morphology of Metal Using a Traveling Video Microscope," LBL-20768 (1985).

Dendritic Zinc Deposition in Flow Batteries

(J. Selman, Illinois Institute of Technology)

The objectives of this project are to investigate the formation and growth rates of dendritic or nodular deposits at Zn electrodes in flowing acidic halide solutions by experimental and analytical methods. Of particular interest are the effect of convection on the growth rate and the influence of solution chemistry (speciation) on the kinetics and mass-transfer characteristics of the deposition process.

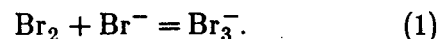
Measurements of the growth rate of dendritic (nodular) deposits from concentrated Zn halide solutions were made using a modified design of the rotating concentric cylinder electrode (RCCE) cell. This cell differed from that used earlier in that the interelectrode distance was only 0.18 to 0.33 cm, with a similar inner electrode diameter (0.65 to 0.78 cm). It was similarly equipped for visual observation and photography of the deposits, but was capable of a better height resolution (approximately 50 μm). It was also equipped with a provision for flushing the gas bubbles from the electrodes by circulating the electrolyte through an external reservoir. The exchange current density of Zn deposition was determined by stationary polarization measurements at the initially smooth

electrode (with accounting of concentration overpotential and ohmic potential drop) and by AC impedance measurements. The value of i_0 for a 1 M ZnCl_2 (+3 M KCl) solution at 25 °C, assuming $\alpha_a = 1.5$ and $\alpha_c = 0.5$, is 1.7 mA/cm^2 .

The growth rate of well-developed protrusion was found to depend on the rotation rate of the electrode to a power of approximately 0.6. Increased convection was found to cause a strong enlargement of the radii of protrusions, with the number density decreasing as electrodeposition proceeds. Higher Zn halide concentrations and higher current densities caused an increase in the growth rate of the protrusions.

The ohmic resistance of the solution was found to be the dominant factor during electrodeposition of Zn from flowing solutions. An explanation of the formation of deposition profiles was given in terms of the amplification of existing microprofiles (roughness, occlusions, striations) by secondary convection patterns in combination with ohmic resistance effects.

The corrosion of Zn by Br_2 dissolved in aqueous ZnBr_2 solution was investigated. Two different aspects were examined. The first one is the solution chemistry of the Br_2/Br^- couple. The second is the kinetics of Zn dissolution in Br_2 -saturated aqueous ZnBr_2 solutions. Limiting-current measurements of Br_2 reduction on a Pt RDE and linear sweep voltammetry of the same reaction on a stationary Pt electrode were applied in order to clarify the role of the complexation reaction:



Results showed that either the complexation rate is very fast, or Br_3^- as well as Br_2 are electroactive species. Under conditions of moderate convection the two cases cannot be distinguished from limiting-current measurements. Reaction (1) is essentially at equi-

brium everywhere in the solution.

Weight-loss measurements of a Zn rotating hemispherical electrode (RHE) were carried out to establish the correlation between mass transfer rate and convection. Diffusivities of Br_2 calculated from these data showed good agreement with the data obtained earlier using a RDE.

The corrosion potential of a Zn RDE was determined as a function of applied current density for various rotation rates. A corrosion mechanism with parallel electrochemical and chemical paths was proposed to explain the data; using this mechanism the simulated potential-current curves showed good agreement with experimental data. From the best fit of these curves, the value of the exchange current density of Zn dissolution in 0.35 M ZnBr_2 solution was determined to be 1.5 mA/cm^2 .

Zinc Electrode Morphology in Acid Electrolytes

(J. McBreen, Brookhaven National Laboratory)

The purpose of this research is to elucidate the factors, other than mass transport, affecting the kinetics and the morphology of Zn deposition in ZnCl_2 and ZnBr_2 electrolytes. A further objective is to devise methods to slow the kinetics in ZnBr_2 electrolytes, and thereby inhibit dendritic growth and achieve higher electrode capacity in Zn/Br₂ batteries. The following research areas were investigated in 1985: (i) investigations of new ZnBr_2 -based electrolytes, (ii) EXAFS studies of Zn halide electrolytes, and (iii) investigations of the effect of additives on Zn single crystals.

New Zinc-Bromide-Based Electrolytes: A systematic study was carried out on the effect of AlCl_3 and AlBr_3 in carefully purified

ZnBr_2 electrolytes on Zn deposition on glassy carbon. Addition of stoichiometric amounts of AlCl_3 yielded results similar to those found in pure ZnCl_2 electrolyte. Additions of AlBr_3 increased the Zn nucleation overvoltage and resulted in slower kinetics than those found in ZnCl_2 . The additions yielded a smooth, fine-grained deposit.

EXAFS Studies of Zinc Halide Electrolytes: Extended X-ray Absorption Fine Structures (EXAFS) studies were carried out in several electrolytes (i.e., 0.1 M solutions of ZnSO_4 , ZnCl_2 , ZnBr_2 and ZnI_2 ; 1 M ZnBr_2 with various additions of HBr and KBr; and 3 M ZnBr_2 with additions of 3 M AlBr_3). EXAFS spectra were also obtained for crystalline ZnBr_2 , ZnO, and ZnO dissolved in KOH.

Preliminary analysis of the data for 1.0 M ZnBr_2 indicate that the Zn in the ZnBr_2 complex is coordinated with both Br^- and water. The Zn-O distance is about 1.9 Å and the Zn-Br distance is about 2.3 Å. Additions of HBr (1.0 M - 9.0 M) to 1 M HBr cause considerable changes in the structure of the electrolyte. Additions of 3 M AlBr_3 to 3 M ZnBr_2 also result in considerable changes in the EXAFS spectra. These results are now being analyzed in more detail.

Effect of Additives on Deposition on Zinc Single Crystals: In these studies single crystals were coated with the equivalent of 5 to 150 monolayers of foreign metals by a displacement reaction. The metals included Bi, Pb, Cd and Cu. Zinc deposition studies were carried out on these modified surfaces in purified 3 M ZnCl_2 . The presence of Bi, Pb and Cd on the surface greatly inhibited layer growth and promoted growth via a nucleation process. Bismuth was unique in that its effects could be seen with large thicknesses of the deposit. It slowed the kinetics of the outward growth of the deposit into the electrolyte. Copper, on

the other hand, did not inhibit layer growth and the kinetics of Zn deposition were accelerated. Bismuth is known to be a beneficial additive while Cu is an undesirable impurity.

Publications

1. J. McBreen and E. Gannon, "Bismuth Oxide as an Additive in Pasted Zinc Electrodes," *J. Power Sources* 15, 169 (1985).
2. J. McBreen and E. Gannon, "Kinetics of Zinc Deposition on Zinc Single Crystals," *Extended Abstracts of the 168th Meeting of the Electrochemical Society* (1985) p. 117.

Transport in Aqueous Battery Systems

(D. Miller and J. Rard,
Lawrence Livermore National Laboratory)

The purpose of this research is to obtain experimental data on mutual diffusion coefficients, which are required to model battery systems of interest to DOE. Diffusion and density measurements were completed for $\text{ZnCl}_2\text{-H}_2\text{O}$ and $\text{ZnCl}_2\text{-KCl-H}_2\text{O}$, and isopiestic/activity coefficient measurements were started for $\text{ZnCl}_2\text{-H}_2\text{O}$. Related measurements will be started for $\text{ZnBr}_2\text{-H}_2\text{O}$, and later for $\text{ZnBr}_2\text{-KBr-H}_2\text{O}$.

Isopiestic measurements were performed for $\text{ZnCl}_2\text{-H}_2\text{O}$ in the concentration range 4.6749 to 13.143 mol/kg. They will be extended to lower concentrations during calendar year 1986. When these measurements are complete, activity coefficients will be calculated.

Mutual diffusion coefficient measurements were completed for $\text{ZnCl}_2\text{-KCl-H}_2\text{O}$ this year. Two more compositions were studied, and the results are given below. Together with previous results, a total of 12 compositions were investigated. Densities were also measured for

these solutions.

The diffusion coefficients for 2.5001 mol/dm³ ZnCl_2 - 0.49996 mol/dm³ KCl at 25.00 °C could not be extracted from the experimental data because of convergence problems with the non-linear least-squares calculations. Alternate computational procedures are being considered. The experimental results for 2.4999 mol/dm³ ZnCl_2 - 1.2500 mol/dm³ KCl are $10^5 D_{11} = 1.2426 \pm 0.0863$, $10^5 D_{12} = 0.0219 \pm 0.0033$, $10^5 D_{21} = -0.1440 \pm 0.0394$, and $10^5 D_{22} = 0.9425 \pm 0.0715$ cm²/s. Subscript 1 denotes ZnCl_2 and subscript 2 denotes KCl.

C. MOLTEN-SALT CELLS

Molten-salt cells based on Li alloy negatives and metal disulfide positives can exhibit very high performance and freeze-thaw capabilities. Two organizations are pursuing techniques to stabilize the performance of FeS_2 electrodes in these cells.

Molten-Electrolyte Cell Research

(L. Redey and T. Kaun,
Argonne National Laboratory)

The objectives of this program are to generate the scientific and technical base of information from which major improvements in the performance of molten-electrolyte cells can be derived. These efforts are directed towards the development of a cell that will deliver a specific energy of 200 Wh/kg at a 4-h discharge rate, a specific power of 200 W/kg at 80% depth of discharge (DOD), and a cycle life of 1000 cycles. A Li-Al/ FeS_2 cell, which employs molten LiCl-LiBr-KBr (mp, 310 °C) as the electrolyte and operates at 390 °C to 430 °C, promises to achieve these performance and cycle-life goals (1).

The performance of Fe and Ni sulfides and their mixtures were investigated to determine their potential as positive electrode materials in electrolytes having the compositions (in mol%) of 22 LiF - 31 LiCl - 47 LiBr (Electrolyte A) and 33 LiCl - 30 LiBr - 37 KBr (Electrolyte B). An intermittent galvanostatic cycling technique was used to measure the ohmic resistance, electrochemical impedance and active material utilization. The peak power and power-sustaining capability of the electrodes were determined by a technique that measures area-specific impedance ($iASR_t$) as a function of duration of high-intensity current pulses.

The most favorable values were obtained with the Fe and Ni sulfide mixture (FeS_x-NiS_x where $x \leq 2$) in a 1:1 mole ratio. Tests also showed that the addition of Li_2S to the electrolyte in a quantity that assured saturation at any cycling condition substantially improved both the utilization and power capability. The combination of Li_2S -saturated electrolyte and mixed sulfide active material showed uniformly low $iASR_t$ over the entire range of the charge and discharge cycle. This was not true for the FeS_x and NiS_x electrodes individually. This effect was observed in both electrolytes A and B.

The area-specific impedances ($iASR_{50s}$) of the $(FeNi)S_x$ electrode in electrolytes A and B were measured during sustained 50-s current pulses of 1 A/cm² at 10, 30 and 71% depth of discharge. The $iASR_{50s}$ values indicate that the highest power capability was present at 10% DOD and the lowest was present at 30% DOD in both electrolytes. In spite of the higher resistances, electrolyte B is more favorable than electrolyte A because of the lower temperature and wider compositional range for operation. The ASR_t values indicate acceptable power performance even in the 370 to 380 °C range for this electrolyte.

The following three conclusions were reached from an analysis of the data. First, the ohmic resistance of the electrode bed is relatively low in the full cycling range compared to the electrochemical impedance of the electrode. Consequently, it is the electrochemical process that controls electrode performance. Second, the active-material utilization in Li_2S -saturated electrolyte is very good, >95% of the theoretical, in contrast to the typically <70% utilizations observed for FeS_x or NiS_x electrodes when cycled under the same conditions. Third, electrochemical impedance and utilization are more favorable at higher temperatures; i.e., the $iASR_{15s}$ values decreased from 2.0 to 0.5 ohm-cm² when the temperature was increased from 370 to 470 °C in electrolyte B.

Design calculations indicated that improved specific energy would be achieved if the FeS_2 electrodes were operated only on the upper of the two plateaus in the voltage versus discharge capacity curves. The specific energy density of this upper-plateau FeS_2 electrode was likely to be greater than that of a two-plateau FeS_2 electrode, with an added advantage of a 0.3 V increase in cell voltage (to about 1.65 V vs. Li-Al) at 80% DOD. Upper-plateau operation takes advantage of the high density of the discharge product of the FeS_2 upper-plateau reaction (Li_2FeS_2) by increasing the electrode loading density from 32 vol% FeS_2 (1.5 Ah/cm²) to 50 vol% FeS_2 (2.4 Ah/cm²).

The objective of the research on the Li-alloy electrode was to increase its specific energy. The capacity densities of the Li-Al, Li-Si, and Li-Al-Si electrodes (within acceptable voltage limits) are quite similar: 1.25 ± 0.05 Ah/cm³. Hence, alloys with increased average Li activity were sought, with the constraint of not sacrificing cell voltage at 80% DOD. A Li-Al alloy with 53 at% Li, rather than the

usual 48 at% Li, provided some improvement toward this end.

A survey of molten-salt compositions uncovered an electrolyte, 25 mol% LiCl - 37 mol% LiBr - 38 mol% KBr (mp, 310 °C), having higher Li content and lower melting point than the 58 mol% LiCl - 42 mol% KCl (mp, 352 °C) eutectic electrolyte. This new electrolyte was chosen to permit a lower cell operating temperature. The lower operating temperature would slow the loss of S from the FeS₂ electrode, which had caused an unacceptable rate of capacity decline in earlier cells.

Two sealed prismatic bi-cells, one with twice the capacity of the other, were employed in evaluating the performance of the Li-Al/LiCl-LiBr-KBr/FeS₂ system. The electrodes (8.7-cm high x 6.3-cm wide) were contained behind perforated-sheet current collectors -- Mo for the central FeS₂ electrode and AISI-1008 steel for the two Li-Al electrodes. The electrode area was 100 cm², based on the projected area of the BN-felt separator. The positive electrodes contained FeS₂ with 15 mol% CoS₂ additive and had a theoretical capacity of either 24 or 48 Ah on the upper plateau. The slurry-formed Li-Al electrodes contained 53 at% Li-Al alloy and had theoretical capacities of either 35 or 70 Ah (0.9 Ah/cm³). Cells were assembled with a BN-powder feedthrough seal and were operated in an argon-atmosphere glovebox. Cycle-life testing at an 8-h charge rate (25 or 50 mA/cm²) and 4-h discharge rate (50 or 100 mA/cm²) was controlled between voltage cutoffs of 2.10 and 1.25 V, respectively. A Ni/Ni₂S₃ reference electrode indicated working-electrode potentials during the deep-discharge cycling.

Testing of the upper-plateau FeS₂ cells at 397 °C showed that they had 50% higher specific energy and power than did Li-Al/LiCl-KCl/FeS₂ cells operated on both voltage plateaus at 427 °C. The specific energy at a 50

mA/cm² discharge current density was enhanced as a result of a 50% higher utilization of the capacity and a 10% higher average discharge voltage. The specific energy at higher discharge current densities (100 and 150 mA/cm²) showed even greater improvement with the utilization of theoretical capacity ranging from 85 to 65% (Fig. 4). The second prismatic cell of the upper-plateau type tested the performance of thicker (8 mm) FeS₂ electrodes having double the capacity (48 Ah). The utilization versus current density curve matched that of the 24-Ah cell. The specific power at 80% DOD was also enhanced by approximately 50% for the new cell because the voltage at that point in the discharge was about 0.3 V higher than that of a cell with a two-plateau FeS₂ electrode.

The improved power and energy density of the upper-plateau FeS₂ cell at the reduced operating temperature of 388 to 427 °C are believed to be due to two factors. The first is improved electronic conductivity of the electrode; it is expected that the increased electrode loading density (from 32 to 50 vol%) would double electronic conductivity of the electrode. The second factor is an increased "dynamic range" with the LiCl-LiBr-KBr electrolyte. At 400 °C, the pure liquid region of this electrolyte extends over a Li⁺/K⁺ ratio of 1.25 to 2.6; for LiCl-KCl, the range is only 1.25 to 1.81. The broader liquid region for the LiCl-LiBr-KBr electrolyte would tend to prevent salt crystallization during cell operation.

The capacity utilization versus cycle number for the upper-plateau FeS₂ cell is shown in Fig. 5 (the coulombic efficiency of the cell is 99%+). Capacity has been constant at about 89% of theoretical capacity (at 50 mA/cm²) through more than 300 cycles and 4000 h, and the cell voltage vs. capacity curve has remained unchanged during this time.

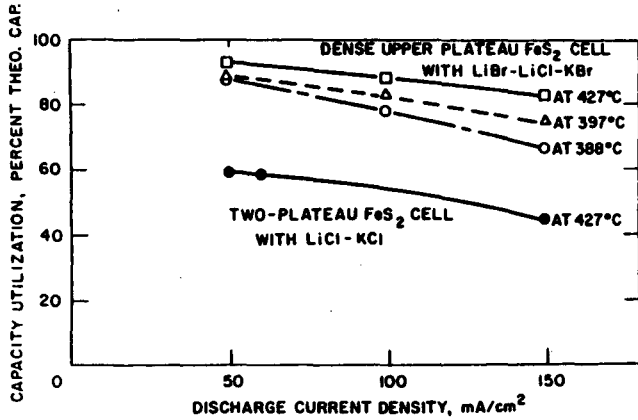


Fig. 4. Utilization versus discharge current density for Li-Al/FeS₂ cells at 388 to 427 °C.

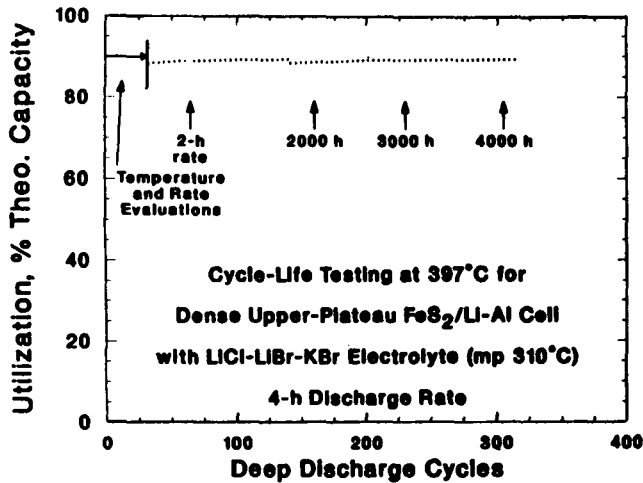


Fig. 5. Capacity utilization versus cycle number for the 24-Ah cell shows stable performance.

Electrode potentials (vs. the Ni/Ni₃S₂ reference electrode) indicate that both electrodes, Li-Al and FeS₂, mutually attain full charge. The discharge capacity is limited by the upper-plateau capacity of the positive electrode.

The dense upper-plateau FeS₂ electrode and the lower melting LiCl-LiBr-KBr electrolyte have eliminated the capacity-loss problem of the previous Li-Al/FeS₂ system. With LiCl-KCl electrolyte, the two-plateau cell would have lost 30% of its capacity in the first 200 cycles. Based on the improved perfor-

mance, a 250 Ah monopolar cell is expected to achieve 175 Wh/kg at a 4-h rate and 200 W/kg at 80% DOD. An advanced bipolar battery design has a projected capability of 200 Wh/kg at a 1-h rate with 600 W/kg at 80% DOD, and a battery specifically designed for continuous high power output is projected to provide greater than 2000 W/kg. These bipolar batteries can be operated nearly isothermally because the unique entropic cooling of the upper-plateau FeS₂ discharge reaction cancels I²R heating.

Reference

1. T.D. Kaun, J. Electrochem. Soc. 132, 3063 (1985).

Publications

1. T.D. Kaun, "Li-Al/FeS₂ Cell with LiCl-LiBr-KBr Electrolyte," J. Electrochem. Soc. 132, 3063 (1985).
2. T.D. Kaun, "Cell Design for Lithium-Alloy/Metal Sulfide Battery," U.S. Patent No. 4,540,642, September 10, 1985.

Investigation of FeS₂ Electrode Capacity Decline in High-Temperature Cells

(G. Barlow, Gould Research Center)

The Li-alloy/FeS₂ couple was considered early in the development of high-temperature, molten-salt battery systems because of its high theoretical specific energy. The failure of this system to live up to its early promise is due primarily to a fairly rapid decay in the capacity of the upper-plateau discharge reaction. Therefore, achieving a stable upper-plateau capacity is critical to further development of the Li/FeS₂ system for electric-vehicle propulsion. The goal of the present research is to develop a better understanding of the mechanisms which lead to upper-plateau capacity decline and attempt to define a solution to the

problem.

The hypothesis, on which the experimental work performed under this contract is based, is that the upper-plateau capacity decline is primarily the result of S loss from the positive electrode due to thermal decomposition of FeS_2 at typical cell operating temperatures of approximately 450°C .

An experimental technique has been established for performing thermal gravimetric analysis on materials which readily form oxides at elevated temperatures and are highly hygroscopic. The rate of decomposition of FeS_2 powder, in a flowing stream of inert gas, has been measured as a function of temperature in the range 350°C to 600°C . The results show that FeS_2 powder is nearly completely decomposed to pyrrhotite, with a loss of elemental S, after a few hours at temperatures above 500°C . Below 400°C , however, extrapolation of the results suggests a lifetime of thousands of hours before FeS_2 is significantly decomposed. The conclusions based on weight loss have been confirmed by X-ray diffraction analysis of the materials before and after exposure to elevated temperatures. The composition of positive-electrode materials from cycled cells has been compared with that of the thermal decomposition products of FeS_2 from the thermogravimetric experiments. The X-ray diffraction patterns of the positive-electrode materials which had lost upper-plateau capacity showed the same diffraction peaks as samples of FeS_2 thermally decomposed in a stream of flowing argon gas. Both pyrite and pyrrhotite were identified as well as constituents of the electrolyte.

In-cell experiments have also been conducted to determine the rate of loss of upper-plateau and total capacity in FeS_2 cells containing different electrolytes at various temperatures. Identical cells containing a LiCl-LiF-LiI electrolyte have been cycled at tem-

peratures of 350 and 450°C . The cell operating at the lower temperature has lost upper-plateau capacity at the rate of 0.1% per cycle, while the high-temperature cell exhibited a decline of 0.23% per cycle. Interestingly, the high-temperature cell shows a lower rate of decline in total (i.e., both plateaux) cell capacity, 0.12% per cycle, as compared to 0.17% per cycle for the lower-temperature cell. These findings are preliminary, because the lower-temperature cell has accumulated 150 cycles over a period of approximately 4000 h, while the cell at 450°C has completed only 64 cycles in about 1700 h. Cells containing a LiCl-LiBr-KBr electrolyte, which has a melting point of 310°C , have only recently been placed on test. Cells with this electrolyte cannot be operated as close to the melting point of the electrolyte as cells containing all-Li-halide electrolytes which typically can be operated at $\sim 20^\circ\text{C}$ above the electrolyte melting point.

D. IMPROVED COMPONENTS FOR ALKALI/SULFUR CELLS

Superior alternatives to the $\beta''\text{-Al}_2\text{O}_3$ ceramic electrolyte and high-temperature sulfur-polysulfide electrode used in Na/S cells and stable Li ion conductors for Li/S cells are under investigation.

Electrochemical Properties of Solid Electrolytes

(L. DeJonghe, Lawrence Berkeley Laboratory)

The purpose of this research is to characterize the electrochemical behavior of $\text{Na } \beta''\text{-Al}_2\text{O}_3$ the Na/S battery, and explore the possibilities of new low-temperature cathode materials. The current emphasis of this program includes the investigation of increased electrolyte performance through transformation toughening, S-side attack on the electro-

lyte, and the role of impurities on cell operation. Work has also been initiated on a novel positive electrode material allowing cell operation below 150 °C and unlimited freeze-thaw cycling.

The effect of a 15-vol% ZrO_2 dispersion on the critical-current density for failure initiation of a β'' - Al_2O_3 solid electrolyte has been examined. Single-phase and composite electrolytes were tested in standard Na/Na test cells and subjected to increasing ionic currents. The onset of degradation in the electrolyte was detected by monitoring acoustic emissions from the cell. Preliminary examination of the electrolyte material showed that the problem of producing a uniform dispersion of ZrO_2 in pure β'' - Al_2O_3 had not been solved. However, the electrolytes were of sufficient quality to draw important conclusions about the potential of transformation toughening for improving electrolyte performance.

A novel low-temperature, high-specific-energy, secondary cell has been developed in this laboratory. In its present form, the new secondary cell is composed of a liquid Na negative, β'' - Al_2O_3 electrolyte, and a novel positive electrode. The cell operates at 120 to 150 °C and can withstand freeze-thaw cycles without harm. The theoretical specific energy of the cell is 360 Wh/kg, and laboratory cells have already been assembled with specific energy of 80 Wh/kg. A practical specific energy of 120 Wh/kg appears readily attainable. These cells can charge and discharge at very high rates, up to 100 to 150 mA/cm², and the technology of cell assembly is simple.

The corrosive nature of the sodium polysulfide electrode toward β'' - Al_2O_3 was evaluated by a series of tests in which samples of electrolyte were immersed in molten polysulfide of various compositions and levels of contamination. It was found that there was significant attack on the electrolyte surface,

particularly in the case of O_2 or H_2O contamination. The polysulfide melt was found to be more corrosive toward the β'' - Al_2O_3 samples as the activity of S increased. Crystalline deposits were observed on the surfaces of the corroded electrolyte; these deposits were identified as $Al_2(SO_4)_3$ and Na_2SO_4 . The crystalline deposits were particularly abundant for the samples contaminated with O_2 or H_2O . Thermodynamic calculations have been made for reaction schemes consistent with the observations.

Publications

1. D. Hitchcock and L.C. DeJonghe, "Solid Electrolyte Degradation with Applied Stress," *J. Mater. Sci. Lett.* **4**, 753 (1985).
2. D. Hitchcock and L.C. DeJonghe, "Time Dependent Degradation in Sodium-Beta"-Alumina Solid Electrolytes," LBL-19223 (1985).
3. D. Hitchcock and L.C. DeJonghe, "Oxygen Depletion and Slow Crack Growth in Sodium-Beta"-Alumina Solid Electrolytes," LBL-19358 (1985).
4. C. Mailhe, S.J. Visco, and L.C. DeJonghe, "Oxygen Activity and Asymmetric Polarization at the Sodium/Sodium-Beta"-Alumina Interface," LBL-19359 (1985).
5. D.A. Olson, "Transformation Toughening of Na-Beta"-Alumina," M.S. Thesis, LBL-19896 (1985).

Improved β'' -Alumina Electrolyte Through Transformation Toughening

(F. Lange, Rockwell International Science Center)

Previous studies have shown that the strength of β'' - Al_2O_3 could be significantly increased with additions of a ZrO_2 -dispersed phase. The relatively large scatter (300 to 400 MPa) in strength of the transformation-toughened material is due to the difficulty of

controlling the distribution of the ZrO_2 phase. Current effort addresses this problem of fabrication reliability. The approach taken was to deagglomerate the two powders, mix them and then consolidate the two-phase mixture by pressure filtration.

Experiments indicate that nonaqueous, colloidal methods can eliminate soft agglomerates and minimize the size of hard agglomerates in both the ZrO_2 and $\beta''-Al_2O_3$ powders. Isopropanol, without an added surfactant, was found to be an effective dispersing medium for both powders. The volume fraction of $\beta''-Al_2O_3$ that could be dispersed without apparent flocculation exceeded 0.50, whereas flocculation was observed for the ZrO_2 powder when its volume fraction exceeded 0.05. Dispersions of either powder could be flocculated with small additions of water (~ 0.5 vol%). Sedimentation is used to minimize the size of the partially sintered hard agglomerates in the ZrO_2 powder and to eliminate the larger particles in the $\beta''-Al_2O_3$ powder. To minimize the water content in the mixed, two-phase slurry, the following procedure was adapted for the two powders. Thirty vol% of $\beta''-Al_2O_3$ was mixed with isopropanol and sedimented to remove particles $\geq 5 \mu m$. The retained dispersion containing particles $\geq 5 \mu m$ was stored for subsequent mixing in the dispersed state. Five vol% ZrO_2 (+3 mol% Y_2O_3) powder was mixed with isopropanol and sedimented to remove all particles (agglomerates) $\geq 2 \mu m$. The retained dispersion was flocculated with small additions of water to concentrate its volume fraction to 0.06. After the volume fractions of solids in each slurry was determined, appropriate weight fractions of each slurry were mixed together by passing the stirred mixture through a chamber containing an ultrasonic horn. Measurements showed that the viscosity of the initial mixture (containing 15 vol% ZrO_2) was relatively shear-

rate independent, whereas the shear-rate dependence of the viscosity increased with the number of passes through the ultrasonic mixing chamber, suggesting that ultrasonic mixing produced flocculation. Observation of sintered microstructures showed that (a) flocculation was desirable to prevent mass segregation due to sedimentation during consolidation, and (b) a minimal amount of ultrasonic agitation was required to break up the ZrO_2 flocs.

To avoid reagglomeration during drying and the formation of crack-like voids during sintering, dry pressing should be avoided. Current slurry consolidation methods (e.g., slip casting, etc.) are limited. For this reason, powder consolidation studies, based on the pressure filtration of slurry states are under investigation. Both Al_2O_3 slurries (which do not require the extended mixing procedure described above) and $\beta''-Al_2O_3/ZrO_2$ slurries are under study. It has been shown that the pressure filtration method can be adapted to iso-press systems and have the potential to produce complex-shaped components.

Studies concerning the kinetics and mechanics of pressure filtration have produced the following results. (i) Consolidation kinetics are parabolic as expected from Darcy's Law. (ii) The density of the consolidated body increases with applied pressure. The effect is most pronounced for flocced slurries, and dispersed slurries produce higher densities at a given applied pressure. Shrinkage due to drying can be avoided when the slurry is consolidated at reasonably low applied pressure (approximately equal to the capillary pressure of drying). (iii) A portion of the stored strain energy is quickly (within a fraction of a second) dissipated upon releasing the applied pressure; the remaining portion is dissipated over a long period (hours). The mechanics of strain energy dissipation are of critical interest since cracks are observed to propagate within the specimen

during the dissipation of strain energy.

Principles of Superionic Conduction

(B. Wuensch, Massachusetts Institute of Technology)

The objective of this program is to provide insight into the principles which control fast-ion conduction in alkali-ion conductors of potential use in high-performance battery systems. Exploratory syntheses and electrical conductivity measurements are performed for either promising types of new structure not yet examined for fast-ion conduction, or new compositions of known conductors which have been modified by crystal-chemical substitutions. Studies during the present year have involved NASICON materials, $\text{Na}_{1+x}\text{Zr}_2\text{Si}_x\text{P}_{3-x}\text{O}_{12}$, and a potential family of new fast-ion conductors, $\text{A}_{2+2x}\text{M}_x^{3+}\text{M}_{1-x}^{4+}\text{Si}_6\text{O}_{15}$, where A^+ is an alkali ion such as Na^+ or K^+ , and M represents an octahedrally-coordinated framework ion such as Y^{3+} , Nd^{3+} , La^{3+} , Ti^{4+} or Zr^{4+} .

Rietveld analysis of the phase transformation and structure at elevated temperature of NASICON solid-solutions with $x = 1.6$ and 2.0 has been completed with neutron powder-diffraction data obtained at 320°C . The results show no evidence for an order-disorder transformation in the Na distribution; the Na(1) site remains fully occupied to this temperature. Only small atomic displacements are involved in the monoclinic to rhombohedral phase transformation, ranging from a few tenths or hundredths of an Angstrom to a maximum of 0.385 \AA for the Na(2) ion in its shallow potential well. Much of these displacements appears due to thermal expansion rather than discontinuous displacements accompanying the phase transition. The rotation of the Si, P tetrahedral units and the radius of the window between neighboring Na sites remain a maximum at $x = 2$, the composition of max-

imum conductivity. The openings between Na sites are considerably larger at 320°C than at room temperature.

To assess the significance of the slight structural changes found in the present Rietveld analyses of neutron powder-diffraction data, a refinement of the silicate end member, $\text{Na}_4\text{ZrO}_2(\text{SiO}_4)_3$, has been completed with room temperature data. A state-of-the-art refinement of this phase (to a residual of 1.9%) with conventional single-crystal X-ray techniques had been reported in the literature. Extraordinarily good agreement was found between the atomic coordinates in the two studies, the average discrepancy being 0.98 standard deviation of the parameters of the precise single-crystal study. The agreement between anisotropic temperature-factor coefficients was, as expected, less precise as Rietveld analysis is known to provide higher standard deviations for variables of this sort. However, the values obtained for all atoms were similar and the nature of the anisotropies of vibration (or lack thereof) were the same. The comparison demonstrates that the structural information presently being obtained through Rietveld analysis of powder samples is quite comparable to that obtained by state-of-the-art single-crystal analyses.

Progress has been made in modeling the framework of the NASICON structure type such that atomic positions and the sizes of "windows" between neighboring alkali sites may be predicted from the ionic radii of the tetrahedral and octahedral framework ions. The objective is to identify a composition with atomic positions and Na^+ concentration identical to NASICON per se (and thus, presumably, comparable conductivity) but without the phosphorus component which leads to degradation in the presence of molten Na. By least-square adjustment of atomic positions to give best fit to sums of known ionic radii, atomic positions have been successfully predicted to

within 0.005 of a cell edge (0.06 Å) on average for the known structure of $\text{Na}_4\text{ZrO}_2(\text{SiO}_4)_3$. The lattice constants a and c were predicted to within 0.63 and 1.71%, respectively.

Glass Electrolytes and Advanced Cell Concepts

(M. Roche and I. Bloom,
Argonne National Laboratory)

The objective of this project is to develop a glass that has low resistivity (100 ohm-cm at 300 °C), will be stable in the hostile Na/S cell environment, and will be easily fabricable at low cost. Soda-rich glasses in the soda-alumina-zirconia-silica system were selected for in-depth study based on early experiments, thermodynamic calculations, and a review of the literature.

Twenty-five glasses were prepared and characterized in terms of their resistivity, activation energy for conduction, and glass transition temperature. The data were analyzed by multiple linear regression using a cubic polynomial in the form appropriate for a mixture of four components, three of which are independent (four linear, six quadratic, and ten cubic terms). A computer search found the best fit using the fewest possible terms with the condition that the linear terms were always included. The resistivity and activation-energy data required five additional terms (two quadratic and three cubic) for squared correlation coefficients of 0.97 and 0.95, respectively. The glass-transition-temperature data were fit with four additional terms (one quadratic and three cubic) for a squared correlation coefficient of 0.98. From the equations, response surfaces and pseudoternary phase diagrams were generated. Such diagrams are useful in making projections for the properties of new glasses in the region where experimental data were collected (up to

46 mol% Na_2O , up to 25 mol% Al_2O_3 , and up to 13 mol% ZrO_2); beyond these regions, the projections should not be expected to be very accurate.

The thermal expansion coefficients of selected glasses have been determined. In each experiment, the expansion of the sample (ca. 20 mm x 4 mm x 4 mm) was measured against a NBS standard Al_2O_3 rod from room temperature to 400 °C using the ASTM standard temperature profile of 1 °C/min. The data indicate that the high-soda glasses have high thermal expansion coefficients (16 to 18.6 x 10⁻⁶/°C).

The glasses were also subjected to chemical-stability tests in high-purity Na, Na_2S_4 , and S at 400 °C for 1000 h. The Dow borate glass and Ceramtec β'' - Al_2O_3 were also included to serve as a basis for comparison. Among the ANL glasses, the high-soda glasses showed the smallest weight change after exposure to the three media. The quaternary glasses that showed acceptable stability include glasses X, IB6, P, R, T, RF5, and RF3. Further testing in Na_2S_3 was performed on selected quaternary glasses. The quaternary glasses that showed acceptable chemical stability included IB51 (P glass made with quartz), RF1, RF2, RF2S, RF4, and T.

Based on these results, an ANL glass electrolyte has been selected for testing in Na/S cells. This electrolyte has a composition (in mol%) of 42 Na_2O , 8 Al_2O_3 , 5 ZrO_2 , and 45 SiO_2 . It has an ionic conductivity (σ) of 7.1 x 10⁻³ ohm⁻¹cm⁻¹ at 300 °C, an activation energy for conduction ($E\sigma$) of 0.53 eV, a glass transition temperature ($T\sigma$) of 534 °C, and a thermal expansion coefficient of 16 x 10⁻⁶/°C. Its chemical stability in the cell environment is comparable to that of Dow glass and β'' - Al_2O_3 . The ANL glass exhibited weight changes of 0.7, -0.5, -0.3 and 0.4 mg/cm² after 1000 h at 400 °C in Na, Na_2S_3 , Na_2S_4 and S, respectively.

Preliminary cell designs and model calculations have been carried out for cells employing tubes of this electrolyte. With a small diameter tube (1.5-mm OD), the cell will contain about 4000 tubes and will yield a specific power of about 2000 W/kg and a specific energy of about 200 Wh/kg. With a larger diameter tube (6-mm OD), the cell will contain about 100 tubes and will yield a somewhat higher specific energy (ca. 300 Wh/kg) at a moderate specific power (ca. 300 W/kg). These modeling results illustrate the versatility of the system design and its excellent combination of energy and power.

Publications

1. P.A. Nelson, I. Bloom, J. Bradley and M.F. Roche, "Sodium-Sulfur Cells with High Conductivity Glass Electrolytes," Proceedings of the 20th IECEC (1985) p. 2.120.
2. I. Bloom, J. Bradley, P.A. Nelson and M.F. Roche, "Chemical Stability of Soda-Alumina-Zirconia-Silica Glasses in Na, Na₂S₄, and S," Extended Abstracts of the 168th Meeting of the Electrochemical Society (1985) p. 87.
3. G.H. Kucera and M.F. Roche, "Glass Electrolyte Composition," U.S. Patent No. 4,544,614 (October 1, 1985).
4. I. Bloom, J. Bradley, G.H. Kucera and M.F. Roche, "High-Conductivity Glass Electrolyte for Sodium/Sulfur Cells," presented at Beta Battery Workshop VI, Snowbird, UT, May 19-23, 1985.

Electrical Conduction and Corrosion Processes in Fast-Ion Conducting Glasses

(H. Tuller, Massachusetts Institute of Technology)

A major objective of this research program has been to develop glasses that exhibit fast-ion conduction (FIC) in the temperature regime of interest (<350 °C) for Li/S batteries,

and that also possess the physical attributes which eliminate the shortcomings of ceramic components, such as current-blocking grain boundaries, anisotropic ion transport (e.g., in β"-Al₂O₃), high-temperature fabrication and relatively large wall thickness. In particular, attention was focused on the transport, electrochemical, and corrosion-resistant properties of alkali-ion-conducting glasses.

Work has continued on electrochemical cells of the type Li-Al/glass/Li-Sn/glass/Li-Al which allow us to examine the transport properties and stability of FIC glasses under a wide range of controlled Li activities as a function of temperature.

The electrochemical cell was used to extend and refine thermodynamic data related to the Li-Sn alloy system. The activity coefficient γ_{Li} of Li in molten Li-Sn alloys was found to follow a quadratic expression of the form

$$\ln \gamma_{\text{Li}} = A + B(1 - X_{\text{Li}})^2$$

up to 30 mol% Li where X_{Li} is the mole fraction Li. Calculation of the partial and integral molar heats of solution indicate strong attractive forces exist between Sn and Li sufficient to induce ordering in the melt.

The examination of alkali ion transport in FIC borate glasses was extended to include K⁺ motion in K₂O · 2B₂O₃ glass. While there are large differences in ion size (r_{Li} = 0.6 Å, r_{Na} = 0.95 Å, and r_K = 1.33 Å), the 0.88 eV activation energy for K⁺ motion was found to be only marginally different from that of Na (0.77 eV) and Li (0.74 eV). This can be rationalized by comparing the respective molar volumes of these glasses, from which it becomes clear that the larger alkali ions induce a dilation in the glass structure to accommodate their larger size. This in turn must compensate at least in part for the larger bottleneck size required for

the larger ions in their motion through the structure.

Research on the influence of other modifiers, whose primary purpose is to improve the stability of glasses against alkali attack, has also been pursued. Electrical conductivity, density and transition temperature measurements have been performed on two families of FIC glasses, a lithium diborate and a lithium metaborate in which 1 to 10 mol% of the Li has been substituted with Ca. The conductivities remain within an order of magnitude of Ca-free glasses, in sharp contrast to the known depressing effect of Ca additions on alkali ion transport in alkali silicate glasses. The fact that the Ca-containing lithium borate glasses remain highly conductive is of technological importance since CaO additions are believed to improve the durability of glasses in contact with Li metal or its alloys.

Measurements of T_g and density on these glasses show that CaO additions markedly influence the dependence of these parameters on the oxygen-to-boron or O/B ratio. Our preliminary interpretation is that Ca additions serve to strengthen and densify the glass structure and thereby result in lower conductivities and higher activation energies.

Publications

1. H.L. Tuller and M.W. Barsoum, "Glass Solid Electrolytes: Past, Present, and Near Future--The Year 2004," *J. Non-Cryst. Solids* 79, 331 (1985).
2. H.L. Tuller and M.W. Barsoum, "Electrolyte Control and Detection of Ionic Species Using Fast-Ion Conducting Glasses," Proceedings of the 3rd International Conference on Solid State Sensors and Actuators, June 11-14, 1985, Philadelphia, PA; IEEE, Piscataway, NJ (1985) p. 256.
3. H.L. Tuller and D.P. Button, "The Role of Structure in Fast Ion Conducting

Glasses," *Transport Structure Relations in Fast Ion and Mixed Conductors*, F.W. Poulson, N. Hessel-Anderson, K. Clausen, S. Skaarup and O.T. Sorenson, eds., Riso National Lab, Roskilde, Denmark (1985) p. 119.

Glass Electrolytes for Lithium/Sulfur Cells

(E. Cairns and F. McLarnon, Lawrence Berkeley Laboratory)

Novel Li/S cells, which employed a fast-Li-ion conducting lithium chloroborate glass as the solid electrolyte, have been built and operated at 400 °C. The composition of glass used for this study, 7.3 mol% Li_2Cl_2 , 25.7 mol% Li_2O and 67.0 mol% B_2O_3 , has an ionic conductivity of $2.9 \times 10^{-3} \text{ ohm}^{-1}\text{cm}^{-1}$ at 400 °C, which is somewhat lower than those of other lithium chloroborate glasses (1).

The current-voltage characteristics of these cells were examined; they were found to be capable of supporting pseudo-steady-state current densities up to 15 mA/cm² for 15 to 20 h. A limiting current was found to exist at ~23 mA/cm². These cells could be charged and discharged with approximately equal polarization in either direction. However, the accumulation of a crystalline reaction layer on the surface of the electrolyte during discharge caused the cells to fail before the completion of a full charge-discharge cycle.

These cells were also used to measure the solubility of Li (as a polysulfide) in S. The solubility limit was found to occur at $0.04_{-0.01}^{+0.03}$ mol% Li at 400 °C, in qualitative agreement with the value reported by Sharma (2).

References

1. D.P. Button, R.P. Tandon, H.L. Tuller and D.R. Uhlmann, *J. Solid State Ionics* 5, 655 (1981).

2. R.A. Sharma, *J. Electrochem. Soc.* **119**, 1439 (1972).

Publication

1. M.L. Smith, F.R. McLarnon and E.J. Cairns, "Investigation of a Vitreous Electrolyte for Use in Lithium/Sulfur Cells," M.S. Thesis, LBL-20737 (1985).

New Battery Materials

(R. Huggins, Stanford University)

The objective of this program is to develop materials for electrolyte or electrode components for high performance Li-based secondary batteries. The emphasis of this work is to understand the important structural, thermodynamic and kinetic properties of these materials which influence their behavior as cell components.

Negative Electrode Materials: Work in this area has continued to be aimed primarily at the investigation of high-Li-activity alloys that undergo displacement reactions and which might be useful as reversible negative electrodes. Following earlier work at higher temperatures, information has been obtained concerning the potentials and capacities of all the constant voltage plateaux at room temperature for binary systems involving Sn, Sb, Bi, Zn, Cd and Pb. Using such information, work has been carried out on the exploration of ternary alloys as part of an investigation of the possibility of using binary alloys as components of mixed-conducting matrix materials in all-solid composite electrodes. In particular, parts of the Li-Cd-Zn, Li-Cd-Sn and Li-Cd-Pb systems have been investigated in some detail, owing to the attractive long, low-potential plateaux found in the Li-Cd system.

Positive Electrode Materials: Several phases in the Li-V-O system have been investigated that have rather high potentials and rapid chemical diffusion rates at room tem-

peratures. In particular, the gamma phase, with nominal composition LiV_2O_5 , has been investigated extensively. Approximately 0.5 Li atoms per mole can be de-intercalated from this structure at potentials of about 3.5 V versus pure Li at room temperature. Also, about 1.0 Li per mole may be added; in this case, two closely spaced plateaux are observed at about 2.45 V versus Li.

Much progress has been made in the investigation of the several phases in the Li-Mo-O ternary bronze system with Mo in initial oxidation state IV. It has been found that there is a large disparity between data obtained under equilibrium and dynamic conditions. Such behavior appears to be due to competition between insertion and displacement reactions in certain composition ranges. It has been shown that the observed behavior on Li insertion may be linked to the known structural properties of this group of compounds.

Work has been performed to investigate the properties of a family of inorganic polymeric materials based upon the parallel chains of edge-sharing tetrahedra found in SiS_2 . Solid solutions of Li_2S in such materials have been found to have large values of Li ionic conductivity. Further work has involved the dissolution of reducible species in SiS_2 ; in particular FeS , FeS_2 , CuS and CuS_2 , together with an examination of what happens when additional highly mobile Li is added. Due to the instability of these materials with respect to Li and the well-known propylene carbonate/ LiClO_4 electrolyte, cells have been constructed which employ a Li-conducting polymeric solid electrolyte and a Li-Pb negative electrode.

Lithium-Conducting Solid Electrolytes:

Three areas of research have been followed. The first concerns the use of a new continuous atmospheric pressure, CVD method for the production of large areas of thin films of Li-

conducting solid electrolytes. In addition to the construction of the apparatus required, preliminary work has been carried out on the deposition of Li-Zr-O phases.

Another area of investigation is the solid-state conductivity of several materials, some of which have attractive stability ranges for use with alkali metal systems, together with attractive values of ionic conductivity at room temperature. For instance, LiAlEt_4 has a room temperature conductivity of about $2 \times 10^{-4} \text{ ohm}^{-1}\text{cm}^{-1}$.

Work has been carried out to evaluate the use of various $\text{Li}_2\text{S}/\text{SiS}_2$ glasses as solid electrolytes. This has necessitated the preliminary evaluation of several ternary phase diagrams, e.g., Li-Si-S, Li-O-S and Si-O-S, both by calculations based on thermodynamic data and electrochemical pulse experiments. These materials have ionic conductivities of the same order as those of the best known inorganic polymeric solid electrolytes.

Publications

1. R.A. Huggins, "Phenomenology of Ionic Transport in Solid-State Battery Materials" *Solid State Batteries*, C.A.C. Sequiera and A. Hooper, eds., NATO ASI Series, Martinus Nijhoff, Dordrecht, Netherlands (1985) p. 5.
2. R.A. Huggins, "Ionically Conducting Inorganic Crystalline Materials," *Solid State Batteries*, C.A.C. Sequiera and A. Hooper, eds., NATO ASI Series, Martinus Nijhoff, Dordrecht, Netherlands (1985) p. 35.

Transport Properties of Sodium/Polysulfide Melts

(J. Newman, Lawrence Berkeley Laboratory)

Mass transport plays an important role in the operation of the positive electrode in a

Na/S cell. Diffusion of reactants and products to and from the electrode surface is especially important. The rate of diffusion in Na_2S_x melts is the focus of this research. The method of restricted diffusion was used to determine differential diffusion coefficients of Na ions as a function of melt composition and temperature. This method is inherently accurate, and each measured coefficient corresponds to a single, unique composition. The theory of restricted diffusion has been developed for both dilute and concentrated solutions.

Diffusion coefficients were measured as a function of melt composition (Na_2S_3 to Na_2S_5) and temperature (300 to 350 °C). The results are in good agreement with predictions based on the microscopic model and fall in the middle of the large range of results of other investigators (2×10^{-7} to $2 \times 10^{-5} \text{ cm}^2/\text{s}$). The following expression summarizes the experimental data:

$$D = 0.0153 \exp(-5.89 \times 10^3/T) \exp(5.30x_e) \text{ cm}^2/\text{s}.$$

This correlation agrees with all but one data point within 6.7%; the largest variation is 17.5%.

Values of the diffusion coefficients based on a thermodynamic driving force, and of the binary interaction coefficients, are calculated from the experimental diffusion coefficients.

Publication

1. S.D. Thompson, "Mass Transport in Sodium Polysulfide Melts," M.S. Thesis, LBL-20762 (1985).

Experimental and Modeling Studies of the Sodium/Sulfur Cell

(E. Cairns and F. McLarnon,
Lawrence Berkeley Laboratory)

A set of equations has been developed to describe the behavior of the S electrode in Na/S cells. The mathematical description takes into account the effects of diffusion, convection and migration on the behavior of the electrode, unlike that of previous work (1,2). An attempt will be made to measure ionic potentials throughout the cathode, in order to confirm the results of modeling. An additional experiment to measure the capillary pressure of S and Na_2S_x in graphite felt has been designed in order to obtain data necessary for predicting convective and wicking effects.

Experimental measurements on the dynamic-polarization and static-corrosion behavior of materials in sulfur/polysulfide melts were completed, and the results were published.

References

1. J. Jacquelin and J.P. Pompon, *Power Sources 7*, J. Thompson, ed., Academic Press, London (1979) p. 713.
2. M.W. Breiter and B. Dunn, *J. Appl. Electrochem.* 9, 291 (1979).

Publications

1. J.C. Dobson, F.R. McLarnon and E.J. Cairns, "Behavior of Metals in Sulfur/Polysulfide Melts," LBL-19518 (1985).
2. J.C. Dobson, F.R. McLarnon and E.J. Cairns, "Voltammetry of Sodium Polysulfides at Metal Electrodes," Extended Abstracts of the 168th Meeting of the Electrochemical Society (1985) p. 708.

3. J.C. Dobson, F.R. McLarnon and E.J. Cairns, "Corrosion in Sulfur/Polysulfide Melts," Extended Abstracts of the 168th Meeting of the Electrochemical Society (1985) p. 86.
4. J.C. Dobson, E.J. Cairns and F.R. McLarnon, "Voltammetry of Lithium Polysulfides at Metal Electrodes," LBL-20248 (1985).
5. J.C. Dobson, E.J. Cairns and F.R. McLarnon, "Voltammetry of Sodium Polysulfides at Metal Electrodes," LBL-20249 (1985).

E. CORROSION PROCESSES IN HIGH-TEMPERATURE, HIGH-SULFUR-ACTIVITY MOLTEN SALTS

The aim of these projects is to develop low-cost containers and current-collector materials for use in alkali-sulfur and other molten-salt cells.

Polysulfide Containment Materials

(J. Battles and A. Brown,
Argonne National Laboratory)

The objective of this project is to develop materials for containment and current collection in cells (e.g., Na/S and Li/FeS₂) that have high S activity and high electrical potential at the positive electrode. During the past year, the corrosion behavior of commercial E-Brite (Fe-26Cr-1Mo) alloys that were modified by the addition of various secondary alloying elements, as well as binary Al-Mg alloys were examined. Tests of these alloys were done in S and Na_2S_3 at 350 °C for up to 2500 h.

To test the effects of secondary alloying elements, two series of experimental Fe-Cr alloys with an E-Brite-26-1 base were prepared and corrosion tested (Table 1). The corrosion penetrations measured for these alloys are compared in Fig. 6. In S, most of these alloys

showed corrosion rates lower than that of pure Cr; the best corrosion resistance was found with the Al-containing E-Brite alloy, which has a corrosion penetration after 2500 h of about one order of magnitude smaller than that of pure Cr. In Na_2S_3 , all of the alloys had corrosion rates higher than that of pure Cr; the worst corrosion resistance was exhibited by the Al-containing E-Brite alloy, which had a corrosion penetration over one order of magnitude larger than that of the pure Cr. To reduce corrosion, the best overall additives are Mo and Y. The corrosion rates for Al-Mg alloys with 1 to 9.6 wt% Mg were determined. In S at 350 °C, all these alloys showed very low corrosion rates. Initially, all the alloys tested in Na_2S_3 had higher corrosion rates than that of pure Al. As testing continued, however, the corrosion rates all became lower than the rate for pure Al, although the alloy containing 9.6 wt% Mg was the only one in which the corrosion rate was effectively reduced to zero after about 100 h.

Electrochemical polarization techniques were utilized to determine the passivation characteristics of the corrosion scales formed on Al and Al-Mg at 350 °C. The experiments involved applying a slow linear potential scan (0.5 mV/s) and recording the current-time

polarization curve. The starting melt composition was Na_2S_3 and the materials examined were Al, Mg, Al-5Mg, Al-9.6Mg, Al-4Mg-1Li, Al-4Mg plus 15 vol% SiC, and electroplated Cr. Over the potential range of +0.5 to -1.2 V versus Mo/ Na_2S_5 , both Al and Mg were passive ($<1 \text{ mA/cm}^2$). However, the two electrodes became active (i.e., polysulfide oxidation or reduction) below about -1.0 V for Al or above +0.1 V for Mg; the activity of the Mg electrode was dependent on its cycling history. The polarization curves of the other materials are shown in Fig. 7. The data clearly show that the film formed on the Al-Mg alloys is far less resistive than the film formed on Al and that increasing the Mg concentration is beneficial to obtaining a less-resistive film.

The polarization curve in Fig. 7 shows that the corrosion scale on Cr is non-passivating. Also, the polarization resistance of the Al-9.6Mg alloy is much larger than would be acceptable for use as a current collector in an Na/S cell. However, the addition of 1 wt% Li or 15 vol% SiC to the Al-4Mg alloy produces a less-resistive film. Preliminary calculations indicate that the total polarization resistance of the Al-4Mg plus 15 vol% SiC alloy is only about a factor of two larger than that of Cr.

Table 1. Composition of the Two Series of Modified E-Brite Alloys

Series 1		Series 2	
Designation	Composition	Designation	Composition
EB-Al	Fe-26Cr-3Al	EB-5Y	Fe-26Cr-5Y-1Mo
EB-Mo	Fe-26Cr-3Mo	EB-Al-Mo	Fe-26Cr-2Mo-1.5Al
EB-Ti	Fe-26Cr-3Ti	EB-Al-Y	Fe-26Cr-3Y-1.5Al
EB-2.5Y	Fe-26Cr-2.5Y	Eb-Zr	Fe-26Cr-3Zr

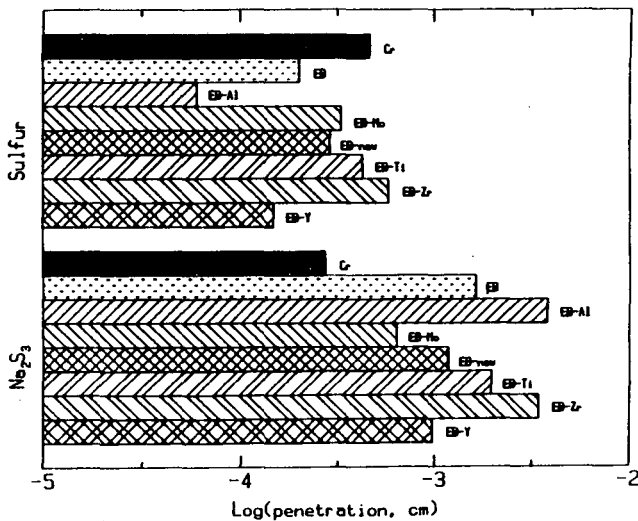


Fig. 6. Comparison of the corrosion penetration of Cr, E-Brite-26-1, and modified E-Brite alloys in S and Na₂S₃ at 350 °C. Test duration was 2500 h.

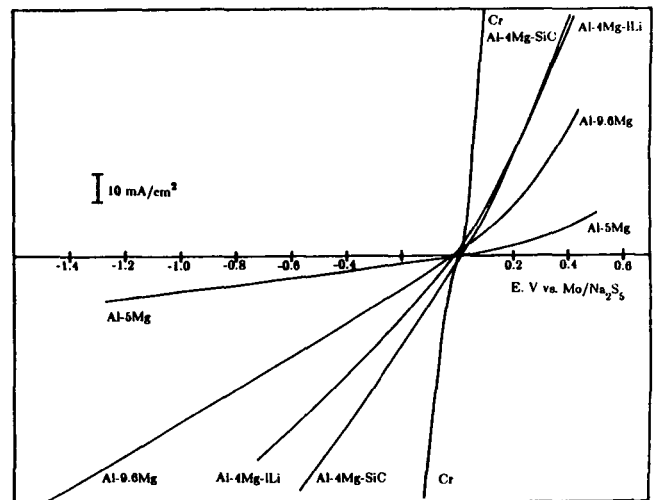


Fig. 7. Polarization curves for various Al-Mg alloys and Cr recorded in Na₂S₅ at 350 °C. Scan rate = 0.5 mV/s.

Corrosion-Resistant Coatings for High-Temperature, High-Sulfur-Activity Applications

(J. Selman, Illinois Institute of Technology)

The objective of this project is to explore molten-salt electrochemical deposition (ECD) and chemical vapor deposition (CVD) as methods to prepare corrosion-resistant coatings of Mo and Mo₂C on low-carbon steel. The principal application will be in the high-temperature S-rich environments of the positive current collectors or containers for Na/S and Li-alloy/FeS₂ cells. The corrosion of solid Mo as well as thin Mo-based coatings on Ni/steel substrates in polysulfide melts is also being investigated.

For the ECD of Mo-based coatings a 3-electrode cell was used for better control of electrolysis parameters and the possibility of obtaining a variety of data about the electrode processes. The anode (Mo rod) and cathode (AISI 1018/Ni interlayer or Ni foil) are arranged as a coaxial set of electrodes to ensure a well-defined geometry with up to three cathode substrates immersed simultaneously in the melt. The typical bath compositions and electrodeposition parameters are presented in Table 2. The SEM micrographs of both Mo and Mo₂C showed a very good polymicrocrystalline growth and a coherent coverage of the substrate surface (Fig. 8). An electrochemical corrosion cell was constructed to permit easy insertion and removal of working and reference electrodes without breaking the inert dry atmosphere. Both anodic and

cathodic current-potential curves are shown for Mo in Na₂S₃ at 300 °C in Fig. 9.

For the CVD of Mo coatings, samples were prepared using the reduction of MoCl₅ with H₂. The factors which most affect the adherence are shown in Table 3. The best experimental results were obtained with rf heating of the samples. Prior to the initiation of vapor deposition, the specimen was heated in a H₂ atmosphere for 20 minutes to ensure a clean surface. After Mo deposition, coated specimens were heat-treated under Ar at 500 °C to outgas adsorbed H₂, which reduces the ductility of the Mo coating. The coatings of Mo were not very uniform; three distinct areas were found. The tip or leading edge of the coupon had a thick deposit and contained some cracks in the coating. The area in the middle of the coupon was smooth, with the Mo layer having good adherence and exhibiting no cracks. The trailing edge of the coupon was only partially covered with Mo. The smooth areas of the leading edge were found to be 100% Mo (determined by EDAX) while the cracks were 81% Mo with the balance Ni. The intermediate areas were all 100% Mo. Analysis of the trailing edge showed Fe, indicating that the Ni interlayer had been destroyed and Mo did not adhere. This was unexpected since Ni is not susceptible to attack by HCl vapors under these conditions, whereas Fe is. Short-duration static corrosion tests conducted in a polysulfide melt indicated that low-carbon steels can be protected from corrosion by CVD of a Mo layer if the layer is dense and defect-free.

Table 2. Experimental conditions for Mo and Mo₂C

Electrolyte Composition	Mo Deposition	Mo ₂ C Deposition
FLINAK	95.7	85.0
K ₂ MoO ₄	4.3	6.5
Na ₂ CO ₃	-	8.5
Temperature, °C	780	850
Current density, A/cm ²	0.076	0.063
Current efficiency, %	22	46
Thickness, μm	6	36

Table 3. Factors affecting the adherence of Mo coatings (CVD).

Temperature	900 ° to 950 °C produces the most-dense coating.
Total system pressure	2.5 to 3.0 kPa is optimum.
Gas phase composition	Slight excess of H ₂ provides complete reduction.
Interlayer	Ni or Cu is necessary.
Mixing of reactants	Complete mixing is required for a uniform coating.

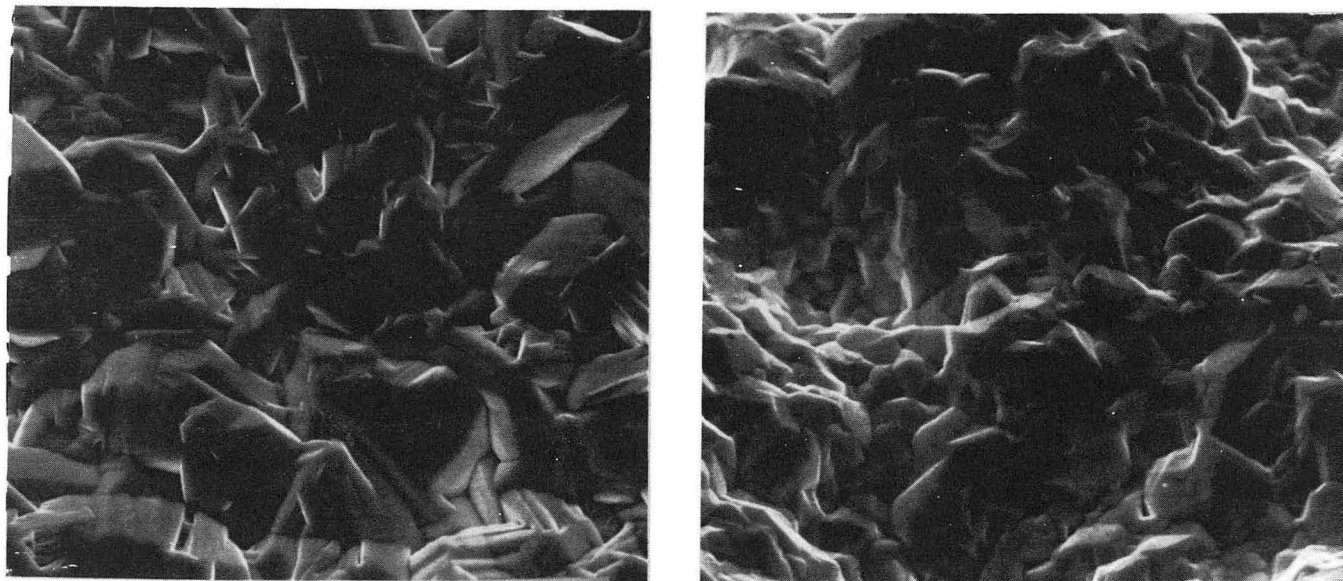


Fig. 8. SEM of Mo coating (left) and Mo₂C coating (right).

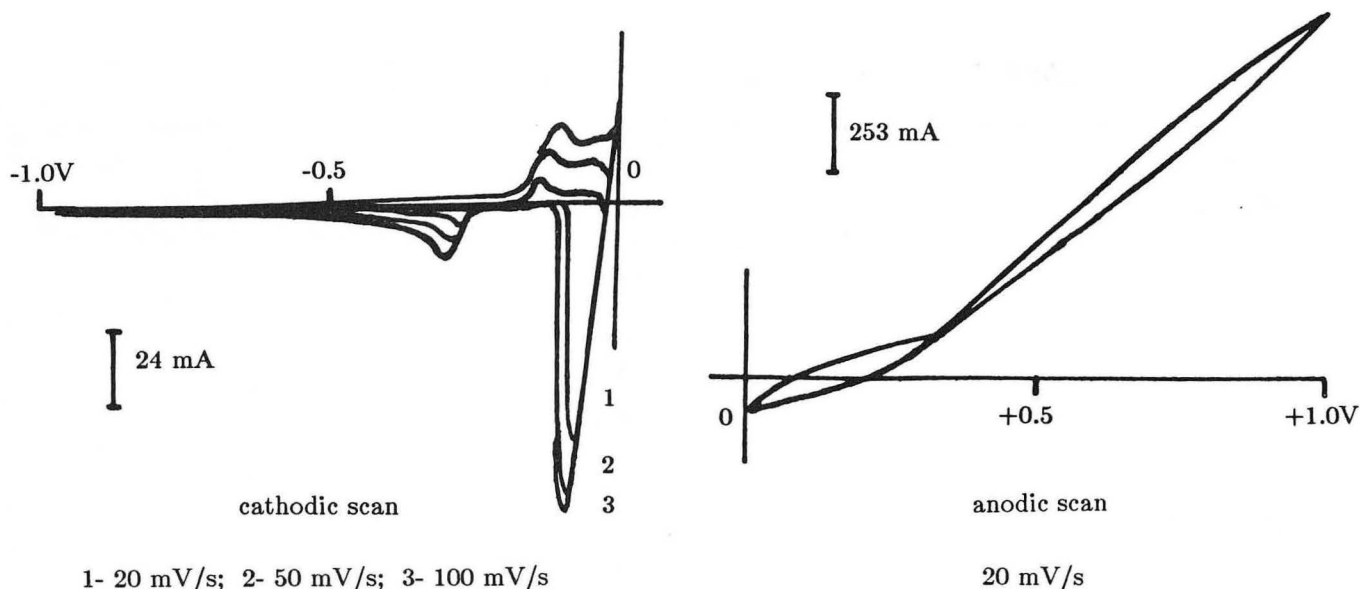


Fig. 9. Cyclic voltammogram of Mo in Na_2S_3 at 300°C .

Microcrystalline (Amorphous) Metal/Alloy Coatings Resistant to Molten Sulfur-Polysulfide

(R. Varma, Argonne National Laboratory)

The objective of this study was to investigate the technical feasibility of depositing thin-layer coatings of microcrystalline (amorphous) Cr coatings on metallic substrates for corrosion protection in molten $\text{Na}_2\text{S}_x/\text{S}$. The experimental measurements demonstrate that amorphous Cr can be electrodeposited from aqueous chromic acid-based electrolytes using high current densities (up to 5 A/m^2). However, results from preliminary corrosion tests suggested that amorphous Cr electrodeposited from aqueous solution does not provide any distinct improvement over the corrosion protection provided by polycrystalline Cr or E-Brite alloy. The observed poor corrosion resistance of the electrodeposit in $0.1 \text{ M H}_2\text{SO}_4$ was attributed to hydrogen incorporation in the

film and the presence of stressed regions.

Electrodeposition experiments were also conducted to investigate the technical feasibility of electrodepositing Cr on steel substrate from molten-salt solution containing 58 mol% LiCl-42 mol% KCl eutectic plus CrCl_2 . The electrodeposition from the molten salt was achieved by using a nucleating pulse followed by potentiostatic growth. The CrCl_2 concentration was kept below 2.2 mol/l in order to produce strongly adhering, pore-free, fine-grained and dense coatings. Analyses of a $40\text{-}\mu\text{m}$ thick Cr layer electrodeposited on Type 304 stainless steel indicates strong adherence of the Cr.

Efforts in the coming year will be restricted to the completion of current experiments on the electrodeposition of microcrystalline Cr from LiCl-KCl- CrCl_2 melts at $<450^\circ\text{C}$.

Publications

1. R. Varma, A. McKiernan and M.J. Klugh, "Electrochemical Deposition of Glassy Chromium on Copper," Extended Abstracts of the 167th Meeting of the Electrochemical Society (1985) p. 943.
2. R. Varma, "Glassy Metal/Alloy Coatings: Status," Extended Abstracts of the 167th Meeting of the Electrochemical Society (1985) p. 940.

F. COMPONENTS FOR AMBIENT-TEMPERATURE NONAQUEOUS CELLS

Metal/electrolyte combinations that improve the rechargeability of ambient-temperature nonaqueous cells are under investigation.

Surface Layers on Battery Materials

(R. Muller, Lawrence Berkeley Laboratory)

The purpose of this work is to provide direct experimental information about formation and properties of surface layers on battery-electrode materials and to find new means for controlling properties that enhance cell performance. Present studies are concerned with anodic oxide formation and the behavior of Li in different ambient-temperature nonaqueous battery electrolytes.

Impedance spectroscopy has been employed to characterize surface layers formed on Li in propylene carbonate-LiClO₄ electrolytes. Film properties derived from the measurements depend on the electrical models used to represent the interface. If two sublayers are assumed to exist, with a solid electrolyte in contact with the metal and a polymer electrolyte in contact with the solution, one can

determine the thickness of the two layers from the measurements. Alternatively, for a surface layer consisting of an intimate dispersion of solid electrolyte in a polymer matrix (solid-polymer interphase), the overall thickness can be determined (Fig. 10). For both models, film thicknesses derived from impedance measurements are in good agreement with those previously obtained from ellipsometer measurements.

Lithium nitride layers are being investigated as ionically conducting protective films on Li electrodes in nonaqueous solutions. Nitride formed by the reaction of Li with gaseous N₂ has been found to be microporous, probably as a result of a 28% decrease in the molar volumes during the conversion of Li to Li₃N. Impedance spectroscopy has shown that N-formed nitride layers are not sufficiently protective to be of interest for rechargeable electrodes. New approaches to forming nonporous nitride coatings are being investigated to take better advantage of the favorable inherent properties of the material.

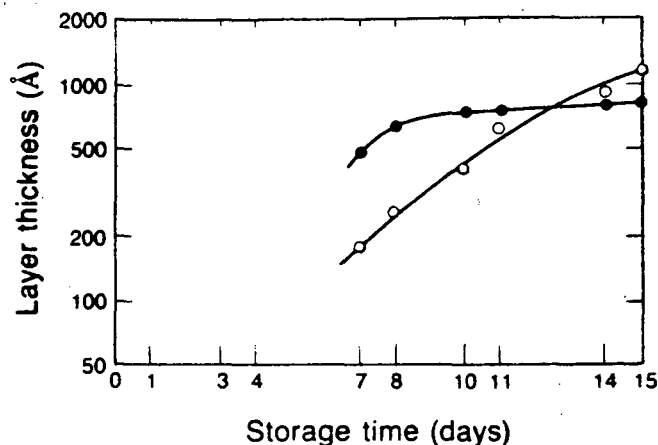


Fig. 10. Film thickness derived from impedance measurements by use of the solid/polymer-interphase model under the assumption of a film conductivity of $5 \times 10^{-8} \text{ ohm}^{-1}\text{cm}^{-1}$ (o) or a dielectric constant of 50 (•). XBL 861-6005

Publications

1. F. Schwager, Y. Geronov and R.H. Muller, "Ellipsometer Studies of Surface Layers on Lithium," *J. Electrochem. Soc.* **132**, 285 (1985).
2. G. Nazri and R.H. Muller, "In-Situ X-Ray Diffraction of Surface Layers on Lithium in Nonaqueous Electrolyte," *J. Electrochem. Soc.* **132**, 1385 (1985).
3. G. Nazri and R.H. Muller, "Composition of Surface Layers on Li Electrodes in PC, LiClO_4 of Very Low Water Content," *J. Electrochem. Soc.* **132**, 2050 (1985).
4. G. Nazri and R.H. Muller, "Effect of Residual Water in Propylene Carbonate on Films Formed on Lithium," *J. Electrochem. Soc.* **132**, 2054 (1985).
5. G. Nazri and R.H. Muller, "Stability of Nonaqueous Electrolytes for Ambient Temperature Rechargeable Lithium Cells," *Chem. Eng. Commun.* **98**, 383 (1985).
6. S.T. Mayer, "Ellipsometric Spectroscopy of Anodically Formed Silver (I) Oxide on Silver," M.S. Thesis, LBL-20503 (1985).
7. J.G. Thevenin and R.H. Muller, "Study of the Impedance Behavior of Surface Layers formed on Lithium Electrodes in a Propylene Carbonate Electrolyte," LBL-20660 (1985).

Spectroscopic Studies of the Passive Film on Alkali and Alkaline-Earth Metals in Nonaqueous Solvents

(D. Scherson, Case Western Reserve University)

The objective of this research is to investigate the nature of the reactions between various non aqueous solvents and sub-, mono- and multi-layers of Li and other alkali and alkaline-earth metals which are vapor deposited on foreign metal substrates under ultrahigh-vacuum conditions. This approach appears particularly attractive because a single monolayer of most of the metals considered

here exhibit bulk-like properties. Most important, however, is the possibility of utilizing highly sensitive and specific probes, such as HREELS, LEED, AES, XPS and UPS, in conjunction with TDS and work-function measurements, which will enable the acquisition of microscopic-level information which may be difficult to obtain by any other means.

During the first year of this project the ultrahigh-vacuum apparatus in which the proposed measurements will be conducted was designed and constructed. The apparatus consists of a conventional pumping station (TNB-X Perkin Elmer Vacuum Products) with BoostiVac filaments and a dual sorption pump (Ultec) capable of reaching pressures in the range between 10^{-10} and 10^{-11} torr. The all-stainless-steel chamber contains low energy electron diffraction optics, LEED, an electron gun (VSW Electronics, Model EG5) for Auger electron spectroscopy AES, a computer-controlled mass spectrometer (Dycor Electronics) and a hemispherical analyzer (VSW Electronics Model HA-100) which can be operated in the constant retarded ratio or constant transmission mode for AES, UPS and XPS. This chamber also houses a custom-made, mechanically driven Kelvin probe, a flood gun for the spectroscopic examination of poorly conducting materials and an XYZ precision manipulator (Perkin Elmer, Model 283-8550) mounted on a differentially pumped rotary feedthrough manipulator.

The initial experiments conducted in this chamber involved exclusively Li and/or propylene carbonate (PC) adsorbed on Ag(111). In each case the metal substrate was cleaned by conventional sputtering-annealing techniques and the quality of the surface was examined with AES and LEED. Lithium that was vapor deposited from commercially available dispensers (SAES, Getters) yielded relatively clean deposits. Carbon monoxide and CO_2 were detected in the mass spectrometer

where Li on Ag(111) surfaces, which had been exposed to PC, was heated. Unfortunately several problems were encountered with the hemispherical analyzer at low electron energies; these problems are being rectified. In the meantime, attention has been focused on K films that are vapor deposited on Ag(100) from the same type of dispenser as that used in the case of Li. Fig. 11 shows the Auger spectrum of clean Ag(100), before (a) and after (b) deposition of about two monolayers of K metal. The apparent absence of spectral features other than those associated with the metal overlayer and the substrate provides a clear

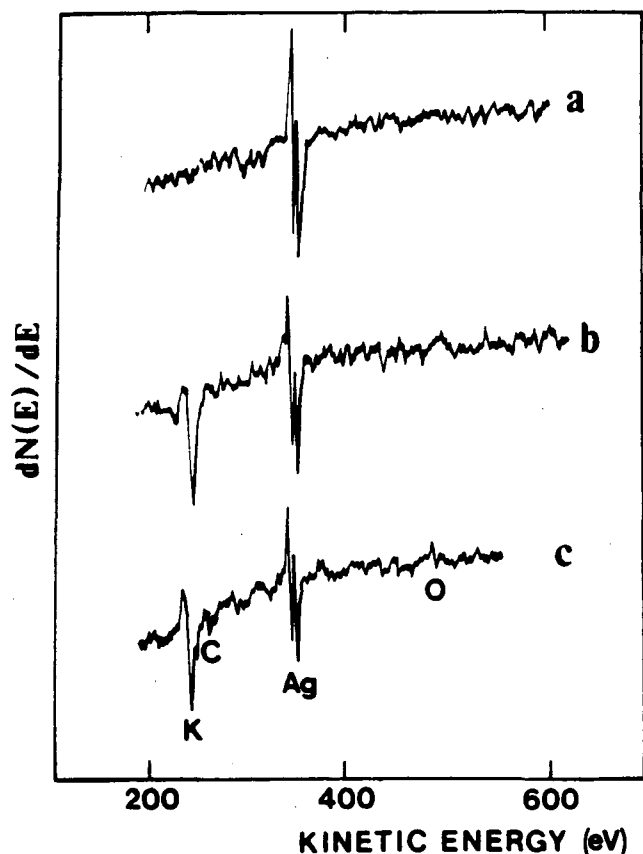


Fig. 11. Auger electron spectra of Ag (100) before (a) and after (b) deposition of about two monolayers of K metal. Curve (c) was obtained after adsorbing propylene carbonate on the K covered Ag surface.

indication that clean K films can indeed be produced with this methodology. Subsequently, the crystal was placed in front of the Kelvin probe and highly purified propylene carbonate was admitted into the chamber, giving rise to a substantial change in the value of the work function. The amount of carbon and oxygen observed in the AES spectrum after adsorption (see curve c in Fig. 11) of PC was very small. It is conceivable that some of the products of the reaction between K and PC may not show any affinity for the surface at room temperature. Additional experiments will be required, however, in order to investigate this possibility.

Polymeric Electrolytes for Ambient-Temperature Lithium Batteries

(G. Farrington, University of Pennsylvania)

The objective of this program is to investigate the chemical and electrochemical characteristics of polymeric electrodes and electrolytes that have been proposed for use in high-specific-energy batteries. Various complexes of alkali-metal salts and poly(ethylene oxide) (PEO) have reasonably high ionic conductivities for alkali cations, and this program has been directed toward exploring whether PEO also forms conductive complexes with various salts of divalent cations and monovalent anions.

PEO complexes with various divalent halides, including $MgCl_2$, $PbBr_2$ and PbI_2 have been synthesized. Films were cast on Teflon plates by slow solvent evaporation. The resulting films were typically 50 to 100- μm thick, flexible, semi-transparent, and easily peeled from the Teflon plate. The following compositions were prepared: $MgCl_2(PEO)_n$ for $n = 4, 8, 12, 16$ and 24 and $PbBr_2(PEO)_n$ for $n = 6, 8, 12, 16, 20$ and 30 . Studies using differential scanning calorimetry (DSC), ther-

mogravimetric analysis (TGA), X-ray, and electron microscopy have shown that many of these complexes are thermally stable to exceptionally high temperatures, generally above $\sim 250^\circ\text{C}$.

Conductivity studies were carried out using complex AC impedance analysis and DC conductivity measurements. Among the PbBr_2 complexes, $\text{PbBr}_2(\text{PEO})_8$ was the best conductor, and $\text{MgCl}_2(\text{PEO})_{16}$ was best of the MgCl_2 complexes. Remarkably, the ionic conductivity of one particular composition, $\text{MgCl}_2(\text{PEO})_{16}$ is about $10^{-5} \text{ ohm}^{-1}\text{cm}^{-1}$ at 80°C , which is as high as that measured for $\text{LiCF}_3\text{SO}_3(\text{PEO})_9$ at the same temperature. The lead halide complexes also are quite conductive. For example, $\text{PbBr}_2(\text{PEO})_8$ has an ionic conductivity of 10^{-6} to $10^{-7} \text{ ohm}^{-1}\text{cm}^{-1}$ at 180°C and about $10^{-5} \text{ ohm}^{-1}\text{cm}^{-1}$ at 250°C .

Preliminary transport number measurements have been carried out only on $\text{PbBr}_2(\text{PEO})_{20}$ at 140°C using complex AC impedance analysis and DC polarization with non-blocking (Pb) and blocking (Pt) electrodes. An initial estimate of the transport number of Pb^{2+} at this temperature is 0.6-0.7.

These investigations clearly demonstrate that PEO easily forms complexes with MgCl_2 and PbBr_2 over a wide range of compositions. The lead halide-PEO complexes are the first polymeric electrolytes with divalent cations that have been reported. This work suggests that many salts of divalent cations and monovalent anions may form conductive complexes with PEO and related polymers.

Metal Couples in Nonaqueous Electrolytes

(C. Tobias, Lawrence Berkeley Laboratory)

The objective of this project is to explore practical alternatives to aqueous or high-

temperature molten-salt systems for the efficient electrochemical reduction and oxidation of reactive metals. Current work includes the exploration of the reduction of Mg, the study of viable reactions for the positive electrode, and investigation of the role of co-solvents in improving stability, solubility and conductivity.

Possibilities for the electroreduction of Mg from its soluble salts are being explored. Attempts to produce adequately dehydrated $\text{Mg}(\text{BF}_4)_2$ have failed so far; a few parts per million of moisture in the electrolyte solutions containing up to 1 Molar salt prevents the formation of detectable amounts of Mg deposits in propylene carbonate (PC). Further efforts are being devoted to finding (or preparing) soluble, dry Mg salts, which exhibit adequate conductivity in PC and allow the reduction of the metal with reasonable current efficiency.

A literature search is being conducted on the nonaqueous electrochemistry of lanthanide metals, with the objective of identifying possibilities for efficient oxidation and reduction of certain of the metals by an ambient-temperature process. The electrochemistry of Mg metal in PC, with or without a co-solvent, will be further investigated to evaluate the promise of this metal in a nonaqueous battery application by studying the reduction of the metal from its salts. Similar exploration will be conducted with the earth alkali series. Finally, reduction of a rare earth in such organic-solvent media will be attempted. The very difficult technology of obtaining these metals in a pure form presents a high incentive for efforts to find an entirely new chemical/electrochemical pathway for their reduction/oxidation.

Publications

1. C.W. Tobias, "Electrochemical Reduction of Potassium from KCl in Propylene

Carbonate Electrolyte with an Aluminum Anode," LBL-9207-rev. (1985).

2. P.H. Johnson, "The Properties of Ethylene Carbonate and Its Use in Electrochemical Applications. A Literature Review." LBL-19886 (1985).

G. CROSS-CUTTING RESEARCH

Cross-cutting research is carried out to address fundamental problems in electrocatalysis and current density distribution, solution of which will lead to improved electrode structures and performance in batteries and fuel cells.

Analysis and Simulation of Electrochemical Systems

(J. Newman, Lawrence Berkeley Laboratory)

The object of this program is to improve the performance of electrochemical cells used in the inter-conversion of electrical energy and chemical energy. Experiments and mathematical models are designed to identify the physical phenomena that govern these systems. The phenomena involved may include hydrodynamics, convective and diffusive mass transfer, ohmic potential drop, charge transfer, and heterogeneous and homogeneous kinetics. A thorough understanding of the interactions among the phenomena governing a given system leads to mathematical models that agree with experiment and predict system behavior. The models are useful in the identification of important parameters, and they aid in the design and scale-up of electrochemical systems.

A mathematical model is being developed to calculate the frequency response of a rotating-disk electrode. Theoretical predictions will be compared to experimental impedance data for zinc/chloride systems. The model has been used to examine the effect of the Schmidt number on the two components of

the faradaic impedance, the mass-transfer (Warburg) impedance, and the charge-transfer resistance. In future work, the effects of surface coverages and double-layer charging will be added to the model.

A mathematical model has been developed to calculate the concentration, potential and current distribution in a thin-gap channel flow cell. The model predictions show the effects of interacting boundary layers on the concentration and current distribution. Preliminary experiments have been carried out to test the model, and the agreement between simulated and experimental results is good. More experimental data will be taken in various Graetz-number regimes to further test the model.

Mathematical models simulating the behavior of LiAl/FeS₂ and Li(Si)/FeS₂ cells employing LiCl-KCl electrolyte have been developed that help identify the factors limiting the cell during operation. The model is also useful to determine the influence of changes in design parameters on the performance of the cells.

A computer model is being developed to predict the response to alternating-current signals of a redox reaction with soluble reactants and products in a flow-through porous electrode. Terms accounting for double-layer capacity have been added to the model. An experimental investigation is under way to accompany the modeling efforts.

Publications

1. D. Bernardi, E. Pawlikowski and J. Newman, "A General Energy Balance for Battery Systems," *J. Electrochem. Soc.* *132*, 5 (1985).
2. V. Edwards and J. Newman, "The Asymmetric Graetz Problem in Channel Flow," *Int. J. Heat Mass Transfer* *28*, 503 (1985).

3. M. Matlosz, "Experimental Methods and Software Tools for the Analysis of Electrochemical Systems," Ph.D. Thesis, LBL-19375 (1985).
4. P. Russell, "Current Oscillations Observed within the Limiting-Current Plateau for Iron in Sulfuric Acid," LBL-19759 (1985).
5. P. Russell, "Anodic Dissolution of Iron in Acidic Sulfate Electrolytes. Part I: Formation and Growth of a Porous Salt Film," LBL-19816 (1985).
6. P. Russell, "Anodic Dissolution of Iron in Acidic Sulfate Electrolytes. Part II: Mathematical Model of Current Oscillations Observed under Potentiostatic Conditions," LBL-19773 (1985).
7. M. Matlosz and J. Newman, "Experimental Investigation of a Porous Carbon Electrode for the Removal of Mercury from Contaminated Brine," LBL-19611 (1985).

Ambient-Temperature Alkaline Sulfur-Polysulfide Electrodes

(E. Cairns and F. McLarnon,
Lawrence Berkeley Laboratory)

Efforts continue to understand the electrochemistry of the aqueous polysulfide redox couple and improve its performance. The studies have concentrated on the fundamental measurement of kinetic and transport parameters by a transient potential step method, steady-state measurements on rotating disk electrodes, modifications of solution chemistry through addition of organic co-solvents, and construction and testing of porous electrodes.

The transient potential-step method was used to obtain data on exchange current density and active species concentration. Cobalt was chosen as the electrocatalyst for most of the studies, but Pt and MoS₂ were also used. Experiments were performed over the temperature range of 25 to 80 °C. At temperatures below ~48 °C it was possible to fit experiment

data to an established analytical expression for a current-time transient for a multi-step redox reaction under diffusion control, but as the temperature increased the fit became poor. Also, it was found that the concentration of the active species determined from the potential step measurements was orders of magnitude lower than the bulk concentrations of the species (S₄²⁻, HS⁻, OH⁻, H₂O) that are included in the proposed overall electrochemical reaction. Instead, the concentration of the radical anion S₂⁻ (supersulfide), which is in equilibrium with S₄²⁻, showed good agreement with the experimentally obtained active species concentrations. This result suggests that supersulfide is the electrochemically active species, and that a homogeneous chemical reaction (equilibrium between S₂⁻ and S₄²⁻) is one of the rate-determining steps. The unexpected presence of an important homogeneous chemical reaction, unaccounted for by the theory, explains the deviation between experiment and theory. The correct form of the material balances and boundary conditions for the electrode reaction with two steps that occur at comparable rates, at least one of which is homogeneous, were formulated. The non-linear partial differential equations were solved numerically using a VAX 8600 computer, and the experimental data showed excellent agreement with the model predictions. The exchange current densities are the order of 1 mA/cm² and are significantly higher than those previously reported.

Steady-state data are needed to estimate the ratio of true to projected area needed for a porous redox electrode, as well as to identify the appropriate hydrodynamic conditions for operation. The rotating disk electrode was chosen for these evaluations, and it was found that at 77 °C a current of about 3 mA/cm² could be sustained on smooth Co electrode at 50 mV polarization and a rotation rate of 1000 rpm. A porous redox electrode should then

require a ratio of true to projected area of about 4, under these hydrodynamic and temperature conditions.

In aprotic, organic solvents containing C=O, S=O and P=O structural units, an increase in equilibrium supersulfide concentration would be expected, along with an improvement in electrode reaction rates. A previous study using N,N-dimethylformamide (DMF) showed that as it was added to an aqueous polysulfide solution, supersulfide was produced at the expense of tetrasulfide (1). Current-voltage curves for a water-DMF and pure aqueous polysulfide solutions were recorded at Co and Pt electrodes. Fig. 12 shows a comparison of the responses. Addition of DMF increases the current density by over 100% at the same temperature and total overpotential.

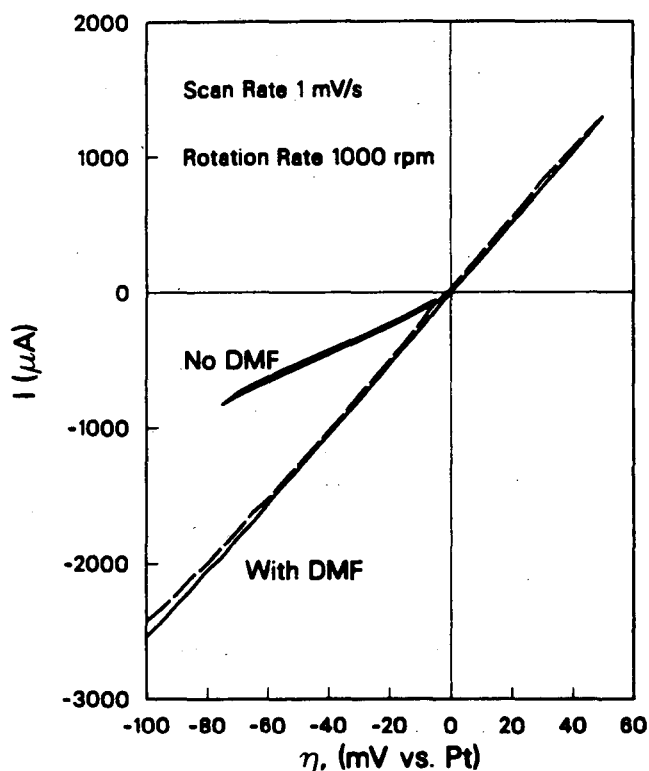


Fig. 12. Addition of DMF to a 1 M Na_2S_4 aqueous solution; response at a 0.2 cm^2 Co electrode, 77°C . XCG 861-7037

Porous flow-through electrodes fabricated from screens could achieve the ratio of true to projected area and hydrodynamic boundary layer thicknesses with only small parasitic power losses. A cell and flow system for evaluating screen electrode performance has been constructed, and screens fabricated from several metals and metal sulfides as well as aqueous solutions containing organic co-solvents will be tested.

Reference

1. W. Giggenbach, *J. Inorg. Nucl. Chem.* **30**, 3189 (1968).

Publications

1. P. Lessner, J. Winnick, F.R. McLarnon and E.J. Cairns, "Porous Counterelectrodes for Polysulfide Photoelectrochemical Cells," Extended Abstracts of the 167th Meeting of the Electrochemical Society (1985) p. 938.
2. P. Lessner, J. Winnick, F.R. McLarnon and E.J. Cairns, "Kinetics of Aqueous Polysulfide Solutions: Part I. Theory of Coupled Electrochemical and Chemical Reactions, Response to a Potential Step," LBL-20989 (1986).
3. P. Lessner, J. Winnick, F.R. McLarnon and E.J. Cairns, "Kinetics of Aqueous Polysulfide Solutions: Part II. Electrochemical Measurement of the Rates of Coupled Electrochemical and Chemical Reactions by the Potential Step Method," LBL-20990 (1986).

Electrode Kinetics and Electrocatalysis

(P. Ross, Lawrence Berkeley Laboratory)

The objective of this project is to develop an atomic level understanding of the processes taking place in complex electrochemical reactions at electrode surfaces. Physically meaningful mechanistic models are essential for the interpretation of electrode behavior and are

useful in directing the research of new classes of materials for electrochemical energy conversion and storage devices.

It is hoped that the anomalous structure-property relations recently observed with Pt single crystal surfaces may be better understood by the study of Au surfaces, since there are characteristic differences in adsorption behavior between Pt and Au which may be exploited to advantage. The basic electrochemistry of Au single-crystal surfaces is also of interest because it is the only known metal surface in which all three low-index surfaces are reconstructed in UHV, i.e., the surface is not a simple termination of the bulk crystal. Preliminary experiments with Au (111) and (100) crystals have produced surprising and interesting results. Unlike Pt, these two Au surfaces produced nearly identical voltammetry in non-adsorbing electrolyte (dilute aqueous fluoride). In the case of (100), the UHV-stable reconstructed surface is not stable in the presence of HF vapor and the surface transforms to (100)-(1x1) before contact with electrolyte. For Au (111), this loss of the UHV-stable structure does not occur until a monolayer of anodic oxide has formed on the surface. Another way in which Au was unlike Pt was the observation that repeated formation/reduction of a monolayer of oxide did *not* change the structure of the surface.

Publications

1. F.T. Wagner and P.N. Ross, "LEED Spot Profile Analysis of Electrochemically Cycled Pt (100) and (111) Surfaces," *Surf. Sci.* **160**, 305 (1985).
2. F.T. Wagner and P.N. Ross, "AES and TDS Studies of Electrochemically Oxidized Pt (100)," *Appl. Surf. Sci.* **24**, 1 (1985).
3. A. D'Agostino and P.N. Ross, "On the Importance of Surface Structure in Electrochemistry: The Well-Defined Au (111)

Single Crystal Electrode Surface," *J. Electroanal. Chem.* **189**, 371 (1985).

Engineering Analysis of Gas Evolution

(C. Tobias, Lawrence Berkeley Laboratory)

The objective of this project is to establish the influence of electrode geometry and surface morphology, and of electrolyte composition, on bubble size and residence time, and to elucidate the role of free and forced convection as it affects overpotential behavior and ohmic resistance in gas evolution processes.

High-speed cinematography is used to characterize the motions of gas bubbles produced at vertical electrodes. The effect of various bubble motions and sizes on mass transfer to a vertical electrode is studied using a microsectioned electrode produced by Hewlett-Packard Corporation and Bell Laboratories. Bubbles produced at an auxiliary electrode located a prescribed distance from the micromosaic electrode rise parallel to the micromosaic surface. Temporal and spatial variations in the mass-transfer rate to the micromosaic are correlated, as well as average mass-transfer rates, as functions of distance of the bubble column to the measuring surface, bubble size, and rate of bubble generation. A continuous bubble stream rising near the measuring electrode is modeled as a cylinder moving parallel to a stationary wall. Mass-transfer predictions from this simplified model agree well with experimental trends.

The effect of electrode surface morphology and of electrolyte composition on the concentration of dissolved gas at the surface of a gas-evolving electrode is studied using electrochemical techniques. Correlations of gas supersaturation versus nominal current density have been obtained for hydrogen evolution in acid and base, and for oxygen evolution in base. The results tend to confirm the usefulness of a surface-renewal model for predicting supersa-

turation at gas-evolving electrodes.

A model is advanced for the numerical determination of current distribution in the vicinity of an attached bubble. These calculations enable the evaluation of the net change in cell resistance caused by the presence of a layer of bubbles on the electrode surface. The mathematics consists of two boundary-value problems that are coupled through two boundary conditions at the electrode. These are a flux-matching condition and a potential matching condition involving the overpotentials. A finite-element or boundary-element routine is used to solve Laplace's equation at each step in a Newton-Raphson iteration scheme which produces the converged solution. The effect of an array of attached bubbles with a given interbubble spacing is simulated by enclosing one bubble in a cylindrical cell whose cross section equals that of the hexagonal symmetry cell characteristic of a hexagonal array. An example of the concentration effect of a layer of attached bubbles on current distribution is shown in Fig. 13. The remarkable feature of Fig. 13 is the enhancement of current density near the bubble-contact area, which results from the local depression of supersaturation overpotential. A strong function of electrode kinetics, this enhancement effect diminishes with increasingly sluggish kinetics and is seen to disappear completely in the limit of Tafel polarization.

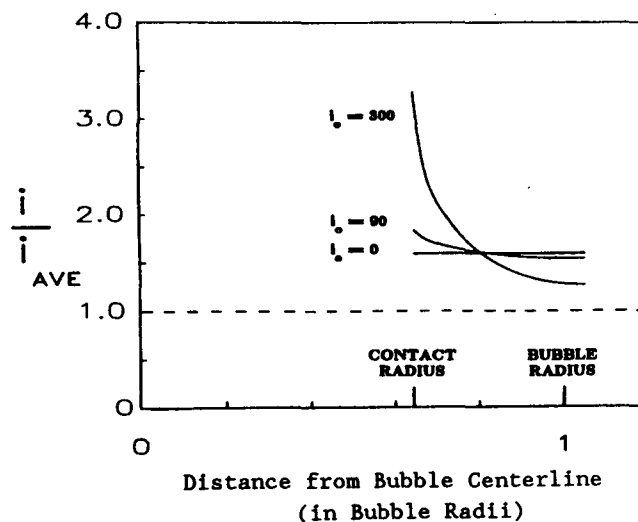


Fig. 13. Current distribution in the vicinity of a bubble, in a close-packed hexagonal arrangement. Conditions: $i = 300 \text{ mA/cm}^2$; electrolyte: 30% NaOH, 80 °C; bubble diameter; 40 μm ; contact angle: 40 °; Nernst boundary-layer thickness: 20 μm . Handbook values are used for conductivity, gas solubility and diffusivity. The exchange-current density, i_0 , given in mA/cm^2 , is a measure of the kinetic facility of the electrode reaction. XBL 862-624

IV. AIR SYSTEMS RESEARCH

The objectives of this project element are to identify, characterize and improve materials for air electrodes; and to identify, evaluate, and initiate development of metal/air battery systems and fuel-cell technology for transportation applications.

A. METAL/AIR CELL RESEARCH

Projects on metal/air cell research address bifunctional air electrodes, which are needed for electrically rechargeable metal/air (Zn/air, Fe/air) cells; and novel alkaline Zn electrode structures which could be used in either electrically recharged or mechanically recharged cell configurations.

Corrosion of Non-Metallic Electrode Materials

(P. Ross, Lawrence Berkeley Laboratory)

The corrosion resistance of carbons, which have potential application in bifunctional air electrodes is under investigation. A large number of furnace-process carbon blacks were examined for corrosion resistance in the potential regime for O_2 evolution (400 to 600 mV vs. Hg/HgO). The carbon blacks studied were chosen to represent a wide range of physical and chemical properties, e.g., Brunauer-Emmett-Teller (BET) surface area, prime particle size, and agglomerate particle size. Relative to acetylene black, all furnace-process carbon blacks exhibited high corrosion rates, factors of 5 to 100 times higher. An interesting and fundamentally important property of these carbons is the one-to-one correlation of surface area measured by physical adsorption (BET) with the area measured by chemisorption ($mg I_2/g C$). This correlation indicates a

uniform distribution of I_2 adsorption sites over the physical surface of the C. When furnace-process carbons are subjected to graphitizing heat treatment ($2700^\circ C$ in He), dramatic changes occur in both chemical and physical properties, with more dramatic changes occurring with increasing surface area, i.e., a larger percentage change in BET area and a larger percentage decrease in corrosion rate. Typically, the I_2 adsorption is changed from a 1:1 relation with BET area to a 1:2 relation, indicating that approximately half of the physical surface of the carbon does not chemisorb I_2 . Since inertness to I_2 is characteristic of the basal plane of graphite, it is concluded that typically half of the surface of a graphitized furnace-black is basal-plane.

As shown by Fig. 14, the corrosion rate is correlated with the BET area (as expected), but there is a separate correlation for both the furnace black and its graphitized form. However, as shown by Fig. 15, the corrosion rate of both forms of C follows the same correlation with I_2 adsorption, indicating that common active sites (for corrosion) exist on both forms of C. The optimum C support is clearly that form of C having the highest possible BET-to- I_2 -adsorption ratio. Graphitization of furnace-black carbons is one way to create new carbons having higher ratios, and there may be other heat treatments and/or precursor carbons that yield new materials having even higher ratios.

Publications

1. N. Staud and P.N. Ross, "The Corrosion of Carbon Black Anodes in Alkaline Electrolyte: II. Acetylene Black and the Effect of Oxygen Evolution Catalysts," LBL-19965 (1985).

2. P.N. Ross, "The Corrosion of Carbon Black Anodes in Alkaline Electrolyte: III. Furnace Process Carbon Blacks and the Effect of Graphitizing Heat-Treatment," LBL-20705 (1985).

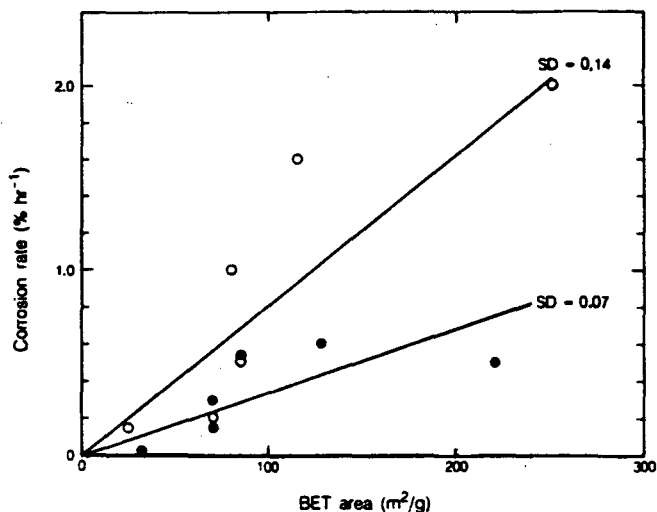


Fig. 14. Correlation between corrosion rate (30% KOH, 50 °C) and BET surface area for furnace-process carbons (open circles) and the graphitized form of these carbons (closed circles). SD = standard deviation.

XBL 8511-12509

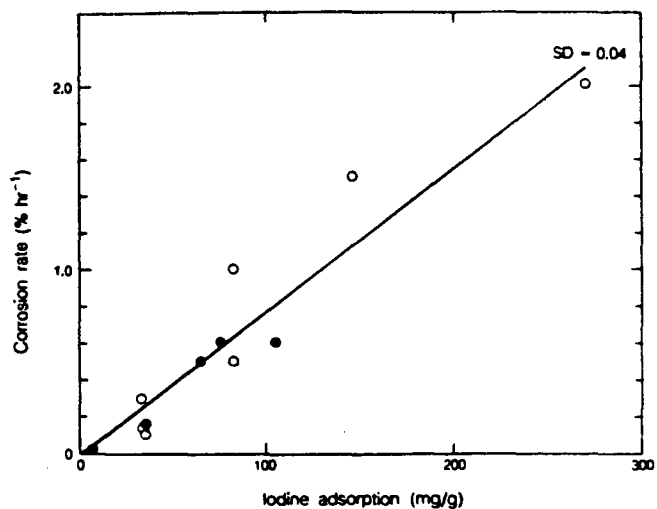


Fig. 15. Correlation between corrosion rate and iodine adsorption number for both forms of carbon black (see Fig. 14 for symbols and conditions).

XBL 8511-12510

Electrocatalysts for Oxygen Electrodes

(E. Yeager, Case Western Reserve University)

The overall objective of the research is the development of much more effective electrocatalysts for O_2 reduction and generation, combining high catalytic activity with long-term stability. Research emphasis is on achieving a fundamental understanding of O_2 electrocatalysis.

Adsorbed Transition Metal Macrocycle Catalysts:

The high catalytic activity for the 4-electron reduction of O_2 with several planar and cofacial macrocycles were investigated. These macrocycles are adsorptively attached to C or metal substrates. Laser Raman and electrochemical studies of the adsorbed tetrasulfonated phthalocyanines (TsPc) indicate the structure of the adsorbed layers is strongly influenced by the nature of the supporting electrolyte. *In-situ* fluorescence emission measurements have been made with the metal-free H_2TsPc adsorbed on various substrates (Ag, Au, Fe, Ni and graphite) in order to better understand the electronic interaction of the macrocycle ligands with the electrode orbitals. Quantum mechanical calculations using the ASED molecular orbital method provide evidence for dioxygen Fe-O-O-N bridging in the iron phthalocyanines where N is a bridging N. This represents an interesting alternative to the intermolecular dioxygen bridging (Fe-O-O-Fe) proposed to explain the 4-electron O_2 reduction with several iron phthalocyanines.

Heat-and Radiation-Treated Macrocycle Catalysts:

Measurements indicate that heat-treated transition metal macrocycles such as Fe- and Co-tetramethoxyphenylporphyrins (TMPP) adsorbed on C have high activity for O_2 reduction in alkaline and acid electrolytes. The transition metal need not be present in the macrocycle during heat treatment. Metal-free macrocycles such as H_2TMPP can be heat

treated and the transition metal subsequently adsorbed on the surface, even *in-situ* from the alkaline electrolyte. The combined use of Fourier transform infrared, transmission electron microscopy, Mossbauer, X-ray diffraction, magnetic susceptibility, and pyrolysis gas chromatograph-mass spectroscopy has provided new insight into the effects of the heat treatment. The macrocycles partially decompose while retaining the pyrrole nitrogen, which then provides binding sites for adsorbed transition metals, such as Co and Fe, with the catalytic activity due mostly to the transition metal in an atomic state of dispersion. Exploratory studies are in progress using γ -radiation to graft the macrocycles to the C surface.

Use of Protonated Nafion as the Electrolyte: Protonated Nafion has been introduced as the electrolyte phase in the interior of porous O₂ electrodes which are in contact with concentrated (85-96%) H₃PO₄. The results with cathodes that are catalyzed with Co- and Fe-TMPP are encouraging. Fluon (ICI) has been used in place of Teflon (duPont) to avoid the high sintering temperatures required with the latter, which would be detrimental to Nafion. The concentrated H₃PO₄ infuses into the Nafion, depressing the vapor pressure of the water and making it feasible to use this ionomer at temperatures approaching the boiling point of the concentrated H₃PO₄. The stability of the macrocycle catalysts is also expected to be greatly improved.

Perovskites Catalysts for Bifunctional Oxygen Electrodes: Sixteen perovskites have been prepared of the type La_xSr_{1-x}MO₃ in which M is a transition metal or combination of transition metals, including Cr, Mn, Fe, Co, Ni and Ru. These compounds have been characterized using X-ray diffraction, BET surface area, elemental analysis and magnetic susceptibility. Encouraging results have been

obtained with some of these perovskites. Plans call for the examination of mixtures of various perovskites as O₂ generation/reduction catalysts using other perovskites as supports. The fundamental studies will also include studies of single crystals.

O₂ Electrocatalytic Properties of Carbon/Graphite: Research has demonstrated that modified carbon surfaces with quinone groups that are chemically or adsorptively attached are effective catalysts for O₂ reduction to peroxide in alkaline electrolytes. In order to establish the role of water and Bronsted/Lewis acids in O₂ reduction, the measurements have been extended to dry acetonitrile and acetonitrile-water mixtures. The O₂ reduction stops at the superoxide radical in the dry aprotic solvent, thus indicating the critical role played by protons in the O₂ reduction to peroxide.

Publications

1. E. Yeager, D. Scherson and C. Fierro, "In-Situ Spectroscopic Studies of Oxygen Electrocatalysts Involving Transition Metal Macrocycles," in *Catalyst Characterization Science: Surface and Solid State Chemistry*, M.L. Deviney and J.L. Gland, eds., ACS Symposium Series 288, American Chemical Society, Washington, DC (1985) p. 537.
2. D.A. Scherson, C.A. Fierro, D. Tryk, S.L. Gupta and E.B. Yeager, "In-Situ Mossbauer Spectroscopy and Electrochemical Studies of the Thermal Stability of Iron Phthalocyanine Dispersed in High Surface Area Carbon," *J. Electroanal. Chem.* 184, 419 (1985).
3. R. Holze and E.B. Yeager, "Sauerstoffreduktionselektroden für Elektrolyse und Brennstoffzellen," *Technische Elektrolysen*, Dechema Monograph, Vol. 98, Verlag Chemie, Weinheim, (1985) p. 499.

4. B. Simic-Glavaski, S. Zecevic and E. Yeager, "Spectroscopic and Electrochemical Studies of Transition-Metal Tetrasulfonated Phthalocyanines. 3. Raman Scattering from Electrochemically Adsorbed Tetrasulfonated Phthalocyanines on Silver Electrodes," *J. Amer. Chem. Soc.* **107**, 5625 (1985).
5. R. Adzic, B. Simic-Glavaski and E. Yeager, "Spectroscopic and Electrochemical Studies of Transition Metal Tetrasulfonated Phthalocyanines. 6. The Adsorption of Iron Tetrasulfonated Phthalocyanine on Single Crystal Silver Electrodes," *J. Electroanal. Chem.* **194**, 155 (1985).
6. S. Zecevic, B. Simic-Glavaski, E. Yeager, A.B.P. Lever and P.C. Minor, "Spectroscopic and Electrochemical Studies of Transition Metal Tetrasulfonated Phthalocyanines. 5. Voltammetric Studies of Adsorbed Tetrasulfonated Phthalocyanines (MTsPc) in Aqueous Solutions," *J. Electroanal. Chem.* **196**, 339 (1985).

Research and Development of Bifunctional Oxygen Electrode

(S. Viswanathan, Energy Research Corporation)

The objective of this research was to develop a relatively inexpensive air electrode that could function effectively both in the O₂ reduction and evolution modes (i.e., bifunctional oxygen electrode). Two approaches were considered in this research effort. The first utilized a low-loading (0.5 to 1.0 mg/cm² on substrates of carbon, graphite, metal and spinel oxides) Au catalyst for O₂ reduction in combination with a Ni layer for O₂ evolution. The second approach utilized a catalyst consisting of a metal oxide perovskite for both O₂ reduction and evolution. The perovskites, with the composition AA¹BO₃ (A is an element of Lanthanide series, A¹ is an alkaline earth metal and B is a first-row transition element) were examined. A number of perovskites were

prepared at different process conditions, using Nd and La for A; Sr, Ba and Cr for A¹; and Ni, Co and Mn for B.

Over 50 different compositions of perovskites were synthesized and tested. The performance data indicate that perovskites show definite possibilities as a viable replacement for Pt in air electrodes. The perovskite La_{0.5}Sr_{0.5}CoO₃ demonstrated stable polarization against a Hg/HgO reference electrode over extended periods of time on anodic (644 mV, at 10 mA/cm² for 860 h) and cathodic (300 mV, at 20 mA/cm² for 1600 h) operation. In addition, the electrode operated as a bifunctional electrode for 800 cycles at 10 mA/cm² (charge) and 20 mA/cm² (discharge). Test results of other perovskites (e.g., LaNiO₃ and Nd_{0.5}Ca_{0.5}Co_{0.8}Ni_{0.2}O₃) showed equal or better performance than La_{0.5}Sr_{0.5}CoO₃. Promising candidates among the ones screened and areas requiring further study have been identified.

In a parallel effort, an engineering analysis of the Zn/air battery system for electric vehicles was conducted. Several possible operating schemes were analyzed with regard to performance characteristics, system problems and cost effectiveness. It is concluded from this study that a Zn/air battery system which is electrically rechargeable by conventional techniques (charge/discharge of bifunctional air electrode and solid Zn electrode) is the optimum configuration for use in electric vehicles.

Publication

1. S. Viswanathan and A. Charkey, "Bifunctional Oxygen Electrodes for Rechargeable Metal-Air Cells," Proceedings of the 20th IECEC, (1985) p. 2.21.

Electrical and Electrochemical Behavior of Particulate Electrodes

(J. Evans, Lawrence Berkeley Laboratory)

The objective of this research is to provide the basic knowledge to enable particulate electrodes to be designed, evaluated and sealed up. One possible particulate electrode is a fluidized-bed electrode where Zn particles are maintained in a state of agitated suspension by the upward-flowing electrolyte. Such electrodes have been the main subject of this investigation to date.

A probe has been used to simultaneously measure the electrolyte and particle potentials within a fluidized-bed electrode. The difference between the two signals then yielded the overpotential. Experiments were performed on beds of copper particles undergoing cathodic deposition from acidified sulfate solution and on beds of Zn-coated particles undergoing deposition or dissolution of Zn with an alkaline zincate electrolyte. Both low-frequency and wide-band noise were observed in the potentials of Cu particles, while the former was much less for Zn-coated polymer particles. An explanation was offered in terms of the hydrodynamics of the electrode, particularly the presence or absence of rising particle-free regions ("bubbles"). The distributions of time-averaged potentials with position in the bed were measured and found to be in qualitative agreement with theory.

In a second part of the study, alternating currents were passed through fluidized beds of Cu particles and Zn-coated polymer particles (Sorapec particles). The sinusoidally varying potential across the bed, and that across a known resistor in series with the bed, were measured. For the Cu particles the former potential showed amplitude variations thought to be due to voids ("bubbles") within the bed.

These amplitude variations depended on bed expansion. Beds of Sorapec particles were free of these variations. Effective bed resistivities were determined and found to increase with bed expansion (rapidly in the case of Cu particles).

The fluidized-bed deposition of Zn from chloride electrolytes has been studied in a laboratory cell. The cell was operated at superficial current densities in the range 1200 to 7500 A/m² with catholytes containing up to 62 kg/m³ Zn and up to 28 kg/m³ HCl. Anolytes examined contained 58 kg/m³ NaCl and up to 100 kg/m³ HCl and, in some instances, had the same composition as the catholyte. Both pure catholytes and ones with deliberate additions of impurities (Ni, Co and Sb) were used. Pure solutions yielded current efficiencies and power consumptions comparable to or better than those of cells with conventional electrodes. Antimony (particularly in combination with Ni and Co) had a detrimental effect on cell performance; this detrimental effect was largely alleviated by simultaneous additions of glue.

Publications

1. N.E. Tuffrey, V. Jiricny and J.W. Evans, "Fluidized Bed Electrowinning of Zinc from Chloride Electrolytes," *Hydrometallurgy* 15, 33 (1985).
2. T. Huh, "The Performance and Electrochemical Behaviour of Fluidized-Bed Electrodes," Ph.D. Thesis, LBL-19621 (1985).
3. T. Huh and J.W. Evans, "Electrical and Electrochemical Behaviour of Fluidized-Bed Electrodes. Part I: Potential Transients," LBL-20820 (1985).
4. T. Huh and J.W. Evans, "Electrical and Electrochemical Behaviour of Fluidized-Bed Electrodes. Part II: Effective Bed Resistivities," LBL-20841 (1985).

Zinc/Air Battery Systems

(P. Foller and J. Morris,
Pinnacle Research Institute)

Pinnacle Research Institute (PRI) began a study of ideas for possible improvement of particulate Zn electrodes for EV batteries. The following areas of focus are planned: (i) a study of the use of electrolyte additives to increase the amount of Zn which may be discharged into a given volume of electrolyte; (ii) a comparison of the discharge behavior and suspension properties of slurries of dendritic Zn powders versus slurries of lower-density Zn-plated particulate substrates; and (iii) a comparison of recharge parameters for fluidized-bed deposition of Zn onto substrate materials versus production of dendritic Zn powder. The intent of this investigation is to produce improvements in the specific energy of the Zn/air battery by complete characterization of discharge-product colloidal stabilizers (such as silicate) and offer a comprehensive comparison of the two particulate electrode approaches.

Various electrochemical cells are being constructed; these include small planar (2 x 100 cm² electrode) discharge cells, a fluidized-bed cell for Zn-plating of substrates, and a cylindrical cell with a glassy-carbon cathode for mechanically assisted production of dendritic Zn powder.

B. ALUMINUM/AIR BATTERY R&D

Projects on Al/air battery R&D, which are managed by LLNL, are directed at improving cell components and solving system integration problems.

Aluminum/Air Power Cell Research and Development

(A. Maimoni, Lawrence Livermore
National Laboratory)

The objectives of this program are to develop an electric power source as an alternative to the internal combustion engine, and to evaluate its ability to provide general purpose vehicles with the range, acceleration performance, and rapid refueling capability of current internal combustion engines. The Lawrence Livermore National Laboratory (LLNL) conducts research and provides program direction on the development of the Al/air battery. Most of the work is carried out under a cost-shared contract with Eltech Systems Corporation, which has formed a consortium with Alcan Aluminum Ltd., CWRU, SRI International, University of Akron and University of Oklahoma.

Integrated Experiments

A number of operational problems in the M4-1 experiment (M4 cell coupled to a crystallizer/hydrocyclone) led to the redesign of the system; the M4-2 experiment was the test of the modified system. The combined duration of the M4-1 and M4-2 experiments was over 9 h; this is sufficient time to indicate satisfactory performance of cell components, but was not long enough to be indicative of long-term problems. The main modifications for M4-2 were: (i) using a diaphragm pump, instead of a peristaltic pump, to feed the hydrocyclone; (ii) direct heating and temperature control of the crystallizer vessel; (iii) upgrading the software used for data acquisition; (iv) pressure filtering the samples, instead of centrifugation to separate the seed from the electrolyte; and (v) using a Sandia automatic titrator to determine Na and aluminate concentrations. A report was published describing the M4-1 and M4-2 experiments (1).

The M4-2 system operated very well. Prior to the electrochemical experiment, the system was operated for 5 h using a hydrargillite/water slurry to determine the particle abrasion characteristics and performance of the diaphragm pump, and the hydrodynamic behavior of the crystallizer. The M4-2 experiment ran for over 5 h at 70°C. A 99.999% pure Al anode was used with sodium stannate in solution to reduce corrosion. Relatively large amounts of metallic Sn in the form of dendritic crystals precipitated from solution. The Sn was carried by the electrolyte flow and embedded into the check valves of the diaphragm pump, causing them to malfunction and leading to termination of the M4-2 experiment. Since the M4-1 was also terminated due to plugging of the lines by metallic Sn/hydrargillite, and the information developed at Alcan indicated that agglomeration is prevented by turbulence and shear, no additional experiments were carried out on the M4 cell system.

The electrical characteristics of the M4 cell agreed very well with the calculated values. The crystallization rate at later times agreed very well with Alcan's correlation, although it was about twice as high as predicted at early times while secondary nucleation was taking place (Fig. 16).

Component Development

Air Cathode: Research continues at CWRU to achieve a basic understanding of the processes and mechanisms of catalysis in heat-treated macrocycles on C. The heat treatment of the macrocycle at temperatures between 400 and 800 °C disturbs the structure considerably, but leaves a surface rich in N. Some of the transition metal (M) remains coordinated to N-containing surface functionalities with different degrees of coordination, i.e., M-N₂, M-N₃, M-N₄. These sites are probably catalytic for both O₂ reduction and peroxide

decomposition. A portion of the transition metal forms hydrated oxide upon contact with the caustic solution and can dissolve and either re-absorb or escape into the bulk solution. The activity of the metal-macrocycle complex depends upon the nature of the transition metal, although it is still not clear what is the exact state of the catalytically active metal. This model gives clues to other materials, which upon pyrolysis, yield N-rich surfaces and has prompted examination of pyrolyzed polymers such as polypyrrole in combination with transition metals.

Recent improvements in the fabrication techniques of gas electrodes have led to a substantial increase in the range through which the Tafel slope is linear; it now extends over 3.5 orders of magnitude. At present the maximum measurable current density is 0.8 A/cm². The polarization curve of CoTMPP on Vulcan XC-72 has a slope of -37 mV/decade, which is likely to be indicative of the rate for peroxide decomposition, because the rate for electron transfer appears to be quasi-equilibrium over almost the entire range of current densities.

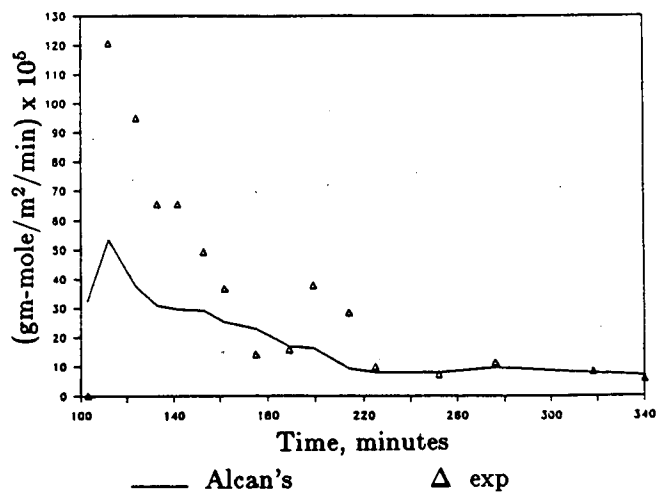


Fig. 16. M4-2 experiments; comparison of experimental crystallization rate with Alcan's correlation.

Great strides were made in increasing the life and the reproducibility of air electrodes at Eltech and Electromedia, and several electrodes have exceeded the project goal of 1400 cycles, which is equivalent to over 2 yr in vehicle life. (The cycles used in this study are not true driving cycles, but represent a comparative test of the electrode cycle life). Manufacturing procedures were standardized for various types of carbons, leading to the Standard Electrode (SE) configurations. Tests of various electrode materials and configurations are continuing and the range of test conditions was extended to 80 °C and now includes experiments with KOH electrolyte.

The electrodes manufactured using Norit carbon have shown exceptionally high life; one early electrode was retired from service after 3000 simulated cycles. The new SE configurations are being tested, one electrode achieved in excess of 2000 cycles (Fig. 17) and another still under test has exceeded 1200 cycles. The performance in KOH is approximately 240 mV higher (at 600 mA/cm²) than, the corresponding voltage in NaOH electrolyte, but the tests have not run long enough to elucidate the effect of the electrolyte on lifetime.

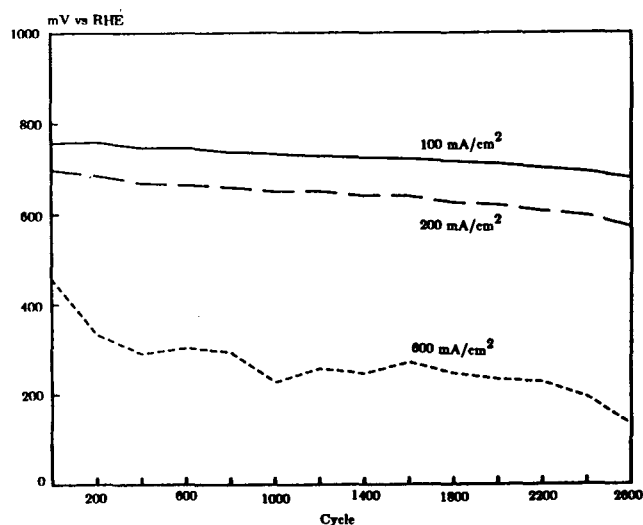


Fig. 17. Evolution of air cathode voltage vs number of cycles, Norit carbon, 60 °C, NaOH.

Failure of the majority of SE electrodes containing RBDA carbon was traced to mechanical failure of the mesh. Heavier meshes are under test, and Electromedia is investigating a structure with additional mechanical rigidity, with performance on par with that of a standard single-grid cathode.

Aluminum Anodes: Superior alloys have been found in this research program, but further work is required to increase their energy yield and decrease their sensitivity to high aluminate concentrations in the electrolyte.

Alcan developed a proprietary alloy, BDW, which has anodic polarization characteristics (Fig. 18) similar to those of RX-808 and corrosion behavior approaching the target of 10 mA/cm² equivalent (Fig. 19). The polarization is not appreciably changed by operation at 80 °C or KOH electrolyte, but the corrosion is somewhat increased at 80 °C. The calculated cell power density using BDW is 0.67 W/cm² at 60 °C (4.2 kWh/kg).

Eltech has standardized the procedure for testing Al alloys. A series of alloys containing varying amounts of Bi, Ga, In, Li, Mn and Sn in 99.99 and 99.999% Al were developed. These alloys along with the Alcan proprietary alloys were tested in NaOH and KOH electrolyte at 80 °C. While many of the alloys developed by Eltech exhibit superior performance, none has exceeded the performance of BDW in energy yield and power density; the polarization and corrosion behavior of one of their alloys, ESC-3, is shown in Figs. 18 and 19, respectively.

The cell developed at SRI International was used to obtain information on the AC impedance of a set of Al alloys in 4 M KOH at 25, 50, 60 and 80 °C. The impedance data were acquired by running frequency sweeps (typically 10 kHz to 0.08 Hz) at various cathodic potentials. A mathematical tech-

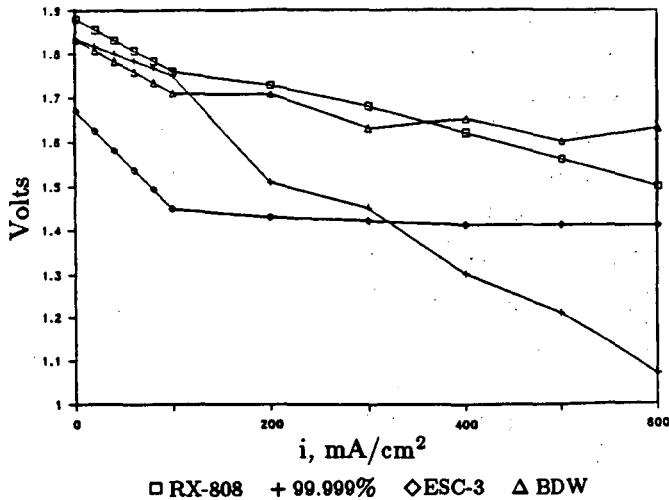


Fig. 18. Polarization in 4 M NaOH at 60 °C for alloys RX-808, BDW, ESC-3 and 99.999% Al.

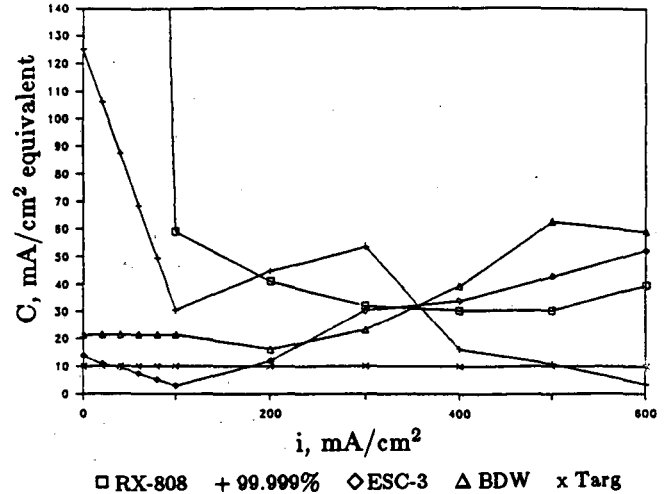


Fig. 19. Corrosion rates in 4 M NaOH at 60 °C for alloys RX-808, BDW, ESC-3 and 99.999% Al. The corrosion target is equivalent to 10 mA/cm².

nique, based upon the Kramers-Konig transformation, was developed to determine the reliability and validity of the complex impedance data. Various models using non-linear least squares are then used to determine the kinetic constants for the postulated chemical reactions.

Cell and Cell Stack Development:

The M4 cell is easy to assemble from its subassembly components and operated reliably, but the assembly and electrical connection of the air electrode was cumbersome and slow. Therefore, Eltech examined in detail all aspects of cell design and evolved their EL-2 cell (Fig. 20). The main improvements attained in EL-2 are:

- A modular air cathode (MAC) subassembly was developed that is easily removed from the cathode compartment. The MAC is made by crimping the air cathode material in a Cu frame which

acts as mechanical support, current distributor, and sealing perimeter.

- A reliable gasket seal on the air compartment was developed.
- An assembly for anode current collection was designed to provide: (i) support to the anode, (ii) constant anode-cathode gap, (iii) a compression member to seal the MAC into the air chamber, (iv) an integral manifold for the electrolyte, and (v) a means for anode current collection and a current path from an old to a new anode. The electrical performance of the EL-2 cell agrees very well with the calculated values. However, a remaining problem with the EL-2 cell has been the failure of the anode to fall freely due to mechanical interferences or friction within the cell; the causes are being investigated.

Calculations by the University of Akron indicate that (i) essentially all the current is carried within the Al anode, only a small fraction is carried by the current collector tines; and (ii) for operating current densities greater than 200 mA/cm², the shunt currents produce less than a 1% performance loss using a worst-case electrolyte manifold design.

Crystallization and Product Separation

Alcan continued to explore the conditions leading to agglomeration and secondary nucleation, measured the conductivity of aluminate solutions over a large range of temperatures and aluminate concentrations in NaOH and KOH electrolytes, and performed initial tests of a tube settler for product separation under crystallization conditions. Since Alcan does not have an electrolytic cell for Al dissolution, they have used the supersaturated aluminate solutions produced by corroding Al in a caustic solution. While this technique has permitted a large number of tests to be made, it has also prevented tests on the new corrosion-resistant alloys.

A very good correlation was found for the crystallization rate in 4 M NaOH. The fastest growth rate (3.1 μm/h linear growth) was obtained at 80 °C; crystallization from KOH proceeds at about the same rate. The following equation was developed

$$G = 3.91 \times 10^9 \exp(-7124/T) \\ \left[\frac{(R - 2.91 \exp(-2351.9/T))}{(1 - 1.04R)} \right]^2$$

where G is growth rate (μm/h), T is temperature (°K), and R is the ratio of Al₂O₃/Na₂CO₃(g/l). This equation yields estimates of growth rate which are about 30% lower than those predicted by an earlier correlation from Alcoa (2).

Agglomeration experiments continue to indicate that the best agglomeration temperature is 80 °C, and low turbulence is essential to obtain agglomerates larger than 20 μm. In one

series of experiments a crystallization rate of 100 g/h per liter of crystallizer volume was achieved without net generation of particles smaller than 40-μm diameter. Thus, a low-turbulence agglomeration vessel, or section of the crystallizer, will be required to attain the desired product size; high solids concentration is not detrimental up to the highest concentration tested, 32 wt%. Agglomerates obtained from KOH are more fragile and agglomeration is slower; crystallization from KOH produced a much higher concentration of fine particles.

The level of alkali impurities in the hydrargillite product after crushing and washing ranged from 0.35 to 0.57%; the higher values was obtained with hydrargillite that was crystallized under low-turbulence conditions. Secondary nucleation can be obtained at will, by increasing supersaturation. A series of samples obtained throughout the secondary nucleation process clearly show the evolution from well-formed crystals to formation of embryonic nuclei on their surfaces.

Experiments at LLNL demonstrated that the conductivity of the electrolyte is sensitive to small amounts of impurities such as stannate ions. This sensitivity prevents its use for quantitative analysis of the electrolyte, but the measurement is a very useful process-control measure. Alcan measured the conductivity of NaOH and KOH solutions (2.5-6 M) containing 1 to 4 M Al. The measurements indicate the KOH solutions have a conductivity about 40% higher than that of NaOH solutions.

Initial tests of lamella settlers for separating agglomerates are underway at LLNL. Lamella settlers are parallel plates, or tubes, inclined at an angle to the vertical (Fig. 21). Clear liquid accumulates under the upper plate and flows upwards, while the settled sludge accumulates and flows downward on the lower plate. In a parallel plate settler the clarification rate can be approximated by an

appropriately chosen settling velocity multiplied by a horizontal projected area. The theoretical models (LAMSET and SETMOD) show good agreement with experiment, and they allow calculation of the clarification rate and material balances, but do not allow calculation of particle size distribution of the product. In contrast to hydrocyclones, lamella settlers have very low shear and energy requirements; the overhead flow rate can be varied over fairly wide limits to obtain a range of products. As found with other particle separation devices, good separation of the fines in the overhead product can be obtained, but the underflow has a wide size distribution. Means for obtaining a sharper bottom product particle distribution are being investigated.

References

1. A. Maimoni, S.A. Muelder and W.C. Hui, Lawrence Livermore National Laboratory, Report UCID-20495 (1985).
2. Aluminum Company of America, Lawrence Livermore National Laboratory, Report UCRL-15503 (1982).

Publications

1. G.D. Chase, and R.F. Savinell, "Current Distribution in a Wedge-Type Aluminum Air Cell," Extended Abstracts of the 168th Meeting of the Electrochemical Society (1985) p. 13.

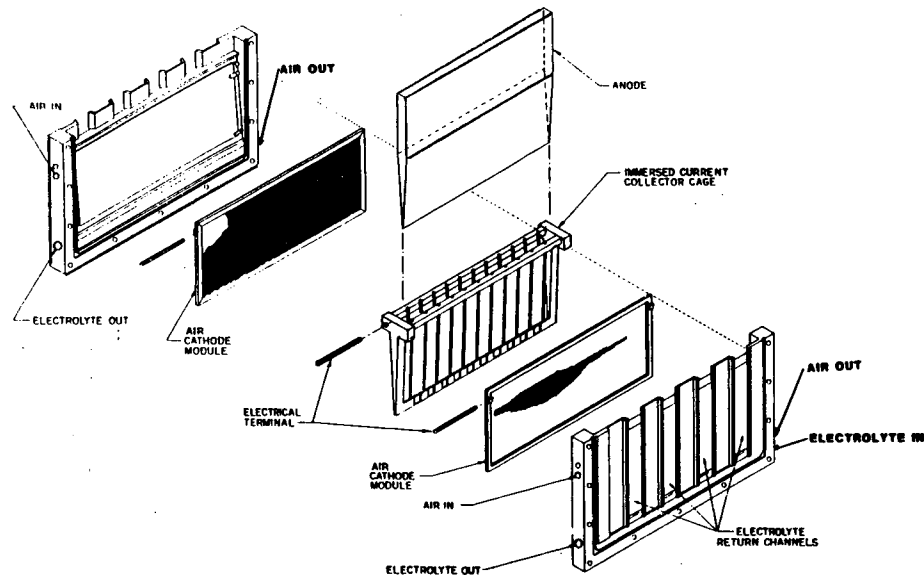


Fig. 20. Eltech's EL-2 cell.

2. S.L. Gupta, D. Tryk, D. Scherson, W. Aldred and E. Yeager, "Oxygen Electrocatalysts for Aluminum-Air Cells," Extended Abstracts of the 168th Meeting of the Electrochemical Society (1985) p. 3.
3. L.A. Knerr and D.J. Wheeler, "Pt Loading Effects on Air Cathode Operation in Alkaline Solution," Extended Abstracts of the 168th Meeting of the Electrochemical Society (1985) p. 1.
4. L.A. Knerr, T.J. Schue, C.L. Krause and D.J. Wheeler, "The Effects of Dissolved Species on Aluminum-Air Battery Anode Performance," Extended Abstracts of the 168th Meeting of the Electrochemical Society (1985) p. 20.
5. A. Maimoni, "Aluminum Air Power Cell -- A Progress Report," Proceedings of the 20th IECEC (1985) p. 2.14.
6. A. Maimoni and S.A. Muelder, "Aluminum-Air Power Cell: The M3-3 Experiment," Lawrence Livermore National Laboratory UCID-20307 (1985).
7. A. Maimoni and S.A. Muelder, "Aluminum-Air Power Cell: The M4-Cell Assembly and Initial Tests," Lawrence Livermore National Laboratory UCID-20495 (1985).
8. A. Maimoni and S.A. Muelder, "Aluminum-Air Power Cell: Overview and Recent Experiments at LLNL," Extended Abstracts of the 168th Meeting of the Electrochemical Society (1985) p. 17.

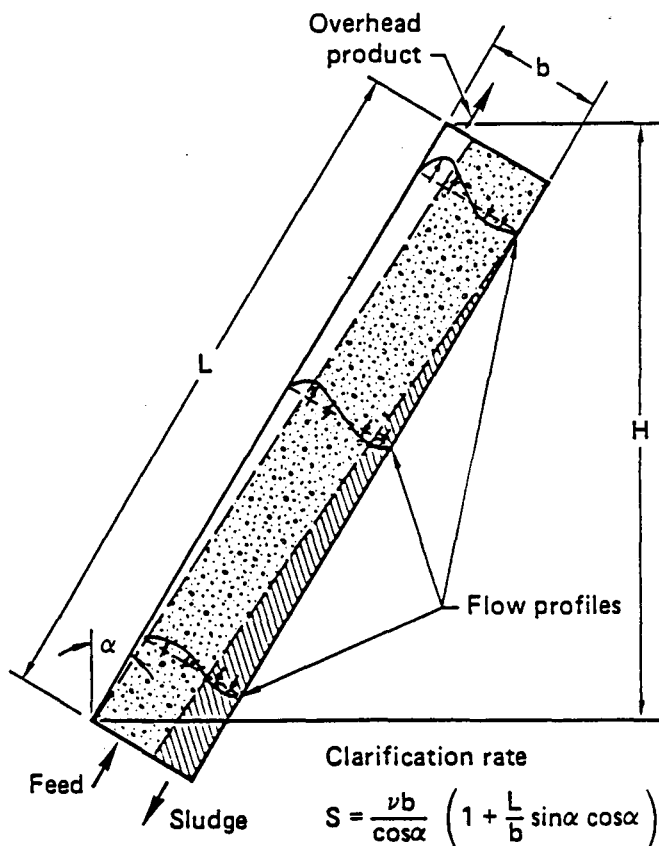


Fig. 21. Lamella settler. For a parallel plate settler the clarification rate is given by a settling velocity times the horizontal projected area.

C. FUEL CELL RESEARCH

Fuel cell research, which is managed by LANL, includes projects in several areas of electrochemistry: theoretical studies, fuel-cell testing, fuel processing and membrane characterization.

Fuel Cells for Vehicles

(J. Huff, Los Alamos National Laboratory)

The objectives of this program are to conduct basic and applied research in electrochemistry necessary to take fuel-cell technology from its present status to a proof-of-concept level where it becomes a practical alternative to internal combustion engines (ICE) for vehicular propulsion. The goals of the effort are to improve the specific power and transient response of the fuel cell system and to reduce the materials and manufacturing costs. The key areas under investigation are: (1) electrocatalytic mechanisms and development of electrocatalysts with faster kinetics and better impurity tolerance; (2) ion and water transport in membranes and use of this understanding to optimize membrane structure and to reduce catalyst loading; (3) catalytic conversion of CH_3OH to H_2 and CO_2 and use of this information to design a fuel processor with lower CO output and better transient performance; and (4) fuel-cell testing under vehicular operating regimes.

Electrocatalysis

Ab initio quantum mechanical calculations are being performed to provide theoretical insight into the character of Pt-O bonding and Pt cluster properties, since Pt has been the most important catalyst for fuel-cell reactions. The effort, at present, is directed primarily at the O_2 electrode, which is the major source of efficiency loss in acid-electrolyte fuel cells.

The ground state and excited wave functions of the PtO molecule have been calculated using several techniques. One important observation is that the ground state of the Pt-O bond is ionic in character, with a major shift of negative charge to the O_2 atom. Wave functions for Pt clusters ranging from Pt_2 to Pt_5 have also been calculated by several techniques. These calculations determine the low-lying energy levels and the geometrical arrangement of the atoms in the cluster. For Pt_3 in the ground state, the three atoms are located at the corners of an equilateral triangle with an internuclear separation of 2.69 Å. This bond distance is much closer to the bulk nearest-neighbor distance in metallic Pt (2.77 Å) than was found for Pt_2 (2.33 Å).

Continuing work on the adsorption and blocking behavior of various atomic species yielded new insights into catalytic mechanisms on single crystal surfaces. Most important, Bi atoms were found to adsorb in a mutually repulsive fashion. The Bi atoms maximize the distance between nearest neighbors on the Pt crystal surface and allows the effects of site blocking on important adsorption reactions to be studied in detail. One intriguing result is that the dissociative adsorption of H_2 and O_2 are blocked in a nonlinear fashion, which can be effectively modeled using Monte Carlo simulation techniques.

Membrane Structure, Transport and Interface Studies

Structures with well-established pore geometries were fabricated in an effort to understand the transport through molecular-sized pores. These materials were prepared by depositing Nafion from solution into Nucleopore polycarbonate membranes that had linear cylindrical pores 0.015 to 0.6 μm in diameter. The composite membranes were positioned over a rotating C disk electrode and studied by voltammetry techniques. The maximum

ionic-transport rate was obtained in membranes with 0.03- μm diameter pores.

Understanding the factors affecting water flow through proton exchange membranes (PEM) is critical for modeling and designing membranes and maintaining water balance in operating fuel cells. Data were determined for water flow through Nafion samples containing different cations such as H^+ , Li^+ , Na^+ , K^+ and Cs^+ . The results showed that the flow rate depends directly on the size of the hydrated ion.

A critical factor determining PEM fuel-cell performance is the electrocatalyst-membrane interface. Experiments were conducted to acquire and analyze complex impedance data on various electrode-membrane configurations. The complex impedance spectroscopy of the H_2 electrode reaction at Pt electrodes contacting a Nafion membrane has allowed the separation of the three elementary steps of the reaction: charge transfer, dissociative chemisorption and mass transport. For both the H_2 oxidation and evolution reactions, the charge transfer step is rapid and the kinetics are determined at steady state by the chemisorption and/or diffusion steps, depending on the potential and the electrode geometry. The electrode kinetics also depend on the polarization history of the interface, perhaps through diffusion of impurities from the membrane or variations of the local water content.

Impedance measurements of CO poisoning on smooth Pt electrodes were also made. A gas mixture containing 1% CO, 80% H_2 and 19% CO_2 was introduced into the electrode compartment. Initially, a significant change in the low-frequency part of the response indicated that mass transport to the electrode was slowed, but the greatest effect was due to blocking of H_2 adsorption sites, which influenced the intermediate frequency response

associated with the rate and extent of the dissociative adsorption process. In addition, the charge-transfer resistance increased significantly. On conventional PEM electrodes, 1% CO reduced the current density at room temperature by about two orders of magnitude.

Perhaps the most significant achievement during 1985 was the demonstration that the catalyst loading in a PEM fuel cell can be dramatically reduced by pretreating commercially available (Prototech) electrodes with solubilized Nafion. The electrodes were painted with a thin layer of Nafion and then air dried. Although these electrodes contain about an order of magnitude less Pt than the conventional PEM electrodes, their performance is comparable for both anode and cathode reactions at moderate temperatures.

Reformer Investigations

Substantial progress was made in understanding the reformer reaction mechanism using isotopic-labeling experiments. In the initial experiments, $^{18}\text{O}_2$ labeled reactants were used in the reforming reaction. It was shown that $^{18}\text{O}_2$ contained in the reactant water could end up in the product CO_2 , indicating rapid exchange of the labeled O_2 with O_2 in the metal-oxide reforming catalyst.

In the second experiment, Zn/CuO catalysts were prepared with $^{18}\text{O}_2$. This was accomplished by anodizing a Cu-Zn alloy in a small vial containing $^{18}\text{O}_2$ water. Starting with $^{16}\text{O}_2$ (normal) CH_3OH , the product CO_2 contained one or $^{18}\text{O}_2$ atoms. This indicates that O_2 atoms are removed from the catalyst lattice and are replaced with O_2 from the reactant water. Therefore, the reforming reaction does not follow the generally accepted cracking-shift route; rather, CH_3OH adds to an oxide vacancy and, in that position, reacts with lattice O_2 atoms to generate CO_2 .

Interestingly, CO showed a tendency not to exchange the O₂ with lattice sites, and thus may result from a different process.

Fuel Cell Testing

Static testing of a 20-kW, state-of-the-art H₃PO₄ fuel cell stack and reformer from Energy Research Corporation was completed. The fuel cell was designed to provide 21-kW gross electrical power with a 31-kW peak capability at sea level. Data were obtained for system operation on reformat at power levels of 14 kW to 26 kW. Below 15 kW, system instabilities were observed that resulted in pulsations in the reformer burner.

The 20-kW reformer performance was examined and the product gas composition was measured as a function of fuel flow rate and distribution of the catalyst bed temperature. Carbon monoxide levels of 0.7% to 1.8% were observed. The transient characteristics of the fuel processor were quantified. A time constant of ~15 minutes was recorded for a change in reformat temperature in response to a step change in the burner temperature.

Publications and Presentations

1. T.E. Springer, H.S. Murray and N.E. Vanderborgh, "On-Board Fuel Processing for Electric Vehicles," National Fuel Cell Seminar, Tucson, AZ (May 1985).
2. M.T. Paffett, C.T. Campbell and T.N. Taylor, "The Influence of Adsorbed Bi on the Chemisorption Properties of Pt(111): H₂, CO, and O₂," *Vac. Sci. Tech. A3* (3), 812 (1985).
3. J.L. Fales, T.E. Springer, N.E. Vanderborgh and P. Stroeve, "Effect of Polymer Morphology on Proton and Water Transport Through Ionomeric Polymers," Extended Abstracts of the 167th Meeting of the Electrochemical Society (1985) p. 596.
4. I. Rubinstein, J. Rishpon and S. Gottesfeld, "An AC-Impedance Study of Electrochemical Processes in Nafion-Coated Electrodes," Extended Abstracts of the 167th Meeting of the Electrochemical Society (1985) p. 708.
5. P.C. Rieke and N.E. Vanderborgh, "Current Voltage Surface Mapping of Solid Polymer Electrolyte Fuel Cell Electrodes Using Micro-Electrode Arrays Created by Photolithography," Extended Abstracts of the 167th Meeting of the Electrochemical Society (1985) p. 709.
6. J.R. Huff, H.S. Murray and N.E. Vanderborgh, "Transportation Applications of Fuel Cell Propulsion Systems," 12th Energy Technology Conference, Washington, D.C. (March 1985).
7. J.B. McCormick and J.R. Huff, "Fuel Cell Propulsion Systems for Lunar Surface Vehicles," The Space Press, Vernuccio Publications, New York (1985).
8. M.T. Paffett, C.T. Campbell and T.N. Taylor, "Surface Chemistry of Bi/Pt(111) Interfaces," New Mexico Chapter of the American Vacuum Society, Albuquerque, NM (April 1985).
9. H.S. Murray, "A 20-kW Indirect Methanol Phosphoric Acid Fuel Cell System Test," National Fuel Cell Seminar, Tucson, AZ (May 1985).
10. M.T. Paffett, C.T. Campbell and T.N. Taylor, "Surface Chemical Properties of Ag/Pt(111): Comparisons Between Electrochemistry and Surface Science," *Langmuir* 1, 741 (1985).
11. I.D. Raistrick, "Hydrogen Oxidation at the Proton Exchange Membrane-Platinum Interface: An Impedance Study," Extended Abstracts of the 168th Meeting of the Electrochemical Society (1985) p. 644.
12. T.E. Springer, H.S. Murray and N.E. Vanderborgh, "Methanol Reformer System and Design for Electric Vehicles," Proceedings of the 20th IECEC (1985) p. 1.723.
13. J. Huff, H.S. Murray, N.E. Vanderborgh, D.K. Lynn, C. Derouin, R. Dooley and J.B. McCormick, "Fuel Cells as Electric Propulsion Power Plants," Proceedings of the 20th IECEC (1985) p. 1.718.

14. C.T. Campbell, T.N. Taylor and M.T. Paffett, "Dispersed and Condensed Phases in Metal Overlayers on Pt(111): Structural Properties and Effects on Chemisorption," German Society for Physical Chemistry on Phase Transitions on Solid Surfaces, University of Erlangen-Numberg, Germany (September 1985).
15. M.T. Paffett, A.F. Voter and C.T. Campbell, "Testing Site Size Requirements in Chemisorption: Experiment and Theory," American Vacuum Society, Houston, TX (1985).
16. J.L. Fales, N.E. Vanderborgh and P. Stroeve, "The Influence of Ionomer Channel Geometry on Ionic Transport," Materials Research Society, Boston, MA (December 1985).
17. P.C. Rieke and N.E. Vanderborgh, "Thin Film Electrode Arrays for Monitoring Transport Processes in Proton-Exchange-Membrane Fuel Cells," Materials Research Society, Boston, MA (December 1985).
18. J. Leddy and N.E. Vanderborgh, "Nafion/Nucleopore Polycarbonate Composite Membranes: Mass Transport Characteristics," Materials Research Society, Boston, MA (December 1985).
19. J.G. Beery, S. Gottesfeld, M. Hollander, M.T. Paffett and C.J. Maggiore, "Electrochemical Applications of Ion Beam Analysis," Ion Beam Analysis Conference, Berlin, Germany (July 1985).
20. I.D. Raistrick, "Application of Impedance Spectroscopy to Solid State Ionics," Fifth International Conference on Solid State Ionics, Lake Tahoe, NV (August 1985).
21. J. Leddy and N.E. Vanderborgh, "Transport Through Membranes: The Effect of Electroactive Species and Electrolyte," Extended Abstracts of the 167th Meeting of the Electrochemical Society (1985) p. 444.

Advanced Chemistry and Materials for Fuel Cells

(J. McBreen, Brookhaven National Laboratory)

The objectives of this project are to develop electrocatalysts that minimize or eliminate the need for noble-metal catalysts in fuel cells and to enhance the kinetics of O_2 reduction and the oxidation of C_1 compounds. In 1985, research was focused on (i) synthesis of new tetrasulfonated metal phthalocyanines (M-TsPc), (ii) reactions of M-TsPc compounds with H_2O_2 and C_1 compounds, (iii) the incorporation of M-TsPc compounds in conductive polymers, and (iv) investigations of the pyrolysis of metal-phthalocyanine (M-Pc) compounds on Vulcan XC-72 carbon.

Synthesis of Tetrasulfonated Metal Phthalocyanines (M-TsPc): Several new M-TsPc compounds including Os-TsPc and H_2 -TsPc were prepared. This brings the total number of M-TsPc compounds prepared to twenty. The H_2 TsPc was successfully used to prepare several M-TsPc compounds by a simple insertion reaction. The inserted ions included Ni^{2+} , Co^{2+} , Fe^{2+} , Mn^{2+} , Zn^{2+} , Cu^{2+d} , Pd^{2+} , Cd^{2+} , and Sn^{2+} . Several ions could not be inserted, i.e., Mg^{2+} , Al^{3+} and Fe^{3+} .

Reactions of M-TsPc Compounds with H_2O_2 and C_1 Compounds): An extensive study of the interaction of M-TsPc compounds with C_1 compounds indicates that none are active for compounds with C-H bonds. However, several are active for π -bonded C_1 compounds (CO and CO_2). There was a particularly

strong interaction between CO and Fe(III)-TsPc in alkaline solution. This was confirmed by X-ray Absorption Near Edge Spectroscopy (XANES), UV/visible spectrophotometry and cyclic voltammetry. The results indicate that CO is a strong ligand for Fe. The ligand field effect lowers one of the Fe d-orbitals below the a_{1u} level of the macrocycle. An electron is transferred to the metal center and the Fe(III) is reduced to Fe(II).

Incorporation of M-TsPc Compounds in Organic Polymers: Several M-TsPc compounds were incorporated into either polypyrrole or poly-3-methylthiophene. In the case of polypyrrole, the metals included Fe, Co, Cu and Ni. Spectroelectrochemical studies indicate that the orientation in which the M-TsPc is incorporated as the counter-ion in the polymers is metal-center dependent. Both Fe-TsPc and Co-TsPc in polypyrrole and poly-3-methylthiophene are active catalysts for O_2 reduction.

Pyrolysis of Fe-Pc and Co-Pc on Vulcan XC-72: Extended X-ray Absorption Fine Structure (EXAFS) spectroscopy was used to investigate the pyrolysis of Fe-Pc and Co-Pc on Vulcan XC-72 carbon. Data were obtained for untreated material and materials treated at 400, 600 and 900 °C for three hours. Considerable changes in the EXAFS spectra were observed, but definitive conclusions will require further analysis and modeling.

Publications

1. J. McBreen, "Voltammetric Studies of Electrodes in Contact with Ionomeric Membranes," *J. Electrochem. Soc.* **92**, 1112 (1985).
2. C.A. Linkous, "C₁ Chemistry on Metal Phthalocyanine Electrocatalysts," Extended Abstracts of the 167th Meeting of the Electrochemical Society (1985) p. 939.

3. A. Melo, W.E. O'Grady, G. Chottiner and R. Hoffmann, "Study of Hydroxyl Formation on Pt(111) Surfaces by EELS and Low Temperature Reaction Quenching," *Appl. Surf. Sci.* **21**, 160 (1985).
4. W.O. Jennings, G.S. Chottiner, C. Natarajan, W.E. O'Grady, I. Lundstrom and W.R. Salaneck, "HREELS and Auger Studies of Conductive Polymers," *Appl. Surf. Sci.* **21**, 80 (1985).

Oxygen Reduction on Platinum in Fuel Cell Electrolytes

(E. Cairns and F. McLarnon,
Lawrence Berkeley Laboratory)

Preliminary rotating ring-disk electrode (RRDE) studies of O_2 reduction in dilute Cs_2CO_3 and KOH showed that solutions with higher carbonate anion concentrations supported higher O_2 reduction currents. These experiments have been supplemented by a series of RRDE experiments in mixed electrolytes (KOH, K_2CO_3 and KF) with the aim to identify the independent effects of ionic strength, pH and carbonate anion concentration. At a constant ionic strength of 0.7 M, both OH^- and CO_3^{2-} appear to have a positive effect on the kinetic current at 0.9 V versus RHE, with the highest kinetic currents observed when both of these ions are present. Peroxide is generated as an unwanted side product and is detected with the ring during a RRDE experiment. Carbonate ion appears to suppress peroxide formation while OH^- appears to increase peroxide formation.

Oxygen reduction experiments in K_2CO_3 and KOH have been completed at concentrations up to 1.0 M. When results are adjusted for differences in O_2 solubility, kinetic currents (at 0.9 V vs RHE) are 2 to 2.5 times higher in K_2CO_3 than in KOH at the same concentration. However, lower O_2 solubilities in carbonate electrolytes may lead to higher mass-transfer overpotentials in a fuel cell.

Two new all-PTFE cells have been designed and built to carry out measurements at elevated temperatures in more concentrated alkaline electrolytes, on both smooth Pt and supported-Pt gas-diffusion electrodes.

Publications

1. K.A. Striebel, P.C. Andricacos, E.J. Cairns, P.N. Ross and F.R. McLarnon, "Oxygen Reduction in Tetrafluoroethane-1,2-Disulfonic Acid," *J. Electrochem. Soc.* **132**, 2381 (1985).
2. K.A. Striebel, F.R. McLarnon and E.J. Cairns, "The Effect of Carbonate Anions on the Reduction of Oxygen at Platinum Electrodes in Dilute Alkaline Electrolytes," *Extended Abstracts of the 167th Meeting of the Electrochemical Society* (1985) p. 923.

Investigation of Alloy Catalysts and Redox Catalysts for Phosphoric Acid Fuel Cells

(J. Bett, International Fuel Cells, Inc.)

The objective of this project was to improve the performance of phosphoric acid fuel cells to meet the goals set for power plants in vehicle applications. Various approaches were investigated to improve cathode performance, increase peak power capability, and to identify anode catalysts with improved low-temperature performance on CO-containing fuels so that the start-up time for the power plant might be reduced.

Metal-organic macrocyclic molecules had been shown in several previous studies to have intrinsic activities rivaling that of Pt, but with limited high-power performance. On the basis of a literature review, six candidate catalysts were selected. They were cobalt tetraazaannulene (CoTAA) and brominated CoTAA, cobalt and iron phthalocyanine (CoPc and FePc), and cobalt and iron tetramethoxyphenylporphyrin (CoTMPP and FeTMPP). In preliminary

tests, FeTMPP in the heat-treated form was clearly the most active and stable. Extensive efforts were made to understand and optimize the activity. The exact form of the active catalyst on a C support, which is heat treated to 950 °C, has not been established but related work at CWRU suggests that the macrocycle partially decomposes while still retaining the N. Thermogravimetric analyses and Mossbauer spectrographic measurements indicated that the central FeN₄ group remained intact in the heat-treated catalysts, with Fe in a zero-valent form.

In tests to determine the factors influencing the performance of the heat-treated FeTMPP, catalysts were prepared on C supports with a range of surface characteristics, particle morphologies, and heat-treatment conditions. These catalysts were evaluated in electrode structures made by wet and dry methods, which permitted a wide variation in the chemistry of the process to optimize performance.

The performance of heat-treated FeTMPP electrodes exceeds that of Pt on a metal weight basis at low current density. Two principal causes were identified for electrode polarizations that limited performance at high current density: diffusion loss due to the morphology of the supporting C, and resistance within the electrode structure. The diffusion loss was reduced by selection of C supports with low internal porosity, but these materials had limited surface area available for dispersion of the FeTMPP molecules. Multilayers of FeTMPP were shown to be less active. Consequently, the ultimate electrode performance was limited by the amount of catalyst that could be introduced into the electrode. The second factor, the resistance within the electrode structure, gave a polarization component that increased linearly with increasing current density. This resistance is most likely caused by a larger-than-normal

ionic resistance caused by the poorly wetting surface of FeTMPP. A second possible source is a resistance between the catalyst and the support, perhaps involving the kinetics of the electron-transfer process.

FeTMPP electrodes in half-cell tests of limited duration gave evidence of stability at 100 °C, but in extended testing in 2" x 2" full cells for many hundreds of hours, FeTMPP electrodes decayed in performance, even at 80 °C. Loss of Fe appeared to be the cause. Stability was not affected by variations in heat-treatment procedures and C supports or by addition of Fe to the electrolyte.

Several candidate anode catalysts were evaluated to establish their activity in CO-containing fuels at low temperature. Candidates were Pt-Ru, Pd-Au and Pt-Bi; and CSV-11, CSV-15 and CSV-34, the last three being proprietary Pt-based catalysts. In screening tests, CSV-11 was selected for further study. The CO tolerance of CSV-11 was measured over a range of temperature from 80 to 200 °C and for CO partial pressures from 0.1 to 5%. This anode operates with significantly improved performance over that of Pt, and may be operated below 140 °C with acceptable polarization.

A New Membrane - Catalyst Combination for Solid-Polymer- Electrolyte Systems

(J. McElroy, Hamilton
Standard-Electrochemical)

The objectives of this project were to develop new membrane-catalyst combinations for solid-polymer-electrolyte fuel cells, and to reduce the cost of membrane and electrode catalysts while still maintaining acceptable performance levels.

A modular test system was designed to provide operating conditions within a range

applicable for vehicle power systems. The operating conditions were: anode pressures from atmospheric to 30 psig, cathode pressures from atmospheric to 135 psig, and operating temperatures to 220 °F. The fuel was pure H₂ or simulated reformer mixtures with varying amounts of CO, and O₂ or air was used as an oxidant.

Development of a low-cost anode catalyst was pursued along two paths: (i) reduction of catalyst cost by direct lowering of the catalyst loading, and (ii) varying catalyst composition and methods of preparation to improve tolerance to fuel gases containing CO. Seven different CO-tolerant anode catalyst compositions were evaluated, with one being established as having a "baseline" performance. Anode tolerance to CO increased with increasing temperature to 220 °F. Above 220 °F, the increase in water vapor pressure results in a water management problem. At 180 and 200 °F, anode performance loss using 0.17% CO-containing reformat gas was 100 mV at 240 and 340 mA/cm², respectively. With a simulated reformat mixture containing 0.3% CO, the anode performance at 100 mV decreased to 170 and 245 mA/cm², respectively, at the same temperature and voltage. A reduction in anode catalyst loading to 2 mg/cm² did not affect anode losses at 300 mA/cm² and 180 °F on 0.17% CO, indicating no affect in CO tolerance with a catalyst weight reduction of 50%.

Reduction in the cost of the cathode catalyst was approached by (i) optimizing the wetproofing structure (i.e., binder content) for improved water management, and (ii) lowering of catalyst content from 4 to 2 mg/cm². The effect of temperature and pressure on cell performance with H₂ and O₂ was studied. Comparison at 220 °F indicates that the cell performance achieved with the 2 mg/cm² electrode was equivalent to that for the cell with a 4

mg/cm² electrode. Attempts to run the cathode on an air endurance test met with varying success during the initial test period. Good initial performance with air was obtained, but cell performance became limited beyond 200 mA/cm² and 60 psig. Modifying the cathode flow-field configuration to improve water/gas flow management corrected the air instability and produced a performance of 0.640 V at 500 mA/cm².

Major conclusions of this study are as follows. The development of a low-cost, ion-exchange membrane that exhibits similar performance to Nafion for over 1000-h operation is feasible. Materials cost for both the anode and cathode catalyst can be reduced by 50% while maintaining similar performance as the baseline fuel cells containing 4 mg/cm² noble metal in the anode and cathode. System analysis and tradeoff studies indicate that an the methanol/air fuel cell with a solid polymer electrolyte is a primary candidate as a power source for automotive applications. Further development is required to improve water management, fuel cell heat removal/humidification, cell scale-up, fuel conditioning, and the air compressor/expander.

The Effects of Heat Treatment and Microstructure on Electrocatalyst Performance

(G. Stoner, University of Virginia)

A series of Pt_xCr_{1-x} alloys were prepared in a planar electrode configuration, characterized, and then tested to determine the effect of several alloying parameters on electrocatalysis. The effects of lattice parameter, atomic ordering, intermetallic crystal structure, and dendritic segregation were examined, primarily with respect to the oxygen reduction reaction (ORR). The lattice parameter within the Pt-rich FCC solid solution decreases linearly with

composition from 0 to 50 at% Cr, with atomic ordering present at room temperature for alloys containing greater than 16 at% Cr. Multiple specimens were prepared with 0, 10, 25, 35, 50, 80 and 100 at%. The 25 at% Cr sample was studied in the as-received, ordered condition, as well as in a metastable, disordered state obtained by quenching from 1100 °C. The 80 at% Cr sample was utilized in its as-received, dendritic state and in a heat-treated, homogenized condition.

Initial calculations of the free energies of formation suggested that the Pt-Cr alloy is, in general, a very stable system relative to the pure components. Experimentally, this was found to be true for the alloys of less than 50 at% Cr, which were stable even during severe electrochemical cycling in phosphoric acid. The 50 at% Cr alloy, however, which thermodynamically was predicted to be the most stable component tested, was found to segregate readily during cycling. This discrepancy may be due to the presence of some form of chromium oxide which was not taken into account in the calculations. This oxide was recently shown to be a very important species in parallel work conducted at LANL on these same alloys. The 80 at% Cr alloy was also found to be very unstable in both its dendritic and homogenized forms.

The Pt-Cr alloys were initially studied utilizing reagent-grade 85 wt% H₃PO₄. The trends of peak currents versus at% Cr indicated that atomic ordering plays an important role in determining the activity for a given reaction. This is evidenced by the fairly large current density for the 25 at% Cr alloy. The presence of additional Cr, however, overrides this ordering effect and causes a drop in current densities.

Tests were also conducted with the Pt-Cr alloys in purified 10 and 85 wt% H₃PO₄. The faradaic resistance of the ORR on the 25 at%

Cr alloy was fairly low, close to Pt, while the 10 at% Cr alloy had a much higher resistance for the ORR reaction. Alloys with greater than 35 at% Cr yielded even greater resistances. The 25 at% Cr alloy gave results very close to those of Pt for a number of the electrochemical parameters investigated, however, it never exceeded Pt in activity. This is contrary to the results obtained with dispersed catalysts, which indicate a higher activity after Cr additions to Pt.

The proposed effect of decreased lattice parameter on the ORR activity (i.e., Pt alloy lattice parameters less than pure Pt yield higher activities) has been shown to be incorrect for bulk Pt_xCr_{1-x} alloys. Solid solution ordering has been shown to substantially increase electrochemical activity relative to similarly random structures. The change in crystal structure occurring at the intermetallic composition appears to have little effect on the electrochemical properties when compared to the addition of Cr.

This report was done with support from the Department of Energy. Any conclusions or opinions expressed in this report represent solely those of the author(s) and not necessarily those of The Regents of the University of California, the Lawrence Berkeley Laboratory or the Department of Energy.

Reference to a company or product name does not imply approval or recommendation of the product by the University of California or the U.S. Department of Energy to the exclusion of others that may be suitable.

*LAWRENCE BERKELEY LABORATORY
TECHNICAL INFORMATION DEPARTMENT
UNIVERSITY OF CALIFORNIA
BERKELEY, CALIFORNIA 94720*